Department of Economics Discussion Paper Series

Policy Transition Risk, Carbon Premiums, and Asset Prices

Christoph Hambel, Frederick van der Ploeg

Number 1075
March, 2025

Department of Economics
Manor Road Building, Manor Road
Oxford, OX1 3UQ

ISSN 1471-0498

Policy Transition Risk, Carbon Premiums, and Asset Prices

Christoph Hambel[a] Frederick van der Ploeg[b]

Revised version: March 2025

Abstract: We analyze the effects of policy transition risk on asset pricing and the green transition using a global two-sector, macro-finance model of climate and the economy. Policy transition risk results from probabilistic changes between three policy states: no, modest, and ambitious carbon pricing. We show that policy transition risk leads to carbon premiums (i.e. higher expected returns on brown than on green assets), especially if the economy is still quite carbon-intensive and close to the temperature cap, and thus accelerate the green transition. Increased transition risk leads to more precautionary saving and falls in the risk-free rate. We offer extensions to deal with physical risks (temperature-related risk of climate disasters and climate tipping), technology transition risk, and more realistic policy tipping with endogenous transition probabilities.

Keywords: carbon premium, green transition, policy transition risks, physical risks

JEL subject codes: D81, G01, G12, Q5, Q54

[a] Tilburg University, Tilburg School of Economics and Management (TiSEM), Department of Econometrics and Operations Research, P.O. Box 90153, 5000 LE Tilburg, The Netherlands, and Netspar. E-mail: C.Hambel@tilburguniversity.edu.

[b] University of Oxford, Department of Economics, Manor Road Building, Oxford OX1 3UQ, U.K., University of Amsterdam, P.O. Box 15551, 1001 NB Amsterdam, the Netherlands, CEPR, and CESifo. Phone: +44 (0) 1865 281285. E-mail: rick.vanderploeg@economics.ox.ac.uk.

Acknowledgements: We are grateful to the Associate Editor and a reviewer for their constructive and helpful comments. We thank Ton van den Bremer, Carina Fleischer, Reyer Gerlagh, Marten Hillebrand, Ivan Jaccard, Holger Kraft, Armon Rezai, Sjak Smulders, Gerhard Stahl, Luca Taschini, and the participants of the CCC Green Seminar Series, seminars at the Climate Change Centre of the ECB, the research department of the Bundesbank, the Seminar series of the University of Freiburg, Tilburg University, University of Rome (Tor Vergata), CREST-CMAP, Paris, and McGill University, and participants of the the EAERE 2024 conference, Leuven, EEA conference 2024, Rotterdam, the T2M 2024 conference, Amsterdam, the SURED 2024 conference, Ascona, the Banca d'Italia/IMF Workshop on Embedded Sustainability in a Credit Risk Assessment, Venice, June 2024, Banca d'Italia/EBANC Conference on Macroeconomic and Financial Dimensions of the Green Transition, June 2024, EUI, Italy, a Workshop at the University of Zurich on Climate Challenge and Economic Policy: Navigating Uncertainties and Agents' Heterogeneity, September 2024, and a Workshop at OsloMet on Climate Change: Global Risks and Cooperation, September 2024 for very helpful comments and suggestions.

Policy Transition Risk, Carbon Premiums, and Asset Prices

Revised version: March 2025

Abstract: We analyze the effects of policy transition risk on asset pricing and the green transition using a global two-sector, macro-finance model of climate and the economy. Policy transition risk results from probabilistic changes between three policy states: no, modest, and ambitious carbon pricing. We show that policy transition risk leads to carbon premiums (i.e. higher expected returns on brown than on green assets), especially if the economy is still quite carbon-intensive and close to the temperature cap, and thus accelerate the green transition. Increased transition risk leads to more precautionary saving and falls in the risk-free rate. We offer extensions to deal with physical risks (temperature-related risk of climate disasters and climate tipping), technology transition risk, and more realistic policy tipping with endogenous transition probabilities.

Keywords: carbon premium, green transition, policy transition risks, physical risks

JEL subject codes: D81, G01, G12, Q5, Q54

1 Introduction

Central bankers, other policy makers, and investors are increasingly concerned about transition risks related to global warming highlighted by the former Governor of the Bank of England in his speech on breaking the tragedy of the horizon (Carney, 2015). Transition risks can originate from a sudden stepping up or reversion of climate policies, a breakthrough in green technologies, or a sudden shifts towards green consumer preferences (e.g. Campiglio and van der Ploeg, 2022). Central bankers have used scenarios developed by the Network for Greening the Financial System (NGFS) and conducted stress tests to see how robust the economy is to transition and physical risks. In contrast, we analyze the effects of transition risk on asset prices and the green transition using a calibrated two-sector macro-finance model of the economy and the climate, and focus mainly on policy transition risk. We do not use fixed scenarios to capture transition risk, but capture policy transition risk by stochastic transitions between various climate policy states (e.g. no, modest, and ambitious carbon pricing). Policy tipping is reversible as it can also go back from ambitious to modest or no carbon pricing. Our objective is to investigate the implications of policy transition risk on emissions, financial markets, and the economy, in particular on carbon premiums and asset prices, and on the speed of the green transition. Our contributions are as follows.

First, we demonstrate that policy transition risk implies that climate policies are on average more ambitious than business as usual but less ambitious than the first-best optimal policies. Furthermore, policy makers may price carbon more aggressively than when policy makers do not face transition risk to make up for time lost by previous policy makers who did not price carbon and thus pushing the economy closer to the temperature cap.

Second, we find that at the time policy tips to modest or ambitious carbon pricing, green share price rises while brown share prices fall, and conversely when carbon pricing becomes more lacklustre. At the time the climate tips, both green and brown share prices fall. At the time negative emissions technology becomes available, green share prices jump down and brown share prices jump up while the carbon price falls. The news effects on share prices are much bigger for policy than for climate or technology tipping.

Third, we show that policy transition risk stemming from a change in the policy state from no to positive carbon pricing, and possibly back again gives rise to positive carbon premiums. A novel feature is that the carbon premiums in our analysis are particularly high if the risk of overshooting the temperature cap is high, since then policy makers will have to ramp up carbon prices to bring fossil use down. These two types of policy risk help to explain the empirical evidence for such premiums since 2015 by

Bolton and Kacperczyk (2021, 2023).[1] and for a wider set of pollutants by Hsu et al. (2023).[2] We thus provide an explanation why risk premiums on carbon-intensive assets have been consistently higher than those on greener, more climate-friendly assets, and why the resulting carbon premiums speed up the green transition. We also provide a mechanism of how the risk of tightening climate policy affects the pricing of brown assets as in Bouman (2023) and Campos-Martins and Hendry (2023).[3] The same mechanism leads political transition risk to increase demand for precautionary savings and curb the risk-free interest rate considerably if temperature is close to its cap. The carbon premiums encourage firms to invest more in green than in brown capital, and accelerate the green transition.

Finally, we consider various extensions to deal with physical risks (i.e., temperature-related risks of recurring climate disasters and irreversible climate tipping), technology transition risk related to negative emissions technology, and more realistic models of policy tipping.

To establish these results, we specify a two-sector DSGE model of climate and the economy with fossil fuel, renewable energy, and a wide array of economic, climate, and damage risks (cf. Hambel et al., 2024). There is limited substitutability between the two types of energy. Investments and capital reallocation from the brown to the green capital stock are subject to intertemporal and intrasectoral adjustment costs. We abstract from directed technical change towards green technologies (e.g. Bovenberg and Smulders, 1996; Acemoglu et al., 2012; Casey, 2023), but instead have learning by doing in renewables production. Temperature is driven by cumulative emissions.[4] We allow global warming to adversely affect output as in the seminal DICE model (e.g., Nordhaus, 2017), but in our extensions also to increase the risk of recurring climate-related disasters (cf. Karydas and Xepapadeas, 2022; Hambel et al., 2024), and the risk of climate tipping (cf. Lemoine and Traeger, 2014; van der Ploeg and de Zeeuw, 2018; Cai and Lontzek, 2019). If policy makers price carbon, they internalize these externalities. Our more realistic climate policy scenarios are calibrated to those in Moore et al. (2022).

In our extensions, we also allow for *technology transition* risk and two types of *physical* risks. The former comes from the emergence of a negative emissions technology at an uncertain future date, and thus

[1] Similarly, Delis et al. (2019) have found that banks price in climate policy exposure, especially after 2015, and also charge higher loan rates to fossil fuel firms. Ivanov et al. (2024) show that high-emission firms face shorter loan maturities, lower access to permanent forms of bank financing, and higher interest rates. Others have found mixed or even contrary evidence and thus challenge the existence of carbon and pollution premiums (e.g. Pastor et al., 2021; Bauer et al., 2022; Ardia et al., 2023; Aswani et al., 2024; Zhang, 2025; Hambel and van der Sanden, 2024 among others). Bolton and Kacperczyk (2024) have given a robust defense of their results in response to Aswani et al. (2024). However, Zhang (2025) argue that emissions grow linearly with firm sales, data is only available to investors with significant lags, and the positive carbon premium arises from the forward-looking firm performance information contained in emissions rather than from risk premiums. They show that, after accounting for the data release lag, the carbon premium turns negative in the U.S. and is insignificant globally.

[2] Hsu et al. (2023) find an annual pollution premium of 4.42% and suggest that this may stem from environmental litigation.

[3] These studies extract climate news from newspapers using textual analysis and show how these news affect risk premiums in the U.S. equity and corporate bond markets.

[4] See Matthews et al. (2009), Allen et al. (2009), and Dietz and Venmans (2019) for discussion and justification.

corresponds to 2 states.[5] The two physical risks correspond to the temperature-related risks of recurring climate-related disasters[6] and irreversible climate tipping. The latter risk is captured by 3 climate states to allow for upward jumps in the sensitivity of temperature to cumulative damages and in damages to aggregate production. We also allow for an intermediate policy tipping state with endogenous transition probabilities. We then have a three-dimensional Markov chain to allow for technological, and climate, and policy tipping with $2 \times 3 \times 3 = 18$ states.

While the effect of climate tipping points and feedback loops in the temperature dynamics on the social cost of carbon have been studied in an aggregate growth model of the economy (e.g. Lemoine and Traeger, 2014, Cai et al., 2016; Cai and Lontzek, 2019; Hambel et al., 2021; Olijslagers et al., 2023), these studies did not adopt a two-sector model of the economy to discuss the effects of physical climate risk on financial markets nor did they discuss policy transition risk. In contrast, we show how those risks are priced in by financial markets, and lead to higher risk premiums and an increased demand for precautionary savings curbing the risk-free interest rate.[7] Hambel et al. (2024) used a two-sector economy to analyze the effects of climate disasters and climate tipping on asset prices and the first-best optimal carbon price, but did not analyze the topical question of the effects of policy transition risk on carbon premiums and the speed of the green transition.

Hsu et al. (2023) use a reduced-form continuous-time model of asset pricing to derive the effects of policy transition risk and exposure to this type of risk for high and low emissions firms on the long-short portfolio of high versus low emission firms' expected stock returns. This demonstrates that the carbon premium compensates investors for uncertainty about whether the strong regulation would be implemented in the future. Furthermore, the carbon premium is higher if policy uncertainty is greater. These partial equilibrium insights guide our discussion of carbon premiums in our full-blown DSGE model of climate and the economy with policy transition risks. Our analysis highlights that a quantitatively additional form of policy transition risk resulting in particular high carbon premiums occurs if the risk of being close to the temperature cap is high.

Barnett (2024) is most closely related to our paper. It investigates transition risk within the context of a DSGE model but we allow for a richer structure and interactions between climate tipping risk, political risk, and risk of a technological breakthrough of negative emissions technology, richer structures of policy tipping, imperfect substitution between the energy types, and intra-sectoral adjustment costs.

[5] Negative emissions technologies such as direct air capture and storage are not yet competitive as their current marginal removal costs exceed by far current carbon prices (e.g., Rebonato et al., 2023). Technological breakthroughs can make those technologies competitive and allow removal of carbon dioxide from the atmosphere. Those technologies are essential for the target of net-zero emissions.

[6] We extend Cai and Lontzek (2019), who focus on climate tipping only with a one-sector DSGE model, by allowing for brown and green capital stocks and for two types of transition risks as well as the recurring risk of extreme weather events in a two-sector DSGE model of climate and the economy.

[7] In contrast to, for example, Kelly and Tan (2015), we abstract from learning about climate parameters.

We also allow for temperature-related risks of recurring climate-related disasters and exogenous risks of recurring Barro-style macro disasters. In contrast, Barnett (2024) shows how climate-changed linked expectations of fossil fuel restrictions can lead to a run on fossil fuel and confirms this empirically with a measure of innovations in the climate-related transition risk likelihood.

Section 2 presents our model of climate and the economy. Section 3 explains how we solve and optimize our model. Section 4 provides our calibration and core simulation results. Section 5 discusses extensions. Section 6 concludes.[8]

2 A Two-Sector Macro-Finance Model of Climate and the Economy

Production of Green and Brown Goods Final goods are produced in two sectors. Total output is the sum of outputs produced in the two sectors, $Y = Y_1 + Y_2$.[9] Outputs of both sectors $n \in \{1,2\}$ follow from the Cobb-Douglas production functions

$$Y_n = A_n K_n^{1-\eta_n} E_n^{\eta_n} \Lambda_n(T), \tag{2.1}$$

where K_n is the capital stock of sector n and E_n is an energy composite consisting of renewable energy and fossil fuel.[10] The Cobb-Douglas weight $0 < \eta_n < 1$ and total factor productivity $A_n > 0$ are sector-specific constants. Here, T denotes global mean temperature relative to the beginning of the industrial revolution. It affects sectoral output negatively via a smooth damage function $\Lambda_n(T)$ with $\Lambda_n(0) = 1$ and $\lim_{T\to\infty} \Lambda_n(T) = 0$. The energy composite is (cf. Golosov et al., 2014)

$$E_n = \left(\kappa_{1,n} G_n^{\rho_n} + \kappa_{2,n} F_n^{\rho_n}\right)^{\frac{1}{\rho_n}}, \tag{2.2}$$

where $\kappa_{i,n} \geqslant 0$ and $\rho_n < 1$ may be positive or negative. Here G_n and F_n denote renewable (or green) energy and fossil fuel use in sector n, respectively.[11] The elasticity of substitution between the two energy sources in sector n is $\zeta_n = \frac{1}{1-\rho_n}$. We suppose that the second sector relies significantly more on fossil fuel use than the first sector. We thus refer to the first sector ($n = 1$) as *green* and to the second sector ($n = 2$) as *brown*.

[8] Proofs, the numerical solution algorithm, calibration details, and further simulation results and robustness checks are presented in the appendices.

[9] We have perfect substitution between the two outputs. Imperfect substitution does not change the qualitative nature of the results much (Hambel et al., 2024).

[10] There is an additional production factor, i.e. labour, which is subsumed in total factor productivity A_n. This production function allows for endogenous technical change, since the Cobb-Douglas weights add up to one.

[11] If $\rho_n < 0$, the elasticity of substitution is smaller than one, and the energy inputs are complements within a sector. For $\rho_n > 0$, the elasticity of substitution is larger than one. Thus, the energy inputs are (imperfect) substitutes within a sector, and it is possible to fully replace one energy form by another within that sector, see Golosov et al. (2014). For $\rho_n = 0$, the energy composite collapses to a Cobb-Douglas aggregator.

Dynamics of Green and Brown Capital Let I_n be the investment rate in sector n and R the rate at which brown capital can be converted into green capital. Investment is subject to quadratic intertemporal adjustment costs (cf. Pindyck and Wang, 2013). The conversion of brown into green capital incurs quadratic intrasectoral adjustment costs. One dollar of brown capital can thus be converted into less than one dollar of green capital where the wedge increases in the amount being converted. The depreciation rates of the physical capital stocks are $\delta_n^k \geqslant 0$, $n \in \{1,2\}$. The capital stock dynamics of the green and brown sector are

$$\begin{aligned} \mathrm{d}K_1 &= \Big(I_1 - \frac{1}{2}\varphi_1 \frac{I_1^2}{K_1} + R - \frac{1}{2}\kappa \frac{R^2}{K_1} - \delta_1^k K_1\Big)\mathrm{d}t + K_1\sigma_1 \mathrm{d}W_1 - K_{1-}\ell \mathrm{d}N \\ \mathrm{d}K_2 &= \Big(I_2 - \frac{1}{2}\varphi_2 \frac{I_2^2}{K_2} - R - \delta_2^k K_2\Big)\mathrm{d}t + K_2\sigma_2\Big(\rho_{12}\mathrm{d}W_1 + \sqrt{1-\rho_{12}^2}\mathrm{d}W_2\Big) - K_{2-}\ell \mathrm{d}N \end{aligned} \tag{2.3}$$

where $\varphi_n > 0$, $n = 1,2$, are the investment adjustment cost parameters, $\kappa > 0$ the capital reallocation cost parameter, and W_1 and W_2 two independent Brownian motions. The parameter ρ_{12} denotes the instantaneous diffusive correlation coefficient between the Brownian shocks of the two capital stocks. The process N is an independent point process modelling the risk of macroeconomic disasters, where the disaster intensity λ is constant (Barro, 2006, 2009; Barro and Jin, 2011). The probability for a jump to occur over a small time interval $\mathrm{d}t$ is $\lambda \mathrm{d}t$ and the expected waiting time to the next jump is $1/\lambda$. The parameter ℓ denotes the corresponding jump size which is drawn from an i.i.d. process, but independent of the Brownian and Poisson shocks in the model. The corresponding recovery rate is denoted by $Z = 1 - \ell$. We suppose that the jump sizes are the same for both types of capital.[12]

The total stock of capital is defined by $K \equiv K_1 + K_2$ and the share of brown capital by $S \equiv \frac{K_2}{K_1+K_2}$. The dynamics of K and S are discussed in Appendix A.3.

Equilibrium Conditions Consumption is output net of investments and energy costs,

$$C_n = Y_n - I_n - b_g(S)G_n - b_f F_n, \tag{2.4}$$

where $b_g = b_g(S)$ denotes the real price of one unit of green energy. During a green transition, green energy becomes more competitive due to learning by doing, so $b_g'(S) > 0$.[13] The technology for producing fossil fuel is mature, so that its unit cost b_f is a constant. Consumption goods are perfect substitutes,

[12] Since this disaster shock affects both types of capital, it significantly increases the total correlation between the capital stocks; see Hambel et al. (2024). Besides, we can allow for different jump sizes for the sectors.

[13] Costs of solar panels, wind mills, and batteries decline as more of these have been used in the past (Wright's law).

so that aggregate consumption is $C = C_1 + C_2$.[14] Our analysis gives qualitatively similar results with imperfect substitutes (e.g., if aggregate consumption is a CES aggregate of the consumption goods).

Dividends Empirically, dividends are more volatile than consumption (e.g. Bansal and Yaron, 2004) and much more so if disasters hit the economy (Longstaff and Piazzesi, 2004; Wachter, 2013). This is because dividends are only a small part of household income, while labour income is the largest part of household income and is much less volatile than dividends. Following Wachter (2013), among others, we thus model dividends as leveraged consumption, $\mathscr{D}_n = C_n^\phi$ with leverage parameter $\phi > 1$.[15]

Climate Part Following Allen et al. (2009) and Matthews et al. (2009), global mean temperature T rises in cumulative net emissions. Hence, we specify the change in temperature by

$$\mathrm{d}T = \vartheta \nu (F_1 + F_2)\,\mathrm{d}t + \sigma_T \mathrm{d}W_3, \tag{2.5}$$

where ϑ is the transient climate response to cumulative emissions (TCRE), W_3 is a third standard Wiener process (independent of W_1, W_2, and N), and σ_T is the temperature diffusion coefficient. Emissions are $\nu(F_1 + F_2)$, where F_n denotes fossil fuel use measured in gigatons of carbon in sector n,[16] and the emission intensity per unit of fossil fuel use, ν, evolves according to $\mathrm{d}\nu = \nu_- \left[g_\nu \mathrm{d}t - \frac{\mathrm{d}K}{K_-} \right]$. If g_ν is smaller than the expected economic growth rate, the emission intensity declines in expectation.

Policy Tipping The Markov chain for policy tipping X^p distinguishes two policy states:

(i) *No carbon pricing (BAU)* In this business-as-usual state ($X^p = 1$) policy makers ignore the adverse effects of climate change on the economy, but financial markets price in policy transitions risks.

(ii) *Carbon pricing (CAP)* In this state ($X^p = 2$), policy makers set the carbon tax to internalize the adverse effects of warming on aggregate production and ensure that temperature stays below a cap of $T_{cap} = 2^\circ$C, in line with the Paris agreement. If the cap is exceeded, a binding constraint comes into force so that fossil fuels cannot be burnt anymore: $F_{1,t} = F_{2,t} = 0$ if $T_t \geqslant T_{cap}$. If this constraint bites, carbon prices exceed the usual social cost of carbon.

[14] Since both consumption goods are perfect substitutes and investment in a sector is much smaller than output, it does not matter much whether investment comes out of the good in that sector or there is a single aggregate resource constraint.

[15] An alternative to this approach is modelling the consumption-dividend ratio as a stationary but persistent process (e.g. Longstaff and Piazzesi, 2004). In order to focus on the novel implications of climate transition risk on asset prices, we keep the setting simple although following this approach would also be feasible in our setting. A more rigorous approach where capital is owned by intermediaries who issue stocks and pay dividends to households is beyond the scope of this paper.

[16] We model fossil fuel as an inexhaustible resource. To test whether exhaustibility matters for our policy simulations, we have studied a model variant that takes account of the constraint $\int_0^t E_s^{ind} \mathrm{d}s \leqslant \overline{E}$, where $\overline{E}$ denotes the maximum amount of total carbon emissions if all fossil fuel resources were to be exploited. We find that this constraint is not binding if $\overline{E}$ is set in line with recent estimates on exhaustible fossil fuel resources, $11,000\mathrm{GtCO}_2$ or $3,000\mathrm{GtC}$ (McGlade and Ekins, 2015).

A transition from one policy regime to another arises if policy makers change their climate ambition or there is a change of policy makers (e.g., due to an election). Financial markets anticipate such policy transition risks and price them in asset returns. For our calibration the binding temperature cap bites as just internalizing damages to output gives temperatures above the cap. The cap introduces not only higher carbon prices but also more urgency: if policy makers have waited too long with switching to carbon pricing, it becomes more and more difficult and costly to get temperature below the cap again.

Recursive Preferences Households have identical recursive preferences (Epstein and Zin, 1989); we use the continuous-time version (Duffie and Epstein, 1992b). The value function (indirect utility function) of the representative household J is recursively defined by

$$J(t,K_1,K_2,T,X^p) = \sup_{F_n,G_n,I_n,R} \mathbb{E}_t\Big[\int_t^\infty f\big(C_s,J(s,K_{1s},K_{2s},T_s,X_s^p)\big)\mathrm{d}s\Big], \tag{2.6}$$

where the aggregator function has the form ($\gamma \neq 1$)

$$f(C,J) = \begin{cases} \delta\theta J\Big[\frac{C^{1-1/\psi}}{[(1-\gamma)J]^{1/\theta}} - 1\Big], & \psi \neq 1, \\ \delta(1-\gamma)J\ln\Big(\frac{C}{[(1-\gamma)J]^{\frac{1}{1-\gamma}}}\Big), & \psi = 1, \end{cases}$$

γ is the coefficient of relative risk aversion (RRA), ψ the elasticity of intertemporal substitution (EIS), $\theta \equiv \frac{1-\gamma}{1-1/\psi}$, and $\delta > 0$ the rate of time impatience. Relative risk aversion typically exceeds $1/\psi$, which reflects preference for early resolution of uncertainty. For $\gamma = 1/\psi$ or $\theta = 1$, one obtains time-additive CRRA utility with $J(t,K_1,K_2,T,X^p) = \sup_{F_n,G_n,I_n,R} \mathbb{E}_t\big[\int_t^\infty e^{-\delta(s-t)}\frac{C_s^{1-\gamma}}{1-\gamma}\,\mathrm{d}s\big]$.

Policies and Decentralization Policy makers that are in an active policy state ($X^p = 2$) maximize social welfare (2.6) subject to the constraints of our model of the climate and the economy while internalizing the global warming externalities and ensuring that the temperature cap is not violated. The no policy state ($X^p = 1$) corresponds to business as usual, where households and firms do not internalize global warming externalities or the temperature cap when maximizing their expected utility and the present discounted value of profits, respectively. Of course, global warming damages do impact the economy but each private agent is too small to take account of them. Both policy states require solving a dynamic programming problem.[17]

A key question is how to implement the social optimum corresponding to the active policy state ($X^p = 2$) in the decentralized market economy. To decentralize the social optimum requires a specific emissions

[17] See Appendix A for the numerical algorithm. The value function must satisfy the Hamilton-Jacobi-Bellman (HJB) equation (A.1), which under mild assumptions can be expressed as $J(t,K_1,K_2,T,X^p) = \frac{1}{1-\gamma}K^{1-\gamma}V\big(t,T,S(K_1,K_2),X^p\big)$ with $S = S(K_1,K_2) \equiv \frac{K_2}{K_1+K_2}$, $K \equiv K_1 + K_2$, and $V = V(t,T,S,X^p)$ satisfies the easier HJB equation (A.12).

tax on brown firms that is set to the SCC (see equation 3.1 below), and to rebate the carbon tax revenues as lump-sum payments to brown firms.[18] In the market economy brown firms thus do not internalize global warming externalities or the temperature cap, but they do take full account of carbon taxes and lump-sum rebates. To decentralize the social optimum it is thus not necessary to subject households or green firms to a carbon tax, and neither do they get rebates. Of course, under business as usual with no climate or disaster policies policies ($X^p = 1$), the carbon tax and rebates are zero.

Our assumption of exogenous transition probabilities and two given policy states is a very stark and simplified presentation of the political process, but in our view it suffices to demonstrate the effects of transition risk on the economy, financial markets and the climate. A full political economy analysis of endogenous transition risks and policy stances is beyond the scope of this paper. Some recent papers offer a political economy analysis of green transitions with dynamic complementarities stemming from evolving green values and technologies getting cheaper with experience and policy makers that cannot commit future policy makers in democratic societies (Besley and Persson, 2019, 2023). These papers do not study the effects of transition risk on asset prices, carbon premiums, macroeconomic outcomes, and the climate. With our assumption of given policy stances, commitment issues do not arise. Neither do we examine the game between current and future policy makers, but when policy makers optimize their climate policies they fully take account of the possibility that they may be removed from office and be replaced by policy makers that do not conduct climate policies or have a different climate policy stance. This can be seen from the dynamic programming framework which allows for transition risks.[19] Since households and firms in our model (in contrast to many integrated assessment models) are forward-looking and anticipate future events and policies, our model should not be subject to the Lucas critique.

Finally, our model is calibrated to the global economy rather than to the U.S. or European economy as this would require assumptions about whether third countries follow U.S. or European policies. The global economy assumptions fit uneasily with the idea of national elections. In our defense, we base our calibration of policy uncertainty in the full model of section 5 on Moore et al. (2022) which has been very influential in the climate science and climate policy literature.

[18] As Pindyck and Wang (2013) have shown, decentralization of the social optimum also requires catastrophic insurance as the Barro-style disaster risks are not internalized by the firms. Under business as usual, one also needs insurance contracts to decentralize, but in equilibrium they are not needed as they are in zero net demand and supply.

[19] Since our dynamic programming problem yields Markov-perfect equilibrium outcomes, the resulting policies in the active policy states are time consistent provided care is taken by policy makers of the risk that they will be removed from office.

3 Optimal Carbon Taxes, Risk-Free Rate, and Carbon Premium

Social Cost of Carbon The SCC, the expected present discounted value of all present and future negative effects of emitting one ton of CO_2, is

$$\tau = -\frac{\vartheta(X^p)\,J_T}{f_c(C,J)} = \frac{\vartheta(X^p)c^{1/\psi}}{\delta(\gamma-1)}\frac{V_T}{V^{1-1/\theta}}K > 0 \tag{3.1}$$

(see Appendix A.2). The SCC is proportional to the total stock of capital as marginal damages are proportional to aggregate economic activity; cf. Golosov et al. (2014) and Olijslagers et al. (2023) for a stochastic setting who find a similar result in settings *without* transition risk.

Risk-free Rate and Precautionary Savings In equilibrium, the risk-free rate r^f is[20]

$$\begin{aligned} r_t^f = {} & \underbrace{\delta}_{\text{Discounting}} + \underbrace{\frac{1}{\psi}\mu_C}_{\text{Smoothing}} - \underbrace{\frac{1}{2}\gamma\Big(1+\frac{1}{\psi}\Big)\|\sigma_C\|^2}_{\text{Standard Diffusion Risk}} - \underbrace{\lambda\mathbb{E}\Big[Z^{-\gamma}-1+\frac{\theta-1}{\theta}\big(1-Z^{1-\gamma}\big)\Big]}_{\text{Macroeconomic Disaster Risk}} \\ & \underbrace{+\frac{\gamma\psi-1}{2\psi^2}\Big(\|\sigma_C-\sigma_k\|^2+\psi\big(\|\sigma_C\|^2-\|\sigma_k\|^2\big)\Big)+\frac{\theta-1}{\theta\psi}\sigma_g^\top(\sigma_C-\sigma_k)}_{\text{Temperature Interaction Risk}} \\ & \underbrace{-\sum_{x\neq X^p}\lambda_x(X^p,x)\Big[(1-j_v^x)^{1-1/\theta}(1-j_c^x)^{-1/\psi}-1+\frac{\theta-1}{\theta}j_v^x\Big]}_{\text{Transition Risk}}, \end{aligned} \tag{3.2}$$

where j_v^x and j_c^x capture the effects of a transition shock to state x on the value function V and the ratio of consumption to capital $c = C/K$, respectively. Here expected consumption growth μ_C and the volatility vectors of capital σ_k and consumption σ_C are state-dependent and computed numerically.[21] This is also the case for the transition risk terms.[22] The first line of (3.2) reflects the role of discounting, the desire to smooth consumption, and the precautionary saving in response to diffusion and macroeconomic disaster risk (cf. Barro, 2006, 2009; Pindyck and Wang, 2013; Wachter, 2013).[23] The second line of (3.2) captures precautionary savings for uninsurable temperature risk. This depends on the state variables, in particular temperature, in a nonlinear manner, but has little effect on the risk-free rate because

[20] Details on the derivation are in Appendix B.1, where we also derive the dynamics of the pricing kernel (B.6).

[21] The volatility vectors are given in (A.13) and (B.9). Note that μ_C as given in (B.8) can suddenly drop after a jump into the CAP state if temperatures are high and one can no longer use fossil fuel. Expected consumption growth and its volatility depend non-linearly on both temperature and the brown capital share, whereby the result is more involved and qualitatively different from one-tree endowment economies. Also, the share of brown capital has a significant effect. This stems from a diversification argument (cf. Cochrane et al., 2007; Hambel et al., 2024), so the need for precautionary savings falls.

[22] While disaster risk affects the capital stock via the loss ℓ, these shocks affect utility and consumption via state-dependent terms j_v^x and j_c^x. These are computed numerically and are given in equations (B.3) and (B.5) of Appendix B.1.

[23] Both precautionary saving terms curb the interest rate, more so if risk aversion γ is large (cf. Wachter, 2013).

consumption volatility σ_C is close to capital volatility σ_k (cf. Hambel et al., 2024). With time-additive CRRA-utility ($\gamma = 1/\psi$, $\theta = 1$), this term vanishes. The last line in (3.2) reflects precautionary savings in response to the risk of policy tipping. A novel feature is that the risk-free rate (3.2) depends on the current state of the political Markov chain X^p and thus reacts abruptly to transition risks. We perform a quantitative analysis on how transition risks affect the risk-free rate in section 4.3 and Appendix D.2.

Asset Prices For the dividend stream $\mathscr{D}_n = C_n^\phi$, the time-t ex-dividend price of asset n equals

$$P_{nt} = \mathbb{E}_t\Big[\int_t^\infty \frac{H_s}{H_t}\mathscr{D}_{ns}\mathrm{d}s\Big], \tag{3.3}$$

where H_s denotes the pricing kernel for discounting from time s to time t (see (B.6)). Its equilibrium expected excess return corresponds to the risk premium of the asset: its expected ex-dividend stock return, μ_n^p, plus the dividend yield, $y_n^d = \mathscr{D}_n/P_n$, minus the risk-free interest rate, r^f, $r_n^p = \mu_n^p + y_n^d - r^f$.[24]

The Carbon Premium A pivotal element of our analysis is the *carbon premium* defined as the difference between the brown and green risk premiums, i.e. $r_2^p - r_1^p$, which is given by

$$\begin{aligned} r_2^p - r_1^p = & \sum_{x\neq \mathbf{X}} \lambda_x\big[\big(1-(1-j_v^x)^{1-1/\theta}(1-j_c^x)^{-1/\psi}\big)\big((1-j_{\Pi_2}^x)(1+j_{\chi_2}^x)-(1-j_{\Pi_1}^x)(1+j_{\chi_1}^x)\big)\big] \\ & + \Big[\Big(\frac{\partial\Pi_2}{\partial S}-\frac{\partial\Pi_1}{\partial S}\Big)S(1-S)\sigma_S + \phi(\sigma_{\chi_2}-\sigma_{\chi_1}) + \Big(\frac{\partial\Pi_2}{\partial T}-\frac{\partial\Pi_1}{\partial T}\Big)\sigma_T\Big]^\top\Big(\gamma\sigma_k - \frac{\theta-1}{\theta}\sigma_v + \frac{1}{\psi}\sigma_c\Big), \end{aligned} \tag{3.4}$$

where $\Pi_n = P_n/\mathscr{D}_n$ denotes the price-dividend ratio of asset n, σ_{χ_n} the volatility of the consumption-capital ratio in sector n, $\chi_n = C_n/K_n$, ϕ the leverage parameter, and $j_{\Pi_n}^x$ and $j_{\chi_n}^x$ denote the effects of a transition shock to state x on the price-dividend ratio, Π_n and the consumption-capital ratio, χ_n, of sector n, respectively. The first line in equation (3.4) for the carbon premium represents the effects of transition risk term on the carbon premium. It increases in the transition risk intensities, λ_x, and the exposure terms in the square brackets. The term $\big(1-(1-j_v^x)^{1-1/\theta}(1-j_c^x)^{-1/\psi}\big)$ reflects the effect of a transition shock on the stochastic discount factor and is similar to the corresponding term in the risk-free rate. The second exposure term $(1-j_{\Pi_2}^x)(1+j_{\chi_2}^x)-(1-j_{\Pi_1}^x)(1+j_{\chi_1}^x)$ reflects the difference in the impact of transition shock on the price-dividend ratios of both sectors. We thus see that, if the price impact of a certain type of shock is more pronounced for the brown sector, a carbon premium emerges.

The second line of the carbon premium (3.4) indicates that the carbon premium can also emerge from diffusive components. First, the carbon premium increases if the volatility of the share of brown capital affects the price-dividend ratio of the brown sector relatively more (high $\frac{\partial\Pi_2}{\partial S}-\frac{\partial\Pi_1}{\partial S}$), especially if the

[24] The price-dividend ratio $\Pi_n = P_n/\mathscr{D}_n$ satisfies the parabolic partial differential equation (B.12), which we solve numerically (Appendices B.3 and B.4). We also provide a semi-closed form expression of the risk premiums in (B.13) of Appendix B.4.

share of brown capital is neither very large or very small (and thus $S(1-S)$ is high). Second, the carbon premium increases if the volatility of the consumption-capital ratio in the brown sector is higher than that in the green sector (high $\sigma_{\chi_2} - \sigma_{\chi_1}$) and firms are leveraged (high ϕ). Third, in the CAP state, a temperature shock with volatility σ_T can have very distinct effects on the price-dividend ratios of the green and the brown sector if temperatures are close to two degrees, and thus the difference between $\frac{\partial \Pi_2}{\partial T}$ and $\frac{\partial \Pi_1}{\partial T}$ can significantly impact the carbon premium. This shows that a positive carbon premium occurs if the price impact of a transition shock is stronger for the brown asset than for the green asset. It turns out that quantitatively this third effect on the carbon premium is the most important one.

Our model of political risk can explain a *transition risk premium* (cf. Engle et al., 2020; Faccini et al., 2023) leading to positive risk premiums of both green and brown assets. This effect is particularly pronounced when tightening climate policy weighs down the economy (i.e. when the share of brown capital is high). Both types of risky assets carry this risk premium, but if the brown asset is stronger affected than the green asset we have a *carbon premium* (cf. Bolton and Kacperczyk, 2021, 2023; Hsu et al., 2023). Our mechanism for generating the carbon premium is purely risk-driven and prices the asymmetric impact of policy shocks. In contrast, Pastor et al. (2021) argue that green investors may be willing to accept a lower return on green assets, which would also contribute to a positive carbon premium. Similar preference-driven mechanisms can be found in Pedersen et al. (2021), Zerbib (2022), Duineveld et al. (2025), which can explain sizable carbon premiums along the transition to a low-carbon economy without relying on a risk channel. On the other hand, Sauzet and Zerbib (2024) find that preference for green consumption goods induces a consumption premium on expected returns, which mitigates the carbon premium stemming from their preferences for green assets.[25]

Finally, we have assumed in equations (2.3) that physical risks load similarly on the two capital stocks as we wanted to generate a carbon risk premium purely endogenously via the fact that the brown sector is more carbon-intensive than the green sector. If physical risk would impact the two sectors differently, this would have additional effects on the the carbon premium.

4 Benchmark Results

We have calibrated our model to the global economy. Table 1 summarizes our benchmark calibration with details in Appendix C.1. We use a transition probability from the BAU to the CAP policy state of $\lambda_x = 4\%$ per year.

[25] We also provide a mechanism for a *temperature risk premium* (cf. Bansal et al., 2017; Donadelli et al., 2017; Hong et al., 2019; Gregory, 2024. We thus find that global warming carries a positive risk premium that is rooted in physical climate risk and increases in the level of temperature.

	Preferences		
δ	time-preference rate	calibrated (Appendix C.1)	0.0346
γ	relative risk aversion	calibrated (Appendix C.1)	2.977
ψ	elasticity of intertemporal substitution	Bansal and Yaron (2004)	1.5
	Economic Model		
Y_0	initial GDP (trillion US $)	Nordhaus (2017)	116
S_0	initial share of brown capital	from World Bank data (Footnote 44)	0.876
$K_{1,0}$	initial green capital (trillion US $)	calibrated (Appendix C.1)	74.3
$K_{2,0}$	initial brown capital (trillion US $)	calibrated (Appendix C.1)	1353.9
A_1	green productivity	calibrated (Appendix C.1)	0.3323
A_2	brown productivity	calibrated (Appendix C.1)	0.3451
φ_n	investment adjustment cost parameter	calibrated (Appendix C.1)	13.61
κ	capital reallocation cost parameter	calibrated to modified RCP8.5 (Appendix C.1)	2
$b_{f,0}$	initial fossil fuel costs ($ per tC)	Hambel et al. (2024)	540
$b_{g,0}$	initial renewable energy costs ($ per etC)	Hambel et al. (2024)	810
k_0	cost function parameter	from Swanson's law (Footnote 43)	0.5107
k_1	cost function parameter	from Swanson's law (Footnote 43)	0.3219
η_n	energy share in production	van den Bremer and van der Ploeg (2021)	0.043
ζ_2	elasticity of energy substitution	Golosov et al. (2014)	2
$\kappa_{1,2}$	renewable energy weight in brown sector	Golosov et al. (2014)	0.356
$\kappa_{2,2}$	fossil fuel weight in brown sector	Golosov et al. (2014)	0.644
$\kappa_{1,1}$	renewable energy weight in green sector	assumption	1
$\kappa_{2,1}$	fossil fuel weight in green sector	assumption	0
ϕ	leverage parameter	Wachter (2013)	2.6
σ_n	annual capital volatility	Wachter (2013)	0.02
ρ_{12}	instantaneous correlation	Cochrane et al. (2007)	0
α	power function parameter for disaster size	calibrated in line with Wachter (2013)	5
λ	macroeconomic disaster intensity	calibrated in line with Wachter (2013)	0.06
λ_x	transition intensity from BAU to CAP	calibrated in line with Moore et al. (2022)	0.04
	Climate Model and Damages		
T_0	initial temperature ($^\circ$C)	temperature data	1.27
ϑ	TCRE ($^\circ$C/TtC)	Hambel et al. (2024)	1.8
σ_T	annual temperature volatility	RCP data (Footnote 46)	0.033
θ	damage function parameter	Tol (2023)	0.0073

Table 1: Benchmark Calibration. Preferences, the economy, the climate, and damages.

We now present our policy optimization and simulation results. We solve our model numerically with the grid-based finite-differences method (see Appendix A.5). use 20,000 sample paths until the year 2100. These paths were generated with the policy functions.[26] Sensitivity exercises with respect to transition probabilities and the tightness of the temperature cap can be found in Appendix E.

4.1 Scenarios without Transition Risks

BAU Scenario First, we discuss the results for a pure business-as-usual (BAU) scenario, which excludes policy transitions to active climate policies (CAP). This aids comparison with transition risk scenarios. The left panels in Figure D.3 show the simulation of macroeconomic key variables until the

[26]The policy functions for key variables as functions of (S, T, X^p) can be found in Appendix D.2 with a brief discussion.

year 2100. The average values of a variable are depicted by solid lines (——) and referred to as the mean path. Dashed lines (- - -) show 5% and 95% quantiles. Since policy makers do not take account of negative global warming externalities and do not enforce the temperature cap, the green transition takes place at a slow pace (Panel a)). The transition is solely driven by the desire to diversify assets and the falling cost of green energy as the share of green capital rises (Hambel et al., 2024). The share of fossil fuel in the energy mix is always a bit below the share of brown capital, since the brown sector can be operated with both fossil fuel and renewable energy. Emissions are high (Panel b)) and global average temperatures reach on average 3.9°C above the pre-industrial average by the end of this century (Panel c)). In contrast to policy makers, financial markets do anticipate the adverse effects of emissions on the economy. The effect of TFP damages on asset pricing moments is almost negligible and not sufficient to explain a temperature risk premium as in Bansal et al. (2019). As can be seen from Figure D.4 in Appendix D.1, the risk-free rate and the risk premiums are almost unaffected in this BAU scenario. This is not the case if we allow for climate-related disaster and climate tipping risks (see section 5).

CAP Scenario without Transition Risks The panels on the right of Figure D.3 show the results for the pure CAP policy without the possibility of reverting back to BAU. Now, the energy transition takes place at a much faster pace, emissions are strongly mitigated, and temperatures stabilize on average slightly below two degrees. In some paths, however, temperatures exceed the two degrees cap due to climate uncertainty. If this happens, policy makers phase out fossil fuels immediately. This stringent climate action requires substantial carbon taxes and massive capital reallocation from the brown sector to the green sector. Although this is costly, it avoids climate damages and leads to stronger economic growth in the long run relative to the BAU scenario.

4.2 Core Results with Transition Risks: Energy Transition

Figure 1 illustrates the transition towards a low-carbon economy until the year 2100, starting with BAU in 2020. The average values of a variable are depicted by solid lines (——). Dashed lines (- - -) show 5% and 95% quantiles. We also illustrate the effects of climate policy on the real economy and asset prices along one selected sample path shown by the thin black lines (——).

Due to policy tipping the share of brown capital and the share of fossil fuel in the global energy mix decline much faster than in the pure BAU scenario but slower than in the pure CAP scenario without transition risk. Still, the transition is characterized by considerable uncertainty as to when policy makers will take climate protection measures. Such uncertainties explain the broad confidence bands of key variables such as the share of brown capital (panel a)), net emissions (panel b)), temperature (panel c)), and carbon prices (panel d)) compared to the scenarios without transition risk. Along our

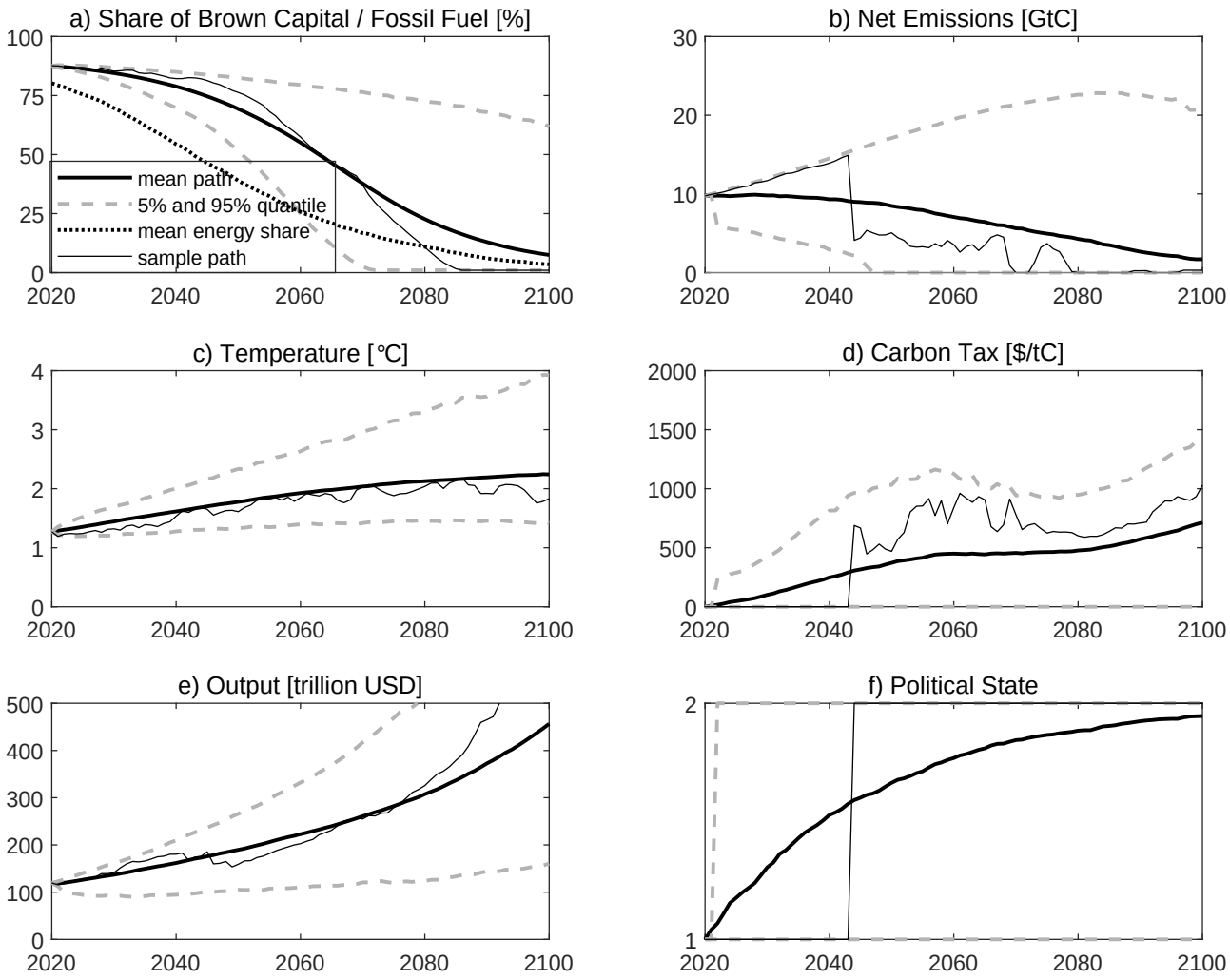

Figure 1: Transition of the Real Economy (starting from BAU with transition risk to the CAP state). Mean paths are depicted by solid lines (——) and dashed lines (- - -) show 5% and 95% quantiles. The dotted line (·····) in Panel a) shows the share of fossil fuel in the global energy mix. The thin black lines (——) shows one illustrative sample path, where society switches from the BAU to the CAP policy state in 2045.

illustrative path, the economy is in the BAU state until the year 2045 when it transitions to the CAP policy state (panel f)). This transition leads to a drastic emission cuts and a sudden implementation of a substantial carbon price of about \$700/tC or \$190/tCO_2.

About 28% of the simulated paths lead to a temperature lower than 1.8°C by the end of the century while 46% of the paths lead to a temperature increase between 1.8°C and 2.5°C. The remaining paths suffer from little or ineffective climate action and lead to significant temperature increases of more than 2.5°C. The 2°C cap is violated for many paths from 2040 onwards, with the number of violations

increasing sharply around 2050. About 45% of the sample paths up to 2100 adhere to the 2°C cap, but a greater proportion of paths temporarily violate the target.

The number of paths with active climate policies increases rapidly over time and reaches 94% by 2100 (panel f)). The illustrative sample path shows that the carbon tax is more volatile than output, which is due to temperature volatility.[27] In about 4% of paths, the carbon tax is implemented in the year 2021 and then starts at an average of \$218/tC or \$60/tCO_2. This figure is about 50% larger than in a scenario with Pigouvian carbon pricing but without a legally enforced temperature cap (see also rows 4 and 6 of Table E.2 for 2025). The reason is that, due to the cap of 2°C, policy makers implement more ambitious carbon taxes than when just correcting for global warming externalities. Further, since the simulations start in BAU, policy makers need to catch up and implement higher carbon prices as the cap is closer.

4.3 Core Results with Transition Risks: Asset Pricing

Figure 2 illustrates the mean path as well as 5% and 95% quantiles of the price-dividend ratios, the green and brown risk premium, the risk-free rate, and the carbon premium until the year 2100. We also illustrate the effects of climate policy on asset prices along the same selected sample path as in section 4.2. Figure D.9 provides additional simulation results for prices and dividends. Equation (3.2) implies that policy shocks affect the risk-free rate, and thus also the price-dividend ratios and risk premiums of the risky assets. Moreover, the asset pricing moments depend in a highly non-linear manner on temperature, especially as the impact of a policy transition to CAP becomes potentially devastating when the 2°C cap is exceeded. We illustrate those non-linearities with policy functions in Appendix D.2. This is reflected in the large extent of variation of the key variables shown in Figure 1.

Asset Prices and the Price-Dividend Ratios A switch from the BAU to the CAP policy state is accompanied by a rise in the demand and price of the green asset and a sharp fall in the price of the brown asset. The effect on prices is stronger than on dividends, whereby the price-dividend ratio of the green asset increases strongly and that of the brown asset decreases. The price reaction is stronger for the green asset if temperature is well below two degrees (see panels a) and b)).[28] In our illustrative sample path, the policy switch happens in the year 2045, causing an immediate increase in the green price of 22%, while the brown share price drops on impact of the switch by 21.5%. The green and brown price-dividend ratios tend to decline over time. The green price-dividend ratio is initially relatively high reflecting the scarcity of this asset. The brown asset becomes worthless when the transition has come to an end and the brown capital stock has been run down completely. When climate policy has already

[27] Appendix D.2 discusses policy functions that show that the carbon tax is extremely sensitive to small changes in temperature, especially if temperature is close to 2°C.

[28] Figure D.9 in Appendix D.3 illustrates the impact of this policy shock on asset prices and dividends.

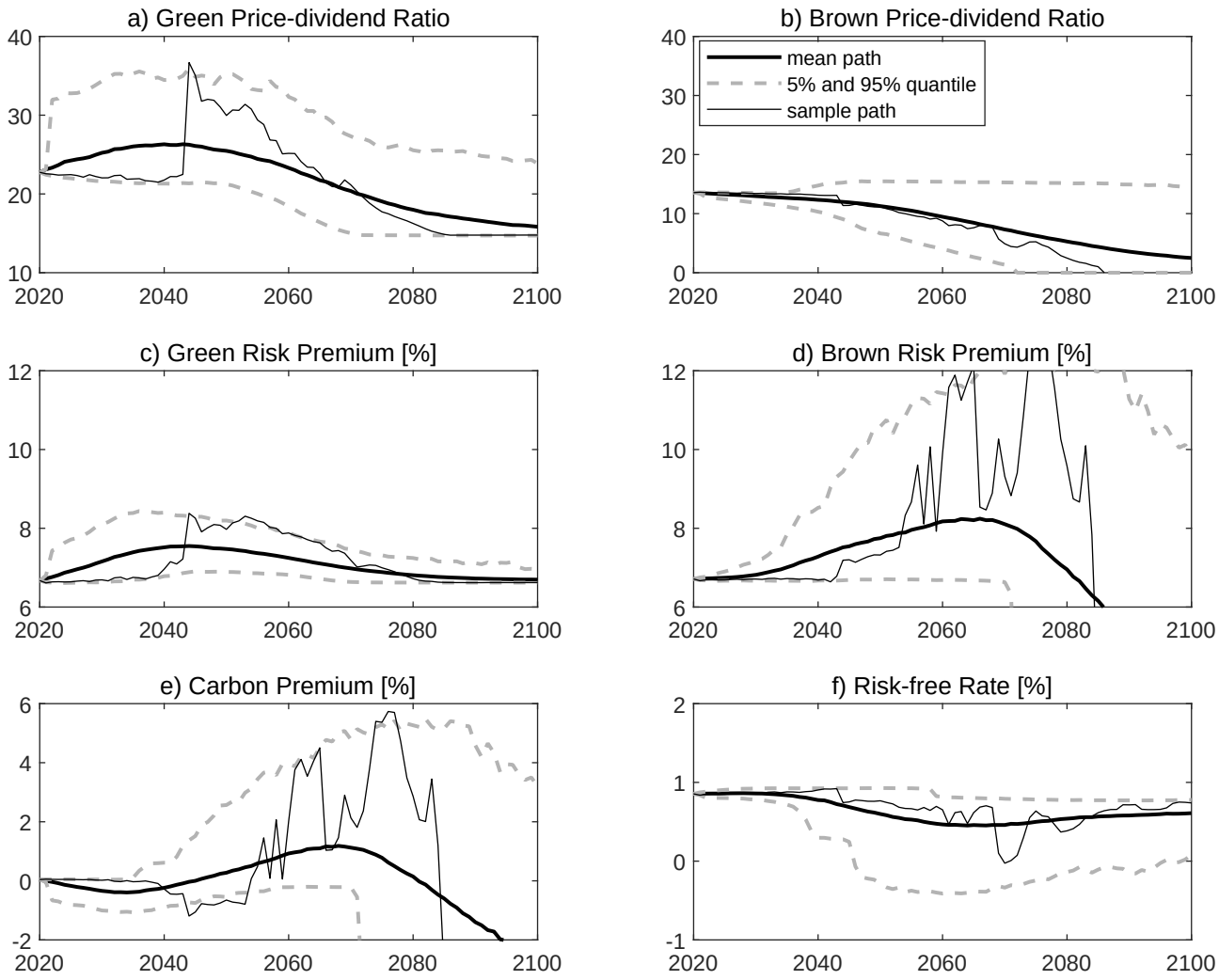

Figure 2: Asset Pricing Results (starting from BAU with transition risk to the CAP state). Average values are depicted by solid lines (——) and 5% and 95% quantiles by dashed lines (- - -). The thin black lines (——) shows one illustrative sample path, where society switches from the BAU to the CAP policy state in 2045.

been implemented and temperature has crossed the 2○C cap, the price of the brown asset also falls. This reflects the effect of asset stranding caused by the fact that fossil fuels may no longer be used.[29]

Risk Premiums The sharp rise in the price-dividend ratio of the green asset after a policy shock causes a decline in its dividend yield. However, the onset of climate policy increases demand for the green asset in the long term, causing the expected growth rate of the price of the green asset to rise sharply. This overcompensates for the decline in the dividend yield and leads to a slight increase in the

[29] Although the brown sector may still be operated, fossil fuel must not be used anymore. This can be interpreted as *partial stranding* of the brown sector in the sense that some of its assets may not be used anymore.

green premium (panel c)). Conversely, the increase in the brown risk premium can be explained by the now significantly increased risk of fossil fuels phasing out. This risk becomes substantial if temperature is close to its cap. This then leads to a sharp rise in brown risk premiums as compensation for investors (panel d)). The 95% quantiles in panels c) and d) indicate that then the risk premiums for both assets go up considerably, but eventually go down again when the transition is complete. This finding can be interpreted as a *transition risk premium* (cf. Engle et al., 2020;Faccini et al., 2023).

Carbon Premium In contrast to Hambel et al. (2024), which abstracts from climate transition risk, our model can generate a sizable carbon premium (see panel e) of Figure 2). The carbon premium is initially close to zero as in the empirical findings of Aswani et al. (2024), Zhang (2025), and Hambel and van der Sanden (2024). Still, our model offers a mechanism to explain sizable carbon premiums in the presence of policy transition risks. Although transition risk affects both assets, it has a larger effect on the brown asset if temperature is already relative high. Then, the term in the second line of (3.4) becomes positive and potentially large. Consequently and in line with the empirical findings of Hsu et al. (2023) and Bolton and Kacperczyk (2021, 2023), a sizable *carbon premium* emerges that reflects the asymmetric impact of policy transition risk (panel e)).

Risk-free Interest Rate The mean risk-free interest rate starts at 0.8% and remains largely stable over time (panel f)). The 5% quantile of this rate reflects extreme transition risks and generally falls with time. This happens especially in paths with temperatures exceeding the 2°C cap. Having switched to the CAP policy state, the risk of phasing out fossil fuel becomes more acute so that demand for precautionary savings increases slightly (see the small decline in the interest rate in 2045). When temperature crosses its cap, expected consumption growth declines as production becomes much more expensive (see the decline in the interest rate around 2070). When the transition continues and the brown capital stock becomes smaller, the impact of ambitious policies to phase out fossil fuels diminishes, which is why demand for precautionary savings fall and interest rates stabilize again.

5 Extensions

5.1 New Building Blocks

Recurring Climate Disasters Gradual damages from global warming form only a part of total damages. There is also the temperature-dependent risk of recurring climate disasters (droughts, fires, storms, floods, etc.). These risks have to be priced in and further increase the SCC. To capture these, we add to the right-hand of equations (2.3) the terms $-K_{1-}l_c dN_c$ and $-K_{1-}l_c dN_c$, respectively, where

Recurring Climate Disasters		
Jump size parameter	$\alpha_c = 65.7$	Hambel et al. (2024)
Marginal disaster intensity	$\widehat{\lambda}_c = 0.096$	Hambel et al. (2024)
Irreversible Climate Tipping Risk		
TCRE	$\vartheta(X^c=1)=1.8$, $\vartheta(X^c=2)=2.1$, $\vartheta(X^c=3)=2.4$ °C/TtC	from Allen et al. (2009)
Damage parameters	$d(X^c=1)=0$, $d(X^c=2)=0.025$, $d(X^c=3)=0.05$	cf. Cai and Lontzek (2019)
Intensity parameters	$\widehat{\lambda}_c^{1,2}=0.012$, $\widehat{\lambda}_c^{1,3}=0.012$, $\widehat{\lambda}_c^{2,3}=0.02$	cf. Cai and Lontzek (2019)
Breakthrough of Negative Emission Technology		
Cost function	$b_1 = 1.77 \cdot 10^{-4}$, $b_2 = 1.19 \cdot 10^{-5}$, $b_3 = 1$	from Rebonato et al. (2023)
	$c_1 = 0.34$, $c_2 = 0.03$, $c_3 = 0.34$, $\zeta = 0.1$	Appendix C.2, Footnote 31
Intensity parameter	$\widehat{\lambda}_t^{1,2} = 0.0224$	assumed
Political Transition Risks		
Intensity parameters	$\widehat{\lambda}_p^{1,2}=0.12$, $\widehat{\lambda}_p^{1,3}=0.05$, $\widehat{\lambda}_p^{2,3}=0.05$, $\widehat{\mu}=0.75$	using Moore et al. (2022)
	$\widehat{\lambda}_p^{2,1}=0.12$, $\widehat{\lambda}_p^{3,1}=0.06$, $\widehat{\lambda}_p^{3,2}=0.10$	

Table 2: Calibration of climate disasters and the Markov chain $\mathbf{X} = (X^p, X^c, X^t)$.

the subscript denotes climate disasters with N_c denoting the point process with loss l_c. The disaster intensity of climate-related disasters $\lambda_c(T)$ increases in temperature (Hambel et al., 2024). We let the intensity of climate-related disasters rise linearly in temperature, so $\lambda_c(T) = \widehat{\lambda}_c T$ with $\widehat{\lambda}_c = 0.096$ and $\lambda_c(T_0) = 0.122$. The expected loss is $\mathbb{E}[\ell_c] = 1.5\%$ (cf. Karydas and Xepapadeas, 2022; Hambel et al., 2024), compared to 25% for economic disasters. Fitting a power distribution, we obtain $\alpha_c = 65.7$. Climate-related disasters thus occur about twice as often as economic disasters but are less severe.

Irreversible Climate Tipping In line with Cai and Lontzek (2019), we now assume that the Earth's climate system is also exposed to tipping risk modeled by the Markov chain X^c. These climate tipping points irreversibly affect the future evolution of the climate system by increasing the TCRE, $\vartheta(X^c)$, and also affect output damages from climate change.[30] We assume that the TCRE can increase from 1.8 to 2.1 and to 2.4 °C/TtC. The probability of transitioning from a TCRE of 1.8 to 2.1 or 2.4 °C/TtC is 0.012 and from a TCRE of 2.1 to 2.4 °C/TtCt is 0.2. The tip from a TCRE of 1.8 to 2.1°C/TtC has an expected duration of 309 years (if temperature remains fixed at $T_0 = 1.27$°C) while the expected tip from a TCRE of 2.1 to 2.4°C/TtC has an expected duration of 50 years. We thus have imminent and slow tips of the climate system. We also assume that TFP damages react to irreversible climate tipping as in Cai and Lontzek (2019). We assume a damage function of the form $\Lambda(T, X^c) = \frac{1-d(X^c)}{1+\theta T^2}$, where the function d models permanent climate damages due to irreversible climate tipping. Following the median damage scenario of Cai and Lontzek (2019), we assume $d(X^c=0)=0$, $d(X^c=1)=0.025$, $d(X^c=2)=0.05$.

[30] An example is the melting of permafrost soils in the Siberian tundra, which is the largest methane reservoir in the Earth. Such a tipping event is irreversible because, for example, the methane cannot be restored once it has been released. Other examples are melting of the Greenland or Antarctic Ice Sheet or dieback of the Amazon rain forest (cf. Cai et al., 2016).

Negative Emissions and Technological Tipping The cost of the negative emission technology once it has become available is proportional to the capital stock, $b_d(S,\mathbf{X},D,K) = \widetilde{b}_d(S,\mathbf{X},D)K$ with

$$\widetilde{b}_d(S,\mathbf{X},D) = \mathbb{1}_{\{D>0\}}\big[a_1(S)D + a_2(S)\exp\big(a_3(S)D\big)\big],$$

where a_j are truncated power functions of the form $a_j(S) = b_j \max(\zeta,S)^{c_j}$, $j \in \{1,2,3\}$. This mimics the exponential marginal cost structure of Rebonato et al. (2023) with some differences. First, the term $a_1(S)D$ ensures that even the first ton of carbon to be removed and stored has non-zero marginal costs. Second, carbon removal becomes cheaper as the green transition progresses via $a_j(S) = b_j \max(\zeta,S)^{c_j}$.[31] Third, carbon removal costs are stochastic as S is stochastic. Fourth, this technology operates at strictly positive but finite marginal costs $\frac{\partial \widehat{b}_d(S,X^t=2,D)}{\partial D} = a_1(S) + a_2(S)a_3(S)\exp(a_3(S)D) > 0$. We have calibrated this cost function to the marginal cost curves in Figure 5 of Rebonato et al. (2023) for 2050 and 2100.[32] The calibration details are given in Appendix C.2 and the fit to the data is shown in Figure C.2. We assume that the negative emission technology becomes competitive somewhere in the period up to the year 2050 with a probability of 50% corresponding to a jump intensity of $\widehat{\lambda}_t^{1,2} = 0.0224$.[33] The two technology states (off or on) are captured by the Markov chain X^t. Costs are shared according to the size of the two sectors, $\varsigma_1 = 1-S$ and $\varsigma_2 = S$, so $-\varsigma_n b_d(S,\mathbf{X},D,K)$ is deducted from the right-hand sides of (2.4). We replace $\vartheta\nu(F_1+F_2)$ on the right-hand side of (2.5) by $\vartheta\nu[(F_1+F_2)-D]$. Finally, in contrast to Barnett et al. (2024) and Jaakkola and van der Ploeg (2019) who investigate the effects of investments on the probability of technological breakthrough, we assume a constant probability of a breakthrough. Demand for CDR must be increased (e.g. via carbon pricing) for innovation to occur and scaling up to be successful (Geden et al., 2024), which also suggests an endogenous arrival intensity. This part of the calibration and the functional forms are tentative, since uncertainty about the arrival intensity, the scale to which things can be scaled up, and the cost are still substantial.

Policy Transition Risks First, we allow for three policy states in the Markov chain X^p: BAU ($X^p = 1$), PIGOU ($X^p = 2$), and CAP ($X^p = 3$) corresponding to no, modest and ambitious carbon pricing, respectively, where the PIGOU policy state internalizes all global warming externalities including the ones operating via the temperature-dependent risks of climate disasters and climate tipping, but

[31] We assume that carbon removal costs no longer fall once the share of green capital reaches 90%, so set $\zeta = 0.1$. The truncation parameter ensures that costs for carbon removal does not fall to zero when the share of green capital approaches 100%. Alternative parametrizations with different truncation parameters or alternative functional forms do not significantly affect the qualitative nature of our results.

[32] These marginal cost curves build upon cost estimates for negative emission technologies of Fuss et al. (2018) and the comprehensive review in the of the Sixth Assessment Report of the IPCC (2022), which has shown the important role for negative emissions technologies in limiting global warming to 2°C.

[33] Alternative calibrations for when the jump intensity depends on the political state or the share of brown capital do not significantly affect our results. Moreover, our main asset pricing implications are hardly affected if we include the possibility of a competitive negative emissions technology.

Scenario		Carbon tax [$/tCO$_2$]				Carbon premium [%]			
	λ_x	2025	2050	2075	2100	2025	2050	2075	2100
PIGOU	–	45	77	127	199	–0.1	0	0.2	0.6
+ Climate Disasters		91	134	194	282	0.0	0.1	0.3	0.5
+ Climate Tipping		121	167	234	343	–0.1	0.1	0.3	0.3
+ Tech. Tipping		120	166	228	309	–0.1	0.1	0.3	0.4
BAU → CAP	4%	11 (73)	99 (153)	122 (143)	190 (202)	–0.2	0.3	1.6	1.1
+ Climate Disasters		18 (108)	127 (192)	182 (210)	277 (293)	–0.1	0.3	1.0	0.4
+ Climate Tipping		22 (134)	145 (220)	212 (245)	326 (344)	0.0	0.3	0.8	0.2
+ Tech. Tipping		22 (134)	141 (214)	206 (239)	300 (318)	0.0	0.3	0.6	0.2
BAU ↔ PIGOU ↔ CAP	endog.	9 (45)	43 (115)	102 (161)	181 (226)	–0.1	–0.2	0.2	0.8
+ Climate Disasters		16 (84)	58 (153)	135 (215)	236 (299)	0.1	0.1	0.3	0.5
+ Climate Tipping		19 (101)	70 (184)	175 (271)	308 (387)	0.1	0.1	0.3	0.4
+ Tech. Tipping		19 (101)	68 (184)	165 (265)	274 (368)	0.1	0.1	0.3	0.4

Table 3: The SCC and the Carbon Premium in Various Scenarios. Average carbon taxes and carbon premiums are reported for the years 2025, 2050, 2075, and 2100. The numbers in brackets refer to the average optimal carbon tax *conditional* on being implemented.

does not impose a temperature cap.[34] Second, we have a Markov chain with endogenous switching probabilities to allow the switch to active climate policy to rise to say 75% if temperature rises beyond 1.5°C. Third, due to brown and green lobbies, we let the probability of a switch to a more active climate policy fall in the share of brown capital S and the switch back to BAU fall in the share of green capital. We base our specification and calibration on Barnett (2024) and Moore et al. (2022).[35]

The calibration details of these extensions are given in Table 2 with details presented in Appendix C.2.[36]

5.2 Effects of the Model Extensions

Table 3 summarizes the effects of the various model extensions on our core results.

Climate Disasters and Climate Tipping Since our core results ignore these two types of physical climate risk and allows for output damages only, our extended model leads to much higher carbon prices.

[34]The social cost of carbon (SCC) coming from our dynamic optimization problem now internalize the adverse effects of temperature on total factor productivities in the two sectors and on the risks of recurring climate disasters and irreversible climate tipping. To decentralize the social optimum requires again a specific carbon tax on brown firms that is set to this extended SCC and the revenues to be rebated as lump sums to brown firms. In addition, catastrophic insurance is required where the insurance premiums will rise with temperature.

[35]The calibration roughly matches the likelihood and resulting temperature increase of the various transition scenarios in Moore et al. (2022): about 48% of their simulations are in their modal scenario, which leads to an average temperature increase of 2.3°C. About 28% of their simulations lead to aggressive climate action limiting global warming to up to 1.8°C. There is less ambitious or less effective climate action in the remaining scenarios (about 24%) with average temperature increases of around 3°C, of which less than two percent of the simulations lead to significantly higher temperatures.

[36]Some of our functional forms may seem ad hoc or hard-coded with some of them obtained from curve fitting. We overcome some of this via robustness checks.

In the Pigouvian scenario with no temperature cap and no transition risk, climate disasters double the optimal carbon tax from \$45/tCO_2 in 2025 to \$91/tCO_2. If we switch on irreversible climate tipping, the SCC is boosted to \$121/tCO_2. Although the effect of climate disasters and tipping points is very strong in this pure PIGOU scenario, the effect is significantly smaller in our core results with political transition risks. The optimal average CO_2 tax rises from \$73/tCO_2 to \$108/tCO_2 if climate disasters are taken into account and \$134/tCO_2 if tipping points are also taken into account. These effects are thus smaller than in the PIGOU scenario, since the CAP policy state also takes into account the risk of a partial asset stranding, i.e., abolishing fossil fuels, if the temperature rises above the cap of 2°C.

Overall, the effect of climate disasters and climate tipping on the carbon premium is very modest as we assume that disasters hit both assets in a symmetric manner. Hence, physical climate risks alone cannot explain a sizable carbon premium. This is not only true on average but also in the quantiles of the simulation.[37] However, these additional climate externalities are priced in on financial markets and can lead to a temperature risk premium that affects all risky assets in the economy (e.g., Bansal et al., 2017; Donadelli et al., 2017). Climate disasters destroy capital and lead, as Barro-style disasters, to a drop in share prices when they occur. Moreover, these additional risks lead to additional precautionary savings that curb the risk-free rate in response to higher temperatures (cf. Karydas and Xepapadeas, 2022; Hambel et al., 2024).[38] Finally, once the climate system tips, climate damages will become more pronounced, reducing output and leading to a drop in share prices for both the green and brown asset.

Technological Breakthroughs and Negative Emissions Table 3 indicates that generally breakthroughs leading to negative emission technologies slightly reduce the optimal carbon tax. This can be explained by the fact that policy makers anticipate that negative emission technologies will be available at a later point in time. As a result, policy makers tend to wait a little with stringent climate policy and remove past emissions from the atmosphere later in the transition. This effect is not pronounced, but negative emission technologies in some paths help to push the temperature back below the cap if it has already been exceeded before. Hence, an already implemented ban on emissions can be reversed and the brown sector can be powered by fossil fuels again.

Policy Transition Risks Adding the PIGOU policy state to the political Markov chain and considering reversible political transitions leads to carbon prices that are slightly lower than in the core model. This is because the CAP policy state plays a much smaller role as only about 30% of the paths end up in this policy state by the end of this century. Hence, carbon prices are on average smaller than in our

[37] Results for the quantiles are available upon request.

[38] These effects can be seen from the decomposition of the risk-free rate (B.7) and the equity premium (B.13).

core results. In addition, the CAP policy state is at the root of a substantial carbon premium, which is why there are now significantly more paths with low to moderate carbon premiums.

5.3 Simulation Results with all Extensions

Energy Transition Figure 3 confirms that our core results are robust to these extensions. Since we have calibrated both our core and extended model of policy tipping to roughly match the different climate scenarios in Moore et al. (2022), the transition of the real economy is on average similar to our core simulation results (panel a) of Figure 3). However, there are some subtle differences. Due to climate disasters and tipping points, economic growth is more negatively affected and leads to significantly reduced output in the long run (panel e)). To compensate for this, policy makers are implementing higher carbon taxes in the PIGOU and CAP policy states (panel d)). In addition, a competitive negative emission technology eventually becomes available in many of the simulated paths, so that net emissions can become negative and the temperature can fall. This will enable the brown sector to operate with fossil fuels again after a short-term overlap of the 2°C cap (panel b)).

To illustrate the implications of several types of climate news, we show an illustrative sample path (——) where society switches several times between the three policy states with the first transition from the BAU policy state to the CAP state in 2029 (Panel f)). Emissions fall (increase) on impact of a switch to the CAP (BAU) policy state. There are also two irreversible climate tipping events in 2055 and 2070 (Panel g)); the latter leads to an immediate increase in the carbon tax as the economy is then in the CAP policy state. Negative emission technology becomes available in 2067 (Panel h)), and society immediately starts implementing it. Global temperatures begin to fall again and then stabilize.

Asset Pricing Figure 4 discusses the asset pricing implications. It turns out that the general intuition from the core model carries over, although the carbon premium is on average smaller than in the core model (panel e). This is because society spends less time in the CAP policy state, which is quantitatively the main reason for the carbon premium in our framework. As in the core model, the carbon premium in our illustrative sample path goes dramatically up around the year 2040 when temperature is close to 2°C and society is in the CAP policy state. After a transition to the PIGOU policy state in 2044, the carbon premium vanishes as the risk of phasing out fossil fuels has been reduced drastically.

When the transition to a low-carbon economy is complete, the risk premium of the brown asset vanishes. Overall, the risk premiums in our model tend to increase rather than stabilize even when the energy transition is complete and the brown sector has been shut down (panels c) and d)). Then, the risk premium of the brown asset and the carbon premium have dissipated. The increase in the risk

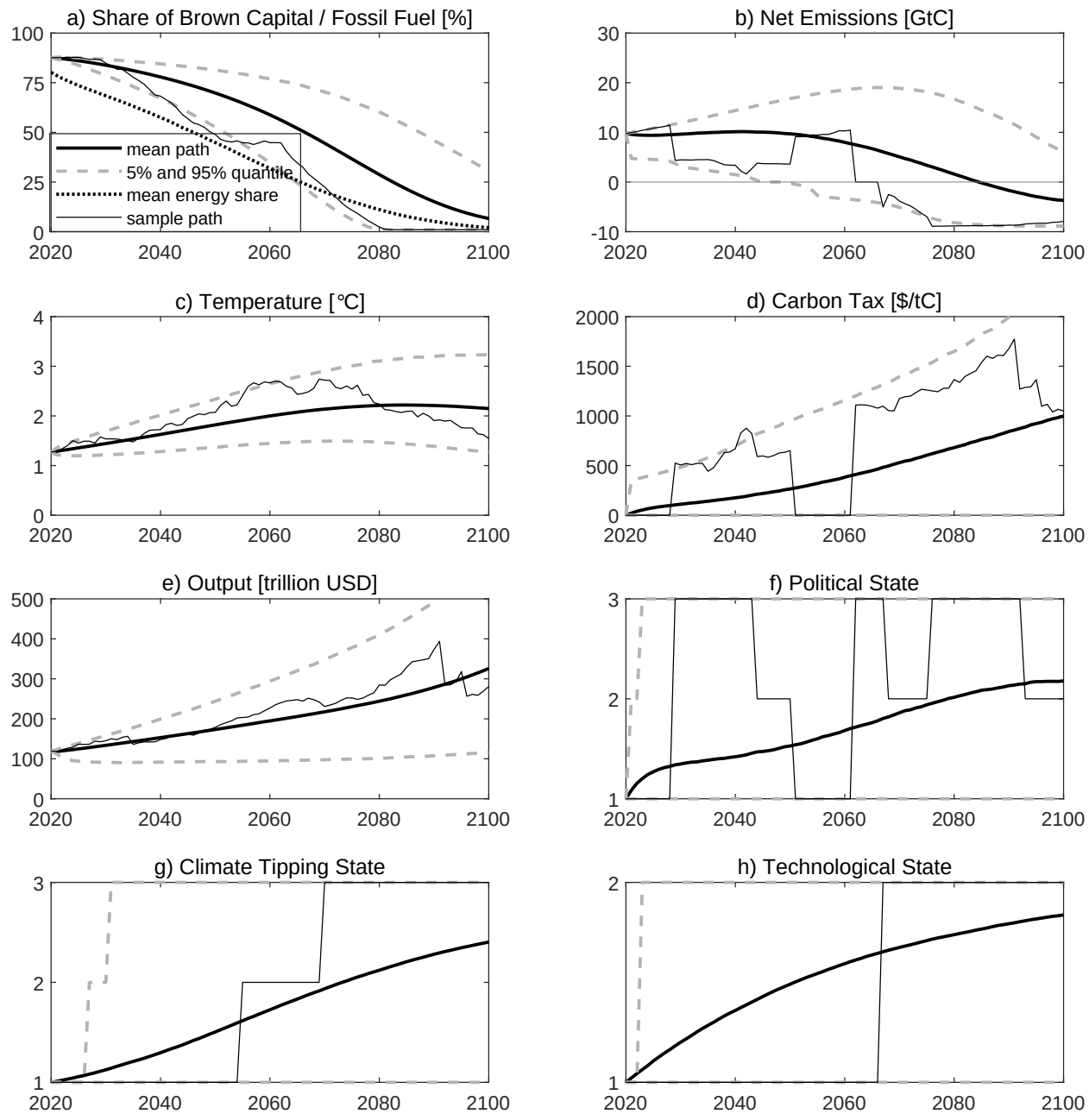

Figure 3: Transition of the Real Economy (starting from BAU with transition risks to PIGOU or CAP policy state). Mean paths are depicted by solid lines (——) and dashed lines (- - -) show 5% and 95% quantiles. The dotted line (·····) in panel a) shows the share of fossil fuel in the global energy mix. The thin black lines (——) shows one illustrative sample path, where society switches several times between the three policy states with the first transition from the BAU policy state to the CAP state in 2029. There are also two irreversible climate tipping events in 2055 and 2070. Negative emissions technology becomes available in 2067.

premiums over time reflects a *temperature risk premium*, i.e. a higher risk of climate-related disasters and climate tipping events (cf. Bansal et al., 2019).

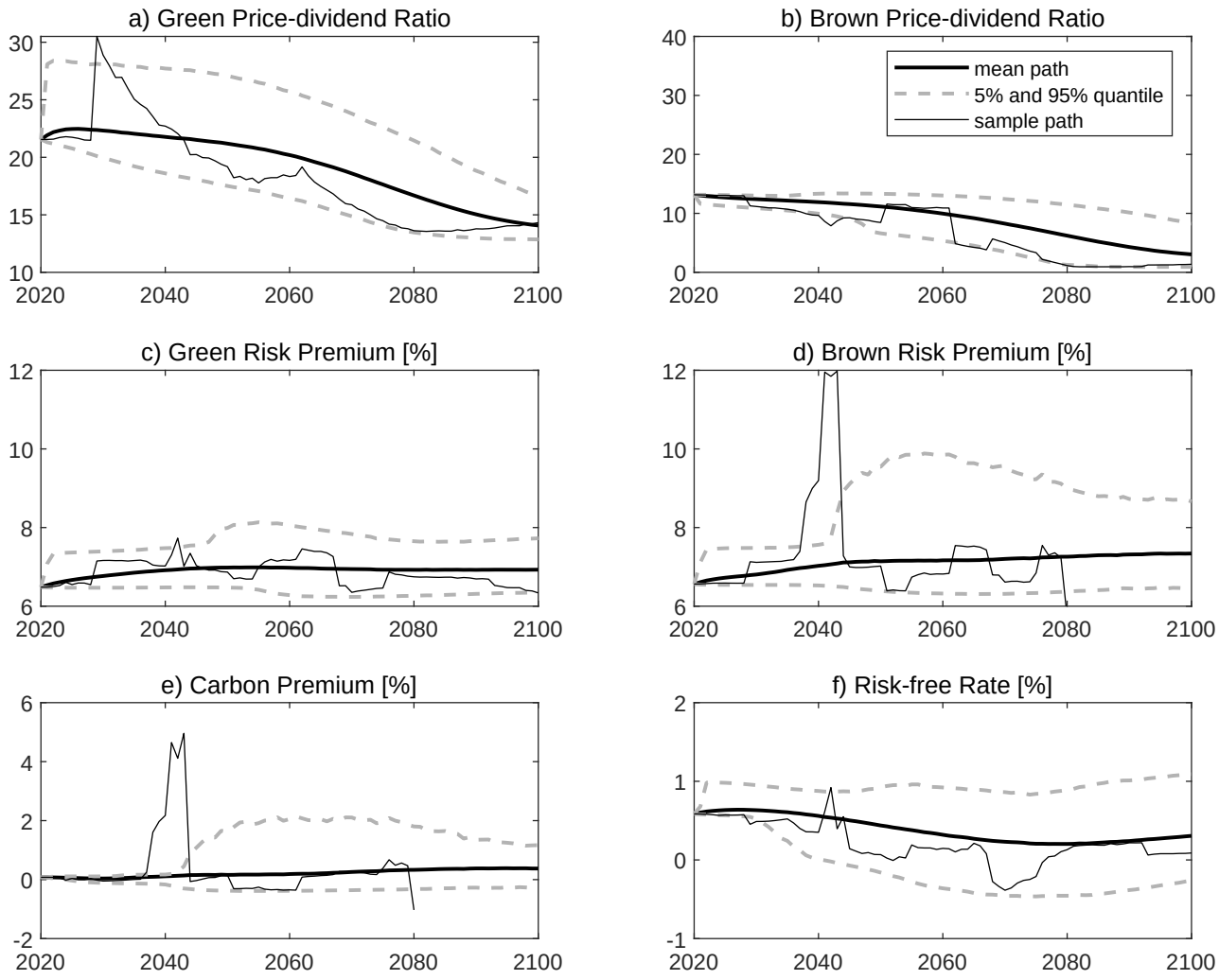

Figure 4: Asset Pricing Results (starting from BAU with transition risks to PIGOU or CAP policy state). Average values are depicted by solid lines (——) and 5% and 95% quantiles by dashed lines (- - -). The thin black lines (——) shows one illustrative sample path, where society switches several times between the three policy states with the first transition from the BAU policy state to the CAP policy state in 2029. There are also two irreversible climate tipping events in 2055 and 2070. Negative emission technology becomes available in 2067.

News about Policy and Climate Tipping Table 4 indicates that the price impact of climate tipping risk and technological breakthroughs on share prices is relatively small compared to policy shocks. For instance, the climate tipping shocks in years 2055 and 2070 imply a drop in share prices between 3 and 5% each. After climate tipping, policy makers implement more stringent taxes provided they are in a state of active climate policy. When the first climate tipping event takes place, the economy is (again) in the BAU and the carbon price remains at zero until society switches to the PIGOU or CAP policy state.

Year	Tipping Type	T	S	$\frac{\Delta P_1}{P_1}$	$\frac{\Delta P_2}{P_2}$	$\frac{\Delta PDR_1}{PDR_1}$	$\frac{\Delta PDR_2}{PDR_2}$	$\Delta\tau$
2029	BAU → CAP	1.5	0.87	13.9%	–26.7%	36.7%	–12.6%	140
2044	CAP → PIGOU	1.8	0.62	–1.2%	61.5%	–1.2%	5.8%	–88
2051	PIGOU → BAU	2.1	0.49	–10.2%	32.5%	–5.0%	44.1%	–178
2055	1st Climate Tipping	2.2	0.46	–3.9%	–3.2%	–3.9%	–3.2%	0
2062	BAU → CAP	2.7	0.45	7.7%	–53.3%	3.6%	–55.1%	295
2067	NET Becomes Available	2.5	0.33	–1.8%	3.8%	–1.1%	1.0%	–10
2068	CAP → PIGOU	2.5	0.29	–1.0%	59.2%	–0.8%	56.4%	–42
2070	2nd Climate Tipping	2.7	0.25	–4.0%	–5.2%	1.1%	–0.2%	41
2076	PIGOU → CAP	2.5	0.11	–0.6%	–29.3%	–0.2%	–29.1%	6
2094	CAP → PIGOU	1.9	0.00	0.0%	0.0%	0.0%	0.0%	0

Table 4: Price Impact of Policy and Climate News. The table reports the relative impact of technological tipping, climate policy transitions, and climate tipping on green and brown share prices and price-dividend ratios with the prevailing state variables temperature T and share of brown capital S along the illustrative path. It also reports the changes in the carbon price measured in \$/tCO_2.

Similarly, the effect of the technological breakthrough in 1967 is relatively small. We find that negative emissions technology coming on stream has a small positive effect on brown share prices and a small negative effect on the price of the green asset. Afterwards, the probability increases that the brown sector will once again use fossil fuels and thus produce more cheaply. This increases the demand for brown assets and the brown share price. This results in a fall in demand for the green asset and a moderate drop in the green share price. Moreover, after the technological breakthrough, policy makers slightly reduce the carbon tax as carbon dioxide can now be removed from the atmosphere.

Building on the intuition gained from the core model, climate policy shocks cause a much stronger price reaction, especially if it happens early in the energy transition. For instance, a tip from the BAU to the CAP policy state causes major market disruptions leading to a 27% fall in the price and a 13% fall in the price-dividend ratio of the brown asset. This price drop of the brown assets is accompanied by a strong price increase of the green asset of about 18% and a sharp increase in the green price-dividend ratio of 42% (cf. panels a) and b) of Figure 4). The policy shocks in 2044 and 2051 to the PIGOU and later back to the BAU policy state lead to sharp rises in the price of the brown asset, as the risk of phasing out is reduced. This also reduces the demand for the green asset and its price falls accordingly. The relative price impact of policy shocks becomes less pronounced over time due to the ongoing transition and the shrinking share of brown capital. When the transition is complete, a policy shock no longer has any noticeable influence on prices as can be seen from the last row in Table 4. Finally, the table confirms that policy makers implement higher taxes in the CAP than in the PIGOU policy state.

6 Concluding Remarks

Our aim has been to better understand how policy transition risks affect carbon pricing, asset returns, carbon premiums, and the risk of stranded assets. For this purpose, we have formulated and calibrated a two-sector DSGE model of the economy and the climate with a wide range of uncertainties. In our core analysis we have distinguished two different policy states: no carbon pricing (business as usual) and carbon pricing to internalize global warming damages and enforce a temperature gap.

If policy makers do not price carbon, the green transition takes place at a slow pace and global mean temperatures rise substantially. Financial markets price in the adverse effects of global warming on output. This gives rise to a tiny carbon risk premium, since transition risks are absent. The risk-free rate falls due to precautionary saving. However, if policy tipping is allowed for, carbon taxes eventually are phased in and emissions and temperature are lower than without transition risks. But temperatures are still a lot higher than if policy makers did not face such transition risk. Financial markets take account of uncertainty including the risk of policy tipping. When the temperature cap kicks in, markets respond with precautionary savings and rapid falls in the risk-free interest rate. As the green transition continues and the brown capital stock falls, precautionary savings will fall again.

We consistently find a positive carbon premium even when policy makers implement carbon taxes. This carbon premium reflects transition risks, especially policy risk, and is particularly large if temperatures are close to or exceed the temperature cap. This premium encourages firms to accelerate the green transition. If policy makers ignore political transition risk and implement first-best carbon taxes, there is a slightly negative carbon premium. With transition risk, policy makers may even set higher carbon taxes than when policy makers do not face transition risk to make up for time lost by previous policy makers who did not price carbon and the economy has become close to the temperature cap. The green asset's price-dividend ratio is initially relatively high reflecting the scarcity of this asset. The brown asset becomes worthless when the transition has come to an end and the brown capital stock has run down completely.

If we allow for the temperature-dependent risks of recurring climate disasters and climate tipping, our main qualitative insights regarding carbon premiums and policy risk are unaffected albeit carbon prices will be higher and the green transition faster. If we also allow for the probability of a competitive emissions technology coming on stream, the qualitative insights are unaffected too but now emissions can be eventually negative and temperature fall. Finally, when we allow for a richer menu of policy states with endogenous transition probabilities our core results remain robust.

We have provided a mechanism for the carbon premium and stranded assets and have shown how these and carbon prices are qualitatively affected by policy and technological tipping (transition risks) and by climate tipping and the risk of climate-related disasters such as extreme weather events (physical risks).

Our insights suggests that empirical work on carbon premiums might be more conclusive if account is taken of the dependence of the carbon premium on temperature and on how green the economy already is. Event studies can be used to empirically test our hypotheses regarding jumps in green and brown asset prices at the time of policy, technological, and climate tipping. In further research we could allow for the risk of stranded assets, credit market constraints, monetary policy, sudden stops, systemic financial risk, political economy, commitment issues, and policies within national jurisdictions.

References

Acemoglu, D., P. Aghion, L. Bursztyn, and D. Hemous, 2012, The environment and directed technical change, *American Economic Review* 102, 131–166.

Allen, M. R., D. J. Frame, C. Huntingford, C. D. Jones, J. A. Lowe, M. Meinshausen, and N. Meinshausen, 2009, Warming caused by cumulative carbon emissions towards the trillionth tonne, *Nature* 458, 1163–1166.

Ardia, D., K. Bluteau, K. Boudt, and K. Inghelbrecht, 2023, Climate change concerns and the performance of green vs. brown stocks, *Management Science* 69, 7151–7882.

Aswani, J., A. Raghunandan, and S. Rajgopal, 2024, Are carbon emissions associated with stock returns?, *Review of Finance,* 28, 75–106.

Bansal, R., D. Kiku, and M. Ochoa, 2017, Price of long-run temperature shifts in capital markets, *Working Paper,* Duke University.

Bansal, R., D. Kiku, and M. Ochoa, 2019, Climate change and growth risks, *Working Paper,* Duke University.

Bansal, R., and A. Yaron, 2004, Risks for the long run: A potential resolution of asset pricing puzzles, *Journal of Finance* 59, 1481–1509.

Barnett, M., 2024, A run on fossil fuel? Climate change and transition risk, *Working Paper,* Arizona State University.

Barnett, M., W. Brock, L.P. Hansen, R. Hu, and J. Huang, 2024, A deep learning analysis of climate change, innovation, and uncertainty, *Arizona State University* Working Paper.

Barro, R. J., 2006, Rare disasters and asset markets in the twentieth century, *Quarterly Journal of Economics* 121, 823–866.

Barro, R. J., 2009, Rare disasters, asset prices, and welfare costs, *American Economic Review* 99, 243–264.

Barro, R. J., and T. Jin, 2011, On the size distribution of macroeconomic disasters, *Econometrica* 79, 1567–1589.

Bauer, M. D., D. Huber, G. D. Rudebusch, and O. Wilms, 2022, Where is the carbon premium? global performance of green and brown stocks, *Journal of Climate Finance* 1, 100006.

Besley, T., and T. Persson, 2019, The dynamics of environmental politics and values, *Journal of the European Economic Association* 17, 993–1024.

Besley, T., and T. Persson, 2023, The political economics of green transitions, *Quarterly Journal of Economics* 138, 1863–1906.

Bilal, A., and D. R. Känzig, 2024, The macroeconomic impact of climate change: global vs. local temperature, *NBER Working Paper* 32450.

Bolton, P., and M. Kacperczyk, 2021, Do investors care about carbon risk?, *Journal of Financial Economics* 142, 517–549.

Bolton, P., and M. Kacperczyk, 2023, Global pricing of carbon-transition risk, *Journal of Finance,* 87, 3677–3754.

Bolton, P., and M. Kacperczyk, 2024, Are carbon emissions associated with stock returns? Comment, *Review of Finance* 28, 107–109.

Bouman, S., 2023, The asset pricing and risk management implications of climate transition risks, *Master Thesis* (Tilburg University).

Bovenberg, A. L., and S. A. Smulders, 1996, Transitional impacts of environmental policy in an endogenous growth model, *International Economic Review* 37, 861–893.

Cai, Y., T. M. Lenton, and T. S. Lontzek, 2016, Risk of multiple interacting tipping points should encourage rapid CO_2 emission reduction, *Nature Climate Change* 6, 520–525.

Cai, Y., and T. S. Lontzek, 2019, The social cost of carbon with economic and climate risks, *Journal of Political Economy* 127, 2684–2734.

Campiglio, E., and F. van der Ploeg, 2022, Macrofinancial risks of the transition to a low-carbon economy, *Review of Environmental Economics and Policy* 16, 173–195.

Campos-Martins, S., and D. F. Hendry, 2023, Common volatility shocks driven by the global carbon transition, *Journal of Econometrics* 105472.

Carney, M., 2015, Breaking the tragedy of the horizon – climate change and financial stability, *Speech,* Bank of England.

Casey, G., 2023, Energy efficiency and directed technical change: Implications for climate change mitigation, *Review of Economic Studies* 90, 0034–6527.

Cochrane, J. H., F. A. Longstaff, and P. Santa-Clara, 2007, Two trees, *Review of Financial Studies* 21, 347–385.

Delis, M. D., K. de Greiff, M. Iosifidi, and S. Ongena, 2019, Being stranded with fossil fuel reserves? climate policy risk and the pricing of bank loans, *Working Paper,* Swiss Finance Institute.

Dietz, S., and F. Venmans, 2019, Cumulative carbon emissions and economic policy: In search of general principles, *Journal of Environmental Economics and Management* 96, 108–129.

Donadelli, M., M. Jueppner, M. Riedel, and C. Schlag, 2017, Temperature shocks and welfare costs, *Journal of Economic Dynamics and Control* 82, 331–355.

Duffie, D., and L. G. Epstein, 1992a, Asset pricing with stochastic differential utility, *Review of Financial Studies* 5, 411–36.

Duffie, D., and L. G. Epstein, 1992b, Stochastic differential utility, *Econometrica* 60, 353–394.

Duineveld, S., C. Hambel, and K. Lessmann, 2025, Green investors and the return on capital in general equilibrium, *Economics Letters* 247, 112149.

Engle, R. F., S. Giglio, B. Kelly, H. Lee, and J. Stroebel, 2020, Hedging climate change news, *Review of Financial Studies* 33, 1184–1216.

Epstein, L. G., and S. E. Zin, 1989, Substitution, risk aversion, and the temporal behavior of consumption and asset returns: A theoretical framework, *Econometrica* 57, 937–969.

Faccini, R., R. Matin, and G. Skiadopoulos, 2023, Dissecting climate risks: Are they reflected in stock prices?, *Journal of Banking & Finance* 155, 106948.

Fuss, S., W. F. Lamb, M. W. Callaghan, J. Hilaire, F. Creutzig, T. Amann, T. Beringer, W. de Oliveira Garcia, J. Hartmann, T. Khanna, G. Luderer, G. F. Nemet, J. Rogelj, P. Smith, J. L. Vicente, J. Wilcox, M. del Mar Zamora Dominguez, and J. C. Minx, 2018, Negative emissions—part 2: Costs, potentials and side effects, *Environmental Research Letters* 13, 063002.

Geden, O., 2024, The state of carbon dioxide removal, *A global, independent scientific assessment of Carbon Dioxide Removal* 2nd edition, 993–1024.

Golosov, M., J. Hassler, P. Krusell, and A. Tsyvinsky, 2014, Optimal taxes on fossil fuel in general equilibrium, *Econometrica* 82, 41–88.

Gregory, R. P., 2024, Risk premiums from temperature trends, *International Review of Economics & Finance* 91, 505–525.

Hambel, C., H. Kraft, and E. S. Schwartz, 2021, Optimal carbon abatement in a stochastic equilibrium model with climate change, *European Economic Review* 132, 103642.

Hambel, C., H. Kraft, and F. van der Ploeg, 2024, Asset diversification versus climate action, *International Economic Review,* 65, 1323–1355.

Hambel, C., and F. van der Sanden, 2024, Reevaluating the carbon premium: Evidence of green outperformance, *Working Paper,* Tilburg University.

Hong, H., F. W. Li, and J. Xu, 2019, Climate risks and market efficiency, *Journal of Econometrics* 208, 265–281.

Hsu, P.-H., K. Li, and C.-Y. Tsou, 2023, The pollution premium, *Journal of Finance* 78, 1343–1392.

IPCC, 2022, *Climate Change 2022 – Impacts, Adaptation and Vulnerability* (Cambridge University Press).

Ivanov, I. T., M. S. Kruttli, and S. W. Watugala, 2024, Banking on carbon: Corporate lending and cap-and-trade policy, *Review of Financial Studies,* 37, 1640–1684.

Jaakkola, N., and F. van der Ploeg, 2019, Non-cooperative and cooperative climate policies with anticipated breakthrough technology, *Journal of Environmental Economics and Management* 97, 42–66.

Karydas, C., and A. Xepapadeas, 2022, Climate change financial risks: Implications for asset pricing and interest rates, *Journal of Financial Stability* 63, 101061.

Kelly, D. L., and Z. Tan, 2015, Learning and climate feedbacks: optimal climate insurance and fat tails, *Journal of Environmental Economics and Management* 72, 98–122.

Lafond, F., A.G. Bailey, J.D. Bakker, D. Rebois, R. Zadourian, P. McSharry, and D. Farmer, 2018, How wel do experience curves predict technological progress? a method for making distributional forecasts, *Technological Forecasting and Social Change* 128, 104–117.

Lemoine, D., and C. P. Traeger, 2014, Watch your step: optimal policy in a tipping climate, *American Economic Journal: Economic Policy* 6, 137–166.

Longstaff, F. A., and M. Piazzesi, 2004, Corporate earnings and the equity premium, *Journal of Financial Economics* 74, 401–421.

Matthews, H. D., N. P. Gillett, P. A. Stott, and K. Zickfeld, 2009, The proportionality of global warming to cumulative carbon emissions, *Nature* 459, 829–832.

McGlade, C., and P. Ekins, 2015, The geographical distribution of fossil fuels unused when limiting global warming to 2 $^{\circ}$C, *Nature* 517, 187–190.

Moore, F. C., K. Lacasse, K. J. Mach, Y. A. Shin, L. J. Gross, and B. Beckage, 2022, Determinants of emissions pathways in the coupled climate–social system, *Nature* 603, 103–111.

Munk, C., and C. Sørensen, 2010, Dynamic asset allocation with stochastic income and interest rates, *Journal of Financial Economics* 96, 433–462.

Nordhaus, W. D., 2017, Revisiting the social cost of carbon, *Proceedings of the National Academy of Sciences* 114, 1518–1523.

Olijslagers, S., F. van der Ploeg, and S. van Wijnbergen, 2023, On current and future carbon prices in a risky world, *Journal of Economic Dynamics and Control* 146, 104569.

Pastor, L., R. F. Stambaugh, and L. A. Taylor, 2021, Sustainable investing in equilibrium, *Journal of Financial Economics* 142, 550–571.

Pedersen, L. H., S. Fitzgibbons, and L. Pomorski, 2021, Responsible investing: The ESG-efficient frontier, *Journal of Financial Economics* 142, 572–597.

Pindyck, R. S., and N. Wang, 2013, The economic and policy consequences of catastrophes, *American Economic Journal: Economic Policy* 5, 306–339.

Rebonato, R., D. Kainth, L. Melin, and D. O'Kane, 2023, Optimal climate policy with negative emissions, *Working Paper,* EDHEC-Risk Climate Impact Institute.

Rennert, K., F. Errickson, B. C. Prest, L. Rennels, R.G. Newell, W. Pizer, C. Kingdon, J. Wingenroth, R. Cooke, B. Parthum, Smith D, K. Cromar, D. Diaz, F.C. Moore, U.K. Müller, R.J. Plevin, A.E. Raftery, H. Ševčíková, H. Sheets, J.H. Stock, T. Tan, M. Watson, T.E. Wong, and D. Anthoff, 2022, Comprehensive evidence implies a higher social cost of CO_2, *Nature* 610, 687–692.

Sauzet, M., and O. D. Zerbib, 2024, When green investors are green consumers, *Working Paper* .

Tol, R. S. J., 2023, Social cost of carbon estimates have increased over time, *Nature Climate Change* 13, 532–536.

van den Bremer, T. S., C. Hambel, and F. van der Ploeg, 2023, Three reasons to price carbon under uncertainty: Accuracy of simple rules, *Working Paper,* Tinbergen Institute.

van den Bremer, T. S., and F. van der Ploeg, 2021, The risk-adjusted carbon price, *American Economic Review,* 111, 2782–2810.

van der Ploeg, F., and A. de Zeeuw, 2018, Climate tipping and economic growth: precautionary capital and the price of carbon, *Journal of the European Economic Association* 16, 1577–1617.

Wachter, J. A., 2013, Can time-varying risk of rare disasters explain aggregate stock market volatility?, *Journal of Finance* 68, 987–1035.

Zerbib, O. D., 2022, A sustainable capital asset pricing model (S-CAPM): Evidence from environmental integration and sin stock exclusion*, *Review of Finance* 26, 1345–1388.

Zhang, S., 2025, Carbon returns across the globe, *Journal of Finance* 80, 615–645.

SUPPLEMENTARY MATERIALS:

Online Appendix to

Policy Transition Risk, Carbon Premiums, and Asset Prices

Revised version: March 2025

Abstract

Here we present additional material such as proofs, a description of the numerical solution algorithm, calibration details, and further simulation results and robustness checks.

Table of Contents

A Solution Approach

In order to give a unified description of the solution procedure, Appendices A and B show the solution procedure for the extended model of section 5. In particular, the derivations include the three-dimensional Markov chain $\mathbf{X} = (X^p, X^t, X^c)$ and climate-related disasters.

A.1 Hamilton-Jacobi-Bellman Equation

Applying the Bellman principle in continuous time, the value function $J = J(t, K_1, K_2, T, \mathbf{X})$ solves a non-linear partial differential equation, which is typically refered to as Hamilton-Jacobi-Bellman equation (e.g., Duffie and Epstein 1992b). This equation is given by

$$\begin{aligned} 0 = \max_{D, F_n, G_n, I_n, R} \Bigg\{ & J_t + \delta\theta J \Big(\frac{\left(\sum_{n=1,2}[Y_n - I_n - b_g G_n - b_f F_n - \varsigma_n b_d(S, \mathbf{X}, D, K)]\right)^{1-1/\psi}}{[(1-\gamma)J]^{\frac{1-1/\psi}{1-\gamma}}} - 1 \Big) \\ & + J_T \vartheta(\mathbf{X}) \big(\nu_t [F_1 + F_2] - D \big) + \frac{1}{2} J_{TT} \sigma_T^2 + J_{K_1} \Big(I_1 - \frac{1}{2}\phi_1 \frac{I_1^2}{K_1} + R - \frac{1}{2}\kappa \frac{R^2}{K_1} - \delta_1^k K_1 \Big) \\ & + \frac{1}{2} J_{K_1 K_1} K_1^2 \sigma_1^2 + J_{K_2} \Big(I_2 - \frac{1}{2}\phi_2 \frac{I_2^2}{K_2} - R - \delta_2^k K_2 \Big) + \frac{1}{2} J_{K_2 K_2} K_2^2 \sigma_2^2 + J_{K_1 K_2} K_1 K_2 \sigma_1 \sigma_2 \rho_{12} \\ & + \sum_{i=c,e} \lambda_i(T, \mathbf{X}) \mathbb{E}\big[J(K_1 Z_i, K_2 Z_i, T, \mathbf{X}) - J \big] + \sum_{x \neq \mathbf{X}} \lambda_x(S, T, \mathbf{X}, x) \big[J(K_1, K_2, T, x) - J \big] \Bigg\}, \end{aligned} \tag{A.1}$$

subject to the constraints $D, F_n, G_n, I_n, R \geqslant 0$. Subscripts of J denote partial derivatives, e.g., $J_{K_1} = \frac{\partial J}{\partial K_1}$.

A.2 Optimal Carbon Tax and Negative Emission Technology

The first-order condition for optimal fossil fuel use is

$$f_C(C, J) \Big(\frac{\partial Y_n}{\partial F_n} - b_f \Big) = -J_T \vartheta(\mathbf{X}) \nu_t.$$

Setting the marginal product of fossil fuel equal its marginal cost b_f plus the external costs of emitting greenhouse gases into the atmosphere,

$$\frac{\partial Y_n}{\partial F_n} = b_f + \tau_f.$$

The optimal Pigouvian social cost for using one unit of fossil fuel is thus

$$\tau_f = -\frac{\vartheta(\mathbf{X}) \nu_t J_T C^{1/\psi}}{\delta [(1-\gamma)J]^{1-1/\theta}}.$$

Taking the different units between fossil fuel and carbon emissions into account, the SCC is

$$\tau = -\frac{\vartheta(\mathbf{X}) J_T C^{1/\psi}}{\delta[(1-\gamma)J]^{1-1/\theta}}. \tag{A.2}$$

Since $\varsigma_1 + \varsigma_2 = 1$, the first-order conditions for optimal carbon removal give

$$f_C(C,J)\frac{\partial b_d(S,\mathbf{X},D,K)}{\partial D} = -J_T \vartheta(\mathbf{X}).$$

A.3 Share of Brown Capital

To solve the Hamilton-Jacobi-Bellman equation (A.1), we first transform it by expressing the decision variables in relative terms and reducing the number of state variables by one. Let $g_n = G_n/K_n$, $f_n = F_n/K_n$, $i_n = I_n/K_n$, $r = R/K_1$ denote the relative control variables. Exploiting the homogeneity property of b_d, we use the notation $\widetilde{b}_d(S,\mathbf{X},D) = b_d(S,\mathbf{X},D,K)/K$. We express the value function in terms of total capital $K = K_1 + K_2$ and share of brown capital $S = K_2/(K_1+K_2)$ (instead of K_1 and K_2). Besides, we set $c = C/K$. Using the notation $S_1 = 1-S$, $S_2 = S$, the production functions can then be expressed as

$$Y_n = A_n S_n K \left(\kappa_{1,n} g_n^{\rho_n} + \kappa_{2,n} f_n^{\rho_n}\right)^{\frac{\eta_n}{\rho_n}} \Lambda_n(T).$$

The amounts of consumption goods produced by each sector are

$$C_n = S_n K\Big[A_n\left(\kappa_{1,n} g_n^{\rho_n} + \kappa_{2,n} f_n^{\rho_n}\right)^{\frac{\eta_n}{\rho_n}} \Lambda_n(T,\mathbf{X}) - i_n - b_g(S) g_n - b_f(S) f_n - \frac{\varsigma_n(S)}{S_n}\widetilde{b}_d(S,\mathbf{X},D)\Big].$$

Therefore,

$$\begin{aligned} c = {} & A_1(1-S)\left(\kappa_{1,1} g_1^{\rho_1} + \kappa_{2,1} f_1^{\rho_1}\right)^{\frac{\eta_1}{\rho_1}} \Lambda_1(T,\mathbf{X}) + A_2 S\left(\kappa_{1,2} g_2^{\rho_2} + \kappa_{2,2} f_2^{\rho_2}\right)^{\frac{\eta_2}{\rho_2}} \Lambda_2(T,\mathbf{X}) - i_1(1-S) - i_2 S \\ & - b_g(S)[g_1(1-S) + g_2 S] - b_f(S)[f_1(1-S) + f_2 S] - \widetilde{b}_d(S,\mathbf{X},D). \end{aligned}$$

The dynamics of the state variables can be written as

$$\begin{aligned} \mathrm{d}K_1 &= K_{1-}\Big[\Big(i_1 - \frac{1}{2}\varphi_1 i_1^2 + r - \frac{1}{2}\kappa r^2 - \delta_1^k\Big)\mathrm{d}t + \sigma_1 \mathrm{d}W_1 - \sum_{i=c,e} \ell_i \mathrm{d}N_i\Big], \\ \mathrm{d}K_2 &= K_{2-}\Big[\Big(i_2 - \frac{1}{2}\varphi_2 i_2^2 - r\frac{1-S}{S} - \delta_2^k\Big)\mathrm{d}t + \sigma_2\Big(\rho_{12}\mathrm{d}W_1 + \sqrt{1-\rho_{12}^2}\mathrm{d}W_2\Big) - \sum_{i=c,e} \ell_i \mathrm{d}N_i\Big], \\ \mathrm{d}T &= \widehat{\vartheta}(t,\mathbf{X})[f_1(1-S) + f_2 S]\mathrm{d}t - \vartheta(\mathbf{X}) D\,\mathrm{d}t + \sigma_T \mathrm{d}W_3 + \kappa_{T-}\mathrm{d}X^c, \end{aligned}$$

where $\widehat{\vartheta}(t,\mathbf{X}) = \vartheta(\mathbf{X})K_0 \mathrm{e}^{\int_0^t g_\nu(s)\mathrm{d}s}$. To shorten the notation, we write $W = (W_1, W_2, W_3)^\top$ and denote the drift of the capital stocks and temperature by μ_{K_i} and μ_T, respectively. The dynamics of K and S can be calculated using Ito's lemma:

$$\begin{aligned}
\mathrm{d}S &= S(1-S)\Big[\mu_S(i_1,i_2,r,S)\mathrm{d}t + (\sigma_2\rho_{12} - \sigma_1)\mathrm{d}W_1 + \sigma_2\sqrt{1-\rho_{12}^2}\mathrm{d}W_2\Big], \\
\mathrm{d}K &= K_-\Big[\mu_K(i_1,i_2,r,S)\mathrm{d}t + [(1-S)\sigma_1 + S\sigma_2\rho_{12}]\mathrm{d}W_1 + S\sigma_2\sqrt{1-\rho_{12}^2}\mathrm{d}W_2 - \sum_{i=c,e}\ell_i \mathrm{d}N_i\Big],
\end{aligned}$$

where the drift rates are given by

$$\begin{aligned}
\mu_S(i_1,i_2,r,S) &= \mu_{K_1} - \mu_{K_2} + S(\sigma_1\sigma_2\rho_{12} - \sigma_2^2) + (1-S)(\sigma_1^2 - \sigma_1\sigma_2\rho_{12}), \\
\mu_K(i_1,i_2,r,S) &= (1-S)\mu_{K_1} + S\mu_{K_2}.
\end{aligned}$$

A.4 Separation and Reduced-Form Value Function

We solve a modified HJB equation with finite differences in terms of only three $(S,T,\mathbf{X})$ instead of four state variables $(K_1,K_2,T,\mathbf{X})$. For this to be possible, we must assume that the transition intensities $\lambda_\ell(\mathbf{S},i,j)$ depend on S and T but not explicitly on K_1 and K_2. The following proposition summarizes our findings for the PIGOU state. The situation for the CAP state is discussed in Corollary A.3.

Proposition A.1 (Value Function and Optimal Controls in the PIGOU state)**.** *Let $\widehat{\vartheta}(t,\boldsymbol{X}) = \vartheta(\boldsymbol{X})K_0\mathrm{e}^{\int_0^t g_\nu(s)\mathrm{d}s}$. Suppose that there is no temperature cap in the current state. The value function (2.6) then has the form*

$$J(t,K_1,K_2,T,\boldsymbol{X}) = \frac{1}{1-\gamma}(K_1+K_2)^{1-\gamma}V\big(t,T,S(K_1,K_2),\boldsymbol{X}\big). \tag{A.3}$$

where V satisfies a certain HJB equation which is given in (A.12) below. Optimal consumption is

$$c = \sum_{n=1,2} S_n\Big[A_n\big(\kappa_{1,n}g_n^{\rho_n} + \kappa_{2,n}f_n^{\rho_n}\big)^{\frac{\eta_n}{\rho_n}}\Lambda_n(T,\boldsymbol{X}) - i_n - b_g(S)g_n - b_f(S)f_n - \frac{\varsigma_n}{S_n}\widetilde{b}_d(S,\boldsymbol{X},D)\Big]. \tag{A.4}$$

Optimal energy use is

$$g_1 = \Big(\frac{b_g(S)}{\eta_1 A_1\big(\kappa_{1,1}+\kappa_{2,1}z^{\rho_1}\big)^{\frac{\eta_1}{\rho_1}-1}\Lambda_1(T,\boldsymbol{X})\kappa_{1,1}}\Big)^{\frac{1}{\eta_1-1}}, \qquad f_1 = g_1 z_1, \tag{A.5}$$

$$g_2 = \Big(\frac{b_g(S)}{\eta_2 A_2\big(\kappa_{1,2}+\kappa_{2,2}z^{\rho_2}\big)^{\frac{\eta_2}{\rho_2}-1}\Lambda_2(T,\boldsymbol{X})\kappa_{1,2}}\Big)^{\frac{1}{\eta_2-1}} \qquad f_2 = g_2 z_2, \tag{A.6}$$

where

$$z_1 = \Big(\frac{\kappa_{1,1}}{\kappa_{2,1} b_g(S)}\Big)^{\frac{1}{\rho_1 - 1}} \Big[b_f(S) - \frac{V_T \widehat{\vartheta}(t,\boldsymbol{X})(1-S)}{\big[(1-\gamma)V - V_S S\big][1-\varphi_1 i_1]} \Big]^{\frac{1}{\rho_1 - 1}},$$
$$z_2 = \Big(\frac{\kappa_{1,2}}{\kappa_{2,2} b_g(S)}\Big)^{\frac{1}{\rho_2 - 1}} \Big[b_f(S) - \frac{V_T \widehat{\vartheta}(t,\boldsymbol{X}) S}{\big[(1-\gamma)V - V_S S\big][1-\varphi_1 i_1]} \Big]^{\frac{1}{\rho_2 - 1}}$$

The condition for the optimal reallocation strategy is

$$r = \frac{1}{\kappa}\Big(\frac{V_S}{V_S S + (\gamma - 1)V}\Big) \tag{A.7}$$

and optimal investment and carbon removal solves the nonlinear system

$$\delta(1-\gamma)V^{1-1/\theta} c^{-1/\psi} = \big[(1-\gamma)V - V_S S\big][1-\varphi_1 i_1], \tag{A.8}$$
$$\delta(1-\gamma)V^{1-1/\theta} c^{-1/\psi} = \big[(1-\gamma)V + V_S (1-S)\big][1-\varphi_2 i_2], \tag{A.9}$$
$$\delta(1-\gamma)V^{1-1/\theta} c^{-1/\psi} = -V_T \vartheta(\boldsymbol{X}) \Big(\frac{\partial \widetilde{b}_d(S,\boldsymbol{X},D)}{\partial D}\Big)^{-1}, \tag{A.10}$$

The optimal carbon tax is

$$\tau = \frac{\vartheta(\boldsymbol{X}) c^{1/\psi}}{\delta(\gamma - 1)} \frac{V_T}{V^{1-1/\theta}} K. \tag{A.11}$$

Proof. Let $i_n = I_n/K_n$, $f_n = F_n/K_n$, $g_n = G_n/K_n$, $r = R/K_1$ denote the control variables in relative terms. Substituting these relative controls into (A.1) leads to the HJB equation:

$$\begin{aligned}
0 = \sup_{D, i_n, f_n, g_n, r} \Big\{ & J_t + \frac{\delta}{1 - 1/\psi}[(1-\gamma)J]^{1-1/\theta} \Big(\sum_{n=1,2} [Y_n - I_n - b_g G_n - b_f F_n - \varsigma_n b_d(S,\mathbf{X},D,K)] \Big)^{1-1/\psi} \\
& - \delta\theta J + J_{K_1} K_1 \big(i_1 - \frac{1}{2}\varphi_1 i_1^2 + r - \frac{1}{2}\kappa r^2 - \delta_1^k\big) + J_{K_2} K_2 \big(i_2 - \frac{1}{2}\varphi_2 i_2^2 - r\frac{K_1}{K_2} - \delta_2^k\big) \\
& + \frac{1}{2} J_{K_1 K_1} K_1^2 \sigma_1^2 + \frac{1}{2} J_{K_2 K_2} K_2^2 \sigma_2^2 + J_{K_1 K_2} K_1 K_2 \sigma_1 \sigma_2 \rho_{12} + J_T[\widehat{\vartheta}(f_1 S_1 + f_2 S_2) - \vartheta D] + J_{TT}\frac{1}{2}\sigma_T^2 \\
& + \sum_{i=c,e} \lambda_i(T) \mathbb{E}[J(K_1 Z_i, K_2 Z_i, T, \mathbf{X}) - J] + \sum_{x \neq X} \lambda_x(S,T,\mathbf{X},x)\big[J(K_1,K_2,T,x) - J\big] \Big\}
\end{aligned}$$

We conjecture that the value function has the form

$$J(t,K_1,K_2,T,\mathbf{X}) = \frac{1}{1-\gamma}(K_1 + K_2)^{1-\gamma} V\big(t,T,S(K_1,K_2),\mathbf{X}\big).$$

The partial derivatives of S are $S_{K_1} = -\frac{S}{K}$, $S_{K_2} = \frac{1-S}{K}$. This specification implies[39]

$$V(t,T,S,\mathbf{X}) > 0, \qquad V_T(t,T,S,\mathbf{X}) > 0.$$

The relevant partial derivatives of the value function J are

$$\begin{aligned}
J_{K_1} &= K^{-\gamma}V + \frac{1}{1-\gamma}K^{1-\gamma}V_S\frac{-S}{K},\\
J_{K_1K_1} &= -\gamma K^{-\gamma-1}V + 2K^{-\gamma}V_S\frac{-S}{K} + \frac{1}{1-\gamma}K^{1-\gamma}\Big[V_{SS}\frac{S^2}{K^2} + 2V_S\frac{S}{K^2}\Big],\\
J_{K_2} &= K^{-\gamma}V + \frac{1}{1-\gamma}K^{1-\gamma}V_S\frac{1-S}{K},\\
J_{K_2K_2} &= -\gamma K^{-\gamma-1}V + 2K^{-\gamma}V_S\frac{1-S}{K} + \frac{1}{1-\gamma}K^{1-\gamma}\Big[V_{SS}\frac{(1-S)^2}{K^2} - 2V_S\frac{1-S}{K^2}\Big],\\
J_{K_1K_2} &= -\gamma K^{-1-\gamma}V + K^{-\gamma}V_S\frac{1-2S}{K} + \frac{1}{1-\gamma}K^{1-\gamma}\Big[V_{SS}\frac{-(1-S)S}{K^2} + V_S\frac{2S-1}{K^2}\Big],\\
J_T &= \frac{1}{1-\gamma}K^{1-\gamma}V_T.
\end{aligned}$$

The aggregator is given by $f(C,J) = K^{1-\gamma}\big[\delta\theta V^{1-1/\theta}c^{1-1/\psi} - \delta\theta V\big]$. Substituting the conjecture and its partial derivatives into the HJB equation leads to the following reduced-form HJB equation

$$0 = \sup_{D,f_n,,g_n,i_n,r}\Big\{V_t + M_0 + M_1V + M_2V_S + M_3V_{SS} + M_4V_T + M_5V_{TT}\Big\} \tag{A.12}$$

We introduce the three-dimensional volatility vectors

$$\sigma_k(S) = \big((1-S)\sigma_1 + S\sigma_2\rho_{12}, S\sigma_2\sqrt{1-\rho_{12}^2}, 0\big)^\top, \tag{A.13}$$

$$\sigma_s = \big(\sigma_2\rho_{12} - \sigma_1, \sigma_2\sqrt{1-\rho_{12}^2}, 0\big)^\top. \tag{A.14}$$

The coefficients M_ℓ ($\ell = 1,\dots,5$) are given by

$$\begin{aligned}
M_0 &= \delta\theta V^{1-1/\theta}c^{1-1/\psi} + \sum_{x\neq\mathbf{X}}\lambda_x(S,T,\mathbf{X},x)V(t,T,S,x),\\
M_1 &= (1-\gamma)\Big[\underbrace{(1-S)\mu_1 + S\mu_2}_{=\mu_k} - \frac{1}{2}\gamma[\underbrace{(1-S)^2\sigma_1^2 + S^2\sigma_2^2 + 2S(1-S)\sigma_1\sigma_2\rho_{12}}_{=\|\sigma_k\|^2}]\Big]\\
&\quad + \sum_{i=c,e}\lambda_i(T)\mathbb{E}[(1-\ell_i)^{1-\gamma} - 1] - \sum_{x\neq\mathbf{X}}\lambda_x(S,T,\mathbf{X},x) - \delta\theta,
\end{aligned}$$

[39] The sign of $V_S(t,T,S,\mathbf{X})$ is ambiguous because S indicates how CO_2 intensive the economy is but also how much the economy is diversified, see Hambel et al. (2024) for an extensive discussion about the interaction of abatement and diversification motives.

$$M_2 = S(1-S)\Big(\mu_2 - \mu_1 - \gamma\big[\underbrace{S\sigma_2^2 - (1-S)\sigma_1^2 + (1-2S)\sigma_1\sigma_2\rho_{12}}_{=\sigma_k^\top \sigma_s}\big]\Big),$$

$$M_3 = \frac{1}{2}(1-S)^2 S^2\big[\underbrace{\sigma_1^2 + \sigma_2^2 - 2\sigma_1\sigma_2\rho_{12}}_{=\|\sigma_s\|^2}\big],$$

$$M_4 = \widehat{\vartheta}(t,\mathbf{X})[f_1(1-S) + f_2 S] - \vartheta(\mathbf{X})D,$$

$$M_5 = \frac{1}{2}\sigma_T^2,$$

where c is given in (A.4) and $\widehat{\vartheta}(t,\mathbf{X}) = \vartheta(\mathbf{X})K_0 \mathrm{e}^{\int_0^t g_\nu(s)\mathrm{d}s}$. Calculating the first-order conditions leads to the system of equations (A.5) – (A.9), which determine the optimal controls. The optimal SCC follows from substituting the value function (A.3) into (A.2). □

This proposition is also valid in the BAU state. Policy makers ignore the negative externalities from emitting CO_2, so behave as if $\Lambda_n(T,\mathbf{X}) = 0$ and $\lambda_c(T) = 0$. This implies in particular $V_T = 0$, $D = 0$, and $\tau = 0$.

Corollary A.2 (Tobin's Q's)**.** *Under the conditions of Proposition A.1, the Tobin's Q's of the green and brown asset, respectively, are given by*

$$q_1 = \frac{(1-\gamma)V - V_S S}{\delta(1-\gamma)V^{1-1/\theta}c^{-1/\psi}}, \qquad q_2 = \frac{(1-\gamma)V + V_S(1-S)}{\delta(1-\gamma)V^{1-1/\theta}c^{-1/\psi}}.$$

Proof. This follows immediately from (A.8) and (A.9). □

Now, we consider the case where a temperature cap is implemented in some state $\mathbf{X}$, i.e., carbon emissions are only allowed as long as $T_t \leqslant T_{cap}$. If the carbon budget has been maxed out, i.e. if temperature exceeds T_{cap}, society is not allowed anymore to release CO_2 into the atmosphere.

Corollary A.3 (Optimal Controls in the CAP state)**.** *Suppose that in state $\mathbf{X}$, carbon emissions are prohibited if temperature exceeds its limit T_{cap}.*

(i) If temperature is below the cap, $T \leqslant T_{cap}$, the indirect utility function and the optimal controls are as stated in Proposition A.1.

(ii) If temperature exceeds T_{cap}, the separation (A.3) still holds, but the release of CO_2 into the atmosphere is no longer allowed, i.e. $f_n = 0$. Then, the optimal energy composites are

$$e_n = g_n \kappa_{1,n}^{\frac{1}{\rho_n}} = \begin{cases} \Big[\frac{b_g(S)}{A_n \eta_n \kappa_{1,n}^{\eta_n/\rho_n}\Lambda_n(T)}\Big]^{\frac{1}{\eta_n - 1}} \kappa_{1,n}^{\frac{1}{\rho_n}}, & \text{if } \rho_n > 0 \\ 0, & \text{if } \rho_n \leqslant 0. \end{cases} \tag{A.15}$$

Optimal consumption is

$$c = \sum_{n=1,2} \Big(S_n \Big[A_n e_n^{\eta_n} \Lambda_n(T) - i_n - b_g(S) g_n - \frac{\varsigma_n}{S_n} \widetilde{b}_d(S,\boldsymbol{X},D) \Big] \Big). \tag{A.16}$$

The optimal reallocation strategy is

$$r = \frac{1}{\kappa} \Big(\frac{V_S}{V_S S + (\gamma - 1)V} \Big) \tag{A.17}$$

and optimal investment and optimal carbon removal solve the nonlinear system

$$\delta(1-\gamma) V^{1-1/\theta} c^{-1/\psi} = \big[(1-\gamma)V - V_S S \big] [1 - \varphi_1 i_1], \tag{A.18}$$

$$\delta(1-\gamma) V^{1-1/\theta} c^{-1/\psi} = \big[(1-\gamma)V + V_S (1-S) \big] [1 - \varphi_2 i_2], \tag{A.19}$$

$$\delta(1-\gamma) V^{1-1/\theta} c^{-1/\psi} = -V_T \vartheta(\boldsymbol{X}) \Big(\frac{\partial \widetilde{b}_d(S,\boldsymbol{X},D)}{\partial D} \Big)^{-1}. \tag{A.20}$$

The optimal SCC is as stated in Proposition A.1 and the Tobin's Q's are as stated in Corollary A.2.

Proof. Along the lines of the proof of Proposition A.1. □

Although the decomposition of the indirect utility function and the optimal controls in (i) are unaffected when the temperature cap kicks in, the values are different. This is because V has a different shape in states with and without temperature cap. In the latter scenario, the value function is much steeper as temperature approaches T_{cap}.

A.5 Numerical Solution Approach

Basic Idea We face a problem with an infinite time horizon. To solve this problem we first compute the steady state $\widetilde{V}(T,S,\mathbf{X})$ on a grid $(T,S,\mathbf{X})$ assuming there is no exogenous time trend. Thus, we first have to solve a similar PDE as in (A.12) but without the time derivative. The resulting steady state $\widetilde{V}(T,S,\mathbf{X})$ is then used as a terminal condition $V(t_{\max},T,S,\mathbf{X}) = \widetilde{V}(T,S,\mathbf{X})$ for the value function in the year 2400 corresponding to $t_{\max} = 380$. Starting with this terminal condition, we proceed backwards through the time grid to analyze the transition towards the steady state.

Definition of the Grid We use a grid-based solution approach to solve the non-linear PDE. We discretize the (t,T,S)-space using an equally-spaced lattice. Its grid points are defined by

$$\big\{ (t_n, T_i, S_j) \,|\, n = 0,\cdots,N_t, i = 0,\cdots,N_T, j = 0,\cdots,N_S \big\},$$

where $t_n = n\Delta_t$, $T_i = i\Delta_T$, and $S_j = j\Delta_S$ for some fixed grid size parameters Δ_t, Δ_T, and Δ_S that denote the distances between two grid points. The numerical results are based on a choice of $N_T = 50$, $N_S = 200$ and one time step per year. Our results hardly change if we use a finer grid or more time steps per year. In the sequel, $V_{n,i,j,k}$ denotes the approximated value function at the grid point $(t_n, T_i, S_j, \mathbf{X} = k)$ and $\pi_{n,i,j,k}$ refers to the corresponding set of optimal controls. We apply an implicit finite-difference scheme.

Finite Differences Approach We now describe the numerical solution approach in more detail. We adapt the numerical solution approach used by Munk and Sørensen (2010). The numerical procedure works as follows. At any point in time, we make a conjecture for the optimal strategy $\pi^*_{n,i,j,k}$. A good guess is the value at the previous grid point since the abatement strategy varies only slightly over a small time interval, i.e. we set $\pi_{n-1,i,j,k} = \pi^*_{n,i,j,k}$. Substituting this guess into the HJB equation yields a semi-linear PDE:

$$0 = V_t + \delta\theta V^{1-1/\theta} c^{1-1/\psi} + \sum_{x \neq \mathbf{X}} \lambda_x(S,T,\mathbf{X},x) V(t,T,S,x) + M_1 V + M_2 V_T + M_3 V_{TT} + M_4 V_S + M_5 V_{SS}$$

with state-dependent coefficients $M_i = M_i(t,T,S,\mathbf{X})$ as stated in Appendix A.4. Due to the implicit approach, we approximate the time derivative by forward finite differences. In the approximation, we use the so-called *up-wind* scheme that stabilizes the finite differences approach. Therefore, the relevant finite differences at the grid point (n,i,j,k) are given by

$$\begin{aligned}
\mathrm{D}_T^+ V_{n,i,j,k} &= \frac{V_{n,i+1,j,k} - V_{n,i,j,k}}{\Delta_T}, & \mathrm{D}_T^- V_{n,i,j,k} &= \frac{V_{n,i,j,k} - V_{n,i-1,j,k}}{\Delta_T}, \\
\mathrm{D}_S^+ V_{n,i,j,k} &= \frac{V_{n,i,j+1,k} - V_{n,i,j,k}}{\Delta_S}, & \mathrm{D}_S^- V_{n,i,j,k} &= \frac{V_{n,i,j,k} - V_{n,i,j-1,k}}{\Delta_S}, \\
\mathrm{D}_{TT}^2 V_{n,i,j,k} &= \frac{V_{n,i+1,j,k} - 2V_{n,i,j,k} + V_{n,i-1,j,k}}{\Delta_T^2}, \\
\mathrm{D}_{SS}^2 V_{n,i,j,k} &= \frac{V_{n,i,j+1,k} - 2V_{n,i,j,k} + V_{n,i,j-1,k}}{\Delta_S^2}, \\
\mathrm{D}_t^+ V_{n,i,j,k} &= \frac{V_{n+1,i,j,k} - V_{n,i,j,k}}{\Delta_t}.
\end{aligned}$$

Substituting these expressions into the PDE above yields the following semi-linear equation for the grid point (t_n, T_i, S_j, k):

$$\begin{aligned}
V_{n+1,i,j,k} \frac{1}{\Delta_t} = V_{n,i,j,k} \Big[-M_1 + \frac{1}{\Delta_t} + \mathrm{abs}\Big(\frac{M_2}{\Delta_T}\Big) + \mathrm{abs}\Big(\frac{M_4}{\Delta_S}\Big) + 2\frac{M_3}{\Delta_T^2} + 2\frac{M_5}{\Delta_S^2} \Big] \\
+ V_{n,i-1,j,k} \Big[\frac{M_2^-}{\Delta_T} - \frac{M_3}{\Delta_T^2} \Big] + V_{n,i+1,j,k} \Big[-\frac{M_2^+}{\Delta_T} - \frac{M_3}{\Delta_T^2} \Big]
\end{aligned}$$

$$+V_{n,i,j-1,k}\Big[\frac{M_4^-}{\Delta_S}-\frac{M_5}{\Delta_S^2}\Big]+V_{n,i,j+1,k}\Big[-\frac{M_4^+}{\Delta_S}-\frac{M_5}{\Delta_S^2}\Big]$$
$$+\delta\theta V_{n,i,j,k}^{1-1/\theta}c_{n,i,j,k}^{1-1/\psi}+\sum_{\widehat{k}\neq k}\lambda(S,T,k,\widehat{k})V_{n,i,j,\widehat{k}}.$$

Therefore, for a fixed point in time each grid point is determined by a non-linear equation. This results in a non-linear system of $(N_S+1)(N_T+1)$ equations for every state k of the Markov chain $\mathbf{X}$ that can be solved for the vector

$$V_{n,k}=(V_{n,1,1,k},\cdots,V_{n,1,N_S,k},V_{n,2,1,k},\cdots,V_{n,2,N_S,k},\cdots,V_{n,N_T,1,k},\cdots,V_{n,N_T,N_S,k}).$$

Using this solution we update our conjecture for the optimal controls at the current point in the time dimension. We apply the first-order conditions as stated in Proposition A.1 and determine the optimal strategies and the optimal SCC with the above-mentioned finite-difference approximations of the corresponding partial derivatives. After we have solved the model, we simulate all state and decision variables in a Monte-Carlo simulation. We simulate 200,000 paths and calculate quantiles, means, and other moments for all relevant variables.

B Asset Pricing

B.1 Dynamics of the Stochastic Discount Factor

Duffie and Epstein (1992a) show that the dynamics of the pricing kernel H are given by

$$\frac{\mathrm{d}H}{H_-}=\frac{\mathrm{d}f_c(C,J)}{f_c(C,J)}+f_J(C,J)\mathrm{d}t.$$

The relevant partial derivatives of the aggregator are

$$f_c(C,J)=\delta V^{1-1/\theta}K^{-\gamma}c^{-1/\psi},\qquad f_J(C,J)=\delta(\theta-1)c^{1-1/\psi}V^{-1/\theta}-\delta\theta.$$

To calculate the dynamics of the SDF, we first compute

$$\frac{\mathrm{d}K^{-\gamma}}{K_-^{-\gamma}}=\Big(-\gamma\mu_k+\frac{1}{2}\gamma(\gamma+1)\|\sigma_k\|^2\Big)\mathrm{d}t-\gamma\sigma_k^\top\mathrm{d}W+\sum_{i=c,e}\big((1-\ell_i)^{-\gamma}-1\big)\mathrm{d}N_i.$$

Secondly, we determine the dynamics of $V^{1-1/\theta}$. According to Ito's lemma, $V=V(t,S,T,\mathbf{X})$ satisfies

$$\frac{\mathrm{d}V}{V_-}=\mu_v\mathrm{d}t+\sigma_v^\top\mathrm{d}W-\sum_{x\neq\mathbf{X}}j_v^x\mathrm{d}N^x$$

where N^x is a point process that indicates a jump to state x, i.e.,

$$N^x_{\tau_x} = \begin{cases} N^x_{\tau_x-} + 1 : & \mathbf{X}_{\tau_x} = x, \mathbf{X}_{\tau_x-} \neq x \\ N^x_{\tau_x-} : & \text{else} \end{cases}$$

with

$$\begin{aligned} \mu_v = \frac{1}{V_-}\Big(& V_t + V_S S(1-S)\mu_s + V_T \vartheta \nu (f_1(1-S) + f_2 S) - V_T \vartheta D \\ & + \frac{1}{2} V_{SS} S^2 (1-S)^2 \|\sigma_s\|^2 + \frac{1}{2} V_{TT} \sigma_T^2 \Big), \end{aligned} \tag{B.1}$$

$$\sigma_v = \frac{1}{V_-}\Big(V_S S(1-S)(-\sigma_1 + \sigma_2 \rho_{12}),\, V_S S(1-S)\sigma_2 \sqrt{1-\rho_{12}^2},\, V_T \sigma_T \Big)^\top, \tag{B.2}$$

$$j_v^x = 1 - \frac{V(t,T,S,x)}{V(t,T,S,\mathbf{X})}. \tag{B.3}$$

Another application of Ito's lemma yields

$$\frac{\mathrm{d}V^{1-1/\theta}}{V_-^{1-1/\theta}} = \Big[\frac{\theta-1}{\theta}\mu_v - \frac{\theta-1}{2\theta^2}\|\sigma_v\|^2 \Big]\mathrm{d}t + \frac{\theta-1}{\theta}\sigma_v^\top \mathrm{d}W + \sum_{x \neq \mathbf{X}} \big((1-j_v^x)^{1-1/\theta} - 1 \big)\mathrm{d}N^x.$$

Therefore, by Ito's product rule,

$$\begin{aligned} \frac{\mathrm{d}(V^{1-1/\theta}K^{-\gamma})}{(V^{1-1/\theta}K^{-\gamma})_-} = & \Big(-\gamma\mu_k + \frac{1}{2}\gamma(\gamma+1)\|\sigma_k\|^2 \Big)\mathrm{d}t + \frac{\theta-1}{\theta}\Big(\mu_v - \gamma\langle \sigma_k, \sigma_s \rangle \frac{V_S}{V} S(1-S) \Big)\mathrm{d}t \\ & - \frac{\theta-1}{2\theta^2}\|\sigma_s\|^2 \frac{V_S^2}{V^2} S^2 (1-S)^2 \mathrm{d}t + \Big(\frac{\theta-1}{\theta}\sigma_v - \gamma\sigma_k \Big)^\top \mathrm{d}W + \sum_{i=c,e} \big((1-\ell_i)^{-\gamma} - 1 \big)\mathrm{d}N_i \\ & + \sum_{x \neq \mathbf{X}} \big((1-j_v^x)^{1-1/\theta} - 1 \big)\mathrm{d}N^x. \end{aligned} \tag{B.4}$$

Notice that according to the simplified HJB equation (A.12),

$$\begin{aligned} \mu_v - \gamma\langle \sigma_k, \sigma_s \rangle \frac{V_S}{V} S(1-S) = & (\gamma-1)\big(\mu_k - \frac{1}{2}\gamma\|\sigma_k\|^2 \big) + \delta\theta - \delta\theta V^{-1/\theta} c^{1-1/\psi} \\ & - \sum_{i=c,e} \lambda_i \mathbb{E}[(1-\ell_i)^{1-\gamma} - 1] + \sum_{x \neq \mathbf{X}} \lambda_x j_v^x, \end{aligned}$$

where we use the short-hand notation $\lambda_x = \lambda_x(\mathbf{S}, \mathbf{X}, x)$. Substituting this term into (B.4) yields

$$\begin{aligned} \frac{\mathrm{d}(V^{1-1/\theta}K^{-\gamma})}{(V^{1-1/\theta}K^{-\gamma})_-} = & \Big(-\gamma\mu_k + \frac{1}{2}\gamma(\gamma+1)\|\sigma_k\|^2 \Big)\mathrm{d}t - \frac{\theta-1}{2\theta^2}\|\sigma_s\|^2 \frac{V_S^2}{V^2} S^2 (1-S)^2 \mathrm{d}t \\ & + \Big(\frac{\theta-1}{\theta}\sigma_v - \gamma\sigma_k \Big)^\top \mathrm{d}W \end{aligned}$$

$$+\frac{\theta-1}{\theta}\Big((\gamma-1)\big(\mu_k-\frac{1}{2}\gamma\|\sigma_k\|^2\big)+\delta\theta-\delta\theta V^{-1/\theta}c^{1-1/\psi}\Big)\mathrm{d}t+\sum_{i=c,e}\big((1-\ell_i)^{-\gamma}-1\big)\mathrm{d}N_i$$
$$+\sum_{x\neq\mathbf{X}}\big((1-j_v^x)^{1-1/\theta}-1\big)\mathrm{d}N^x-\frac{\theta-1}{\theta}\Big(\sum_{i=c,e}\lambda_i\mathbb{E}[(1-\ell_i)^{1-\gamma}-1]-\sum_{x\neq\mathbf{X}}\lambda_x j_v^x\Big)\mathrm{d}t.$$

Furthermore, the consumption-capital ratio $c=C/K$ has the following dynamics

$$\frac{\mathrm{d}c}{c_-}=\mu_c\mathrm{d}t+\sigma_c^\top\mathrm{d}W-\sum_{x\neq\mathbf{X}}j_c^x\mathrm{d}N^x$$

for auxiliary functions $\mu_c(t,T,S,\mathbf{X})$ and $\sigma_c(t,T,S,\mathbf{X})$, which can be determined numerically, and

$$j_c^x=1-\frac{c(t,T,S,x)}{c(t,T,S,\mathbf{X})}. \tag{B.5}$$

In turn,

$$\frac{\mathrm{d}c^{-1/\psi}}{c_-^{-1/\psi}}=-\frac{1}{\psi}(\mu_c\mathrm{d}t+\sigma_c^\top\mathrm{d}W)+\frac{1+\psi}{\psi^2}\|\sigma_c\|^2\mathrm{d}t+\sum_{x\neq\mathbf{X}}\big((1-j_c^x)^{-1/\psi}-1\big)\mathrm{d}N^x$$

Consequently, the pricing kernel dynamics are given by

$$\begin{aligned}\frac{\mathrm{d}H_-}{H_-}=&-r_t^f\mathrm{d}t+\Big(-\gamma\sigma_k+\frac{\theta-1}{\theta}\sigma_v-\frac{1}{\psi}\sigma_c\Big)^\top\mathrm{d}W+\sum_{i=c,e}\big((1-\ell_i)^{-\gamma}-1\big)\mathrm{d}N_i-\lambda_i\mathbb{E}[(1-\ell_i)^{-\gamma}-1]\mathrm{d}t\\&+\sum_{x\neq\mathbf{X}}\Big[\big((1-j_v^x)^{1-1/\theta}(1-j_c^x)^{-1/\psi}-1\big)\mathrm{d}N^x-\lambda_x\big((1-j_v^x)^{1-1/\theta}(1-j_c^x)^{-1/\psi}-1\big)\mathrm{d}t\Big],\end{aligned} \tag{B.6}$$

where the risk-free rate is given by

$$\begin{aligned}r_t^f=&\,\delta+\frac{1}{\psi}\mu_k-\frac{1}{2}\gamma\Big(1+\frac{1}{\psi}\Big)\|\sigma_k\|^2-\Big(\frac{1+\psi}{\psi^2}\|\sigma_c\|^2-\frac{\theta-1}{2\theta^2}\|\sigma_v\|^2-\frac{1}{\psi}\sigma_c^\top\Big(\frac{\theta-1}{\theta}\sigma_v-\gamma\sigma_k\Big)\Big)\\&-\sum_{i=c,e}\lambda_i\mathbb{E}\Big[(1-\ell_i)^{-\gamma}-1+\frac{\psi^{-1}-\gamma}{1-\gamma}\big(1-(1-\ell_i)^{1-\gamma}\big)\Big]\\&-\sum_{x\neq\mathbf{X}}\Big[\lambda_x\big((1-j_v^x)^{1-1/\theta}(1-j_c^x)^{-1/\psi}-1\big)+\frac{\theta-1}{\theta}\lambda_x j_v^x\Big].\end{aligned} \tag{B.7}$$

An application of Itô's lemma gives the drift and volatility vector of optimal consumption as

$$\mu_C(t,T,S)=\mu_k(S)+\mu_c(t,T,S)+\sigma_c(t,T,S)^\top\sigma_k(S), \tag{B.8}$$
$$\sigma_C(t,T,S)=\sigma_k(S)+\sigma_c(t,T,S). \tag{B.9}$$

Substituting (B.8) and (B.9) into the pricing kernel dynamics and some algebra completes the proof. □

B.2 Dividend Dynamics

The amount of consumption goods produced by asset n are

$$C_n = Y_n - I_n - b_f F_n - b_g G_n - b_d(S,\mathbf{X},D,K) = \chi_n K_n$$

with $\chi_n = \left[A_n\left(\kappa_{1,n} g_n^{\rho_n} + \kappa_{2,n} f_n^{\rho_n}\right)^{\frac{\eta_n}{\rho_n}} \Lambda_n(T) - i_n - b_g(S) g_n - b_f(S) f_n - \widetilde{b}_d(S,\mathbf{X},D)\right]$. An application of Ito's lemma shows that χ_n evolves according to

$$\frac{\mathrm{d}\chi_n}{\chi_{n-}} = \mu_{\chi_n}\mathrm{d}t + \sigma_{\chi_n}^\top \mathrm{d}W - \sum_{x\neq\mathbf{X}} j_{\chi_n}^x \mathrm{d}N^x$$

for auxiliary functions μ_{χ_n}, σ_{χ_n}, $j_{\chi_n}^x$ that can be determined numerically along the lines of (B.1) – (B.3). Notice that χ_n is unaffected when the economy is hit by an economic Barro-type disaster shock N^d.

Empirically, dividends are more volatile than consumption (e.g. Bansal and Yaron 2004) and dividends fall more than consumption when a disaster hits the economy (e.g. Longstaff and Piazzesi 2004). Following Wachter (2013), among others, we thus model dividends as levered consumption, i.e. $\mathscr{D}_n = C_n^\phi$ for $\phi \geqslant 1$.[40] An application of Ito's product rule yields the dividend dynamics

$$\frac{\mathrm{d}\mathscr{D}_n}{\mathscr{D}_{n-}} = \mu_{\mathscr{D}_n}\mathrm{d}t + \sigma_{\mathscr{D}_n}^\top \mathrm{d}W + \sum_{i=c,e} j_{\mathscr{D}_n}^i \mathrm{d}N^i + \sum_{x\neq\mathbf{X}} j_{\mathscr{D}_n}^x \mathrm{d}N^x$$

with

$$\begin{aligned}
\mu_{\mathscr{D}_n} &= \phi(\mu_{K_n} + \mu_{\chi_n} + \sigma_{\chi_n}^\top \sigma_{K_n}) + \frac{1}{2}\phi(\phi-1)\|\sigma_{K_n} + \sigma_{\chi_n}\|^2,\\
\sigma_{\mathscr{D}_n} &= \phi(\sigma_{K_n} + \sigma_{\chi_n}),\\
j_{\mathscr{D}_n}^i &= (1-\ell_i)^\phi - 1,\\
j_{\mathscr{D}_n}^x &= (1-j_{\chi_n}^x)^\phi - 1.
\end{aligned}$$

In a next step, we determine the dynamics of discounted dividends, $\widehat{\mathscr{D}}_n = H\mathscr{D}_n$. Another application of Itô's product rule implies

$$\frac{\mathrm{d}\widehat{\mathscr{D}}_n}{\widehat{\mathscr{D}}_{n-}} = \mu_{\widehat{\mathscr{D}}_n}\mathrm{d}t + \sigma_{\widehat{\mathscr{D}}_n}^\top \mathrm{d}W + \sum_{i=c,e} j_{\widehat{\mathscr{D}}_n}^i \mathrm{d}N_i + \sum_{x\neq\mathbf{X}} j_{\widehat{\mathscr{D}}_n}^x \mathrm{d}N^x$$

[40] A popular alternative to this approach is modelling the consumption-dividend ratio as a stationary but persistent process, as in Longstaff and Piazzesi (2004), among others. In order to focus on the novel implications of climate transition risk on asset prices, we keep the setting simple although following this approach would also be feasible in our setting.

with

$$\begin{aligned}
\mu_{\widehat{\mathscr{D}}_n} &= \mu_H + \mu_{\mathscr{D}_n} + \sigma_H^\top \sigma_{D_n}, \\
\sigma_{\widehat{\mathscr{D}}_n} &= \sigma_H + \sigma_{\mathscr{D}_n}, \\
j^i_{\widehat{\mathscr{D}}_n} &= (1-\ell_i)^{\phi-\gamma} - 1, \\
j^x_{\widehat{\mathscr{D}}_n} &= (1-j^x_{\chi_n})^{\phi}(1-j^x_v)^{1-1/\theta}(1-j^x_c)^{-1/\psi} - 1.
\end{aligned}$$

B.3 Price-dividend Ratios of Dividend Claims

Let $\Pi_n = \frac{P_n}{\mathscr{D}_n}$ denote the price-dividend ration of asset n, and $\pi_n = \log\left(\frac{P_n}{\mathscr{D}_n}\right)$ the log price-dividend ratio. Due to the representation of the dividends, the dynamics of K_n, and the pricing equation, the price is linear in K_n and thus the price-dividend ratio is independent of K_n. Therefore, it is not driven by the disaster risk process N^d, and the dynamics of the log price-dividend ratio can be written as

$$\frac{\mathrm{d}\pi_n}{\pi_{n-}} = \mu_{\pi_n}\mathrm{d}t + \sigma_{\pi_n}^\top \mathrm{d}W - \sum_{x\neq \mathbf{X}} j^x_{\pi_n}\mathrm{d}N^x,$$

where the drift and the volatility vector are given by

$$\begin{aligned}
\mu_{\pi_n} &= \frac{1}{\pi_n}\Big[\pi_{n,t} + \pi_{n,S}S(1-S)\mu_S + \pi_{n,T}\mu_T + \frac{1}{2}\pi_{n,TT}\|\sigma_T\|^2 + \frac{1}{2}\pi_{n,SS}S^2(1-S)^2\|\sigma_S\|^2\Big], \\
\sigma_{\pi_n} &= \frac{1}{\pi_n}\Big[\pi_{n,T}\sigma_T + \pi_{n,S}S(1-S)\sigma_S\Big], \\
j^x_{\pi_n} &= 1 - \frac{\pi_n(t,T,S,x)}{\pi_n(t,T,S,\mathbf{X})}.
\end{aligned}$$

In particular, the price-dividend ratio $\Pi_n = \mathrm{e}^{\pi_n}$ satisfies the following dynamics

$$\frac{\mathrm{d}\Pi_n}{\Pi_{n-}} = \big(\pi_n\mu_{\pi_n} + \frac{1}{2}\pi_n^2\|\sigma_{\pi_n}\|^2\big)\mathrm{d}t + \pi_n\sigma_{\pi_n}^\top \mathrm{d}W - \sum_{x\neq\mathbf{X}} j^x_{\Pi_n}\mathrm{d}N^x,$$

where

$$j^x_{\Pi_n} = 1 - \frac{\Pi_n(t,T,S,x)}{\Pi_n(t,T,S,\mathbf{X})}.$$

We rewrite the discounted asset price HP_n as $\widehat{P}_n(\widehat{\mathscr{D}}_n,\pi_n) = \widehat{\mathscr{D}}_n\mathrm{e}^{\pi_n}$. An application of Itô's lemma implies

$$\frac{\mathrm{d}\widehat{P}_n}{\widehat{P}_{n-}} = \big(\mu_{\widehat{\mathscr{D}}_n} + \pi_n\mu_{\pi_n} + \frac{1}{2}\pi_n^2\|\sigma_{\pi_n}\|^2 + \pi_n\sigma_{\pi_n}^\top\sigma_{\widehat{\mathscr{D}}_n}\big)\mathrm{d}t + (\pi_n\sigma_{\pi_n} + \sigma_{\widehat{\mathscr{D}}_n})^\top \mathrm{d}W$$

$$+\sum_{i=c,e}\big((1-\ell_i)^{\phi-\gamma}-1\big)\mathrm{d}N_i+\sum_{x\neq\mathbf{X}}\big((1-j^x_{\Pi_n})(1+j^x_{\widehat{\mathscr{D}}_n})-1\big)\mathrm{d}N^x.$$

An application of the Feynman-Kač Theorem yields

$$\mathscr{L}\widehat{P}_n+\mathrm{e}^{-\pi_n}\widehat{P}_n=0, \tag{B.10}$$

where $\mathscr{L}\widehat{P}_n$ denotes the infinitesimal generator. The no-arbitrage condition implies

$$\begin{aligned}\frac{\mathscr{L}\widehat{P}_n}{\widehat{P}_{n-}}&=\mu_{\widehat{\mathscr{D}}_n}+\pi_n\mu_{\pi_n}+\frac{1}{2}\pi_n^2\|\sigma_{\pi_n}\|^2+\pi_n\sigma_{\pi_n}^\top\sigma_{\widehat{\mathscr{D}}_n}+\sum_{i=c,e}\lambda_i(T)\mathbb{E}\big[(1-\ell_i)^{\phi-\gamma}-1\big]\\&\quad+\sum_{x\neq\mathbf{X}}\lambda_x\big((1-j^x_{\Pi_n})(1+j^x_{\widehat{\mathscr{D}}_n})-1\big).\end{aligned} \tag{B.11}$$

Substituting (B.11) into (B.10) yields

$$\begin{aligned}0&=\mu_{\widehat{\mathscr{D}}_n}+\pi_n\mu_{\pi_n}+\frac{1}{2}\pi_n^2\|\sigma_{\pi_n}\|^2+\pi_n\sigma_{\pi_n}^\top\sigma_{\widehat{\mathscr{D}}_n}+\sum_{i=c,e}\lambda_i(T)\mathbb{E}\big[(1-\ell_i)^{\phi-\gamma}-1\big]+\mathrm{e}^{-\pi_n}\\&\quad+\sum_{x\neq\mathbf{X}}\lambda_x\big((1-j^x_{\Pi_n})(1+j^x_{\widehat{\mathscr{D}}_n})-1\big).\end{aligned}$$

Consequently, we obtain the following partial differential equation for the log price-dividend ratio π_n:

$$\begin{aligned}0&=\mathrm{e}^{-\pi_n}+\mu_{\widehat{\mathscr{D}}_n}+\pi_{n,t}+\pi_{n,S}S(1-S)\mu_S+\pi_{n,T}\mu_T+\frac{1}{2}(\pi_{n,TT}+\pi_{n,T}^2)\|\sigma_T\|^2\\&\quad+\frac{1}{2}(\pi_{n,SS}+\pi_{n,S}^2)S^2(1-S)^2\|\sigma_S\|^2+\big(\pi_{n,T}\sigma_T+\pi_{n,S}S(1-S)\sigma_S\big)^\top\sigma_{\widehat{\mathscr{D}}_n}\\&\quad+\sum_{i=c,e}\lambda_i(T)\mathbb{E}\big[(1-\ell_i)^{\phi-\gamma}-1\big]+\sum_{x\neq\mathbf{X}}\lambda_x\big((1-j^x_{\Pi_n})(1+j^x_{\widehat{\mathscr{D}}_n})-1\big).\end{aligned}$$

Notice that this PDE is nonlinear since it involves squared partial derivatives of π_n. To simplify the numerical solution approach, we transform this PDE into a linear, parabolic PDE that can be solved using finite differences. We substitute $\Pi_n=\mathrm{e}^{\pi_n}$ and end up with

$$\begin{aligned}0&=1+\sum_{x\neq\mathbf{X}}\lambda_x\Pi_n(t,T,S,x)(1+j^x_{\widehat{\mathscr{D}}_n})+\Pi_n\Big(\mu_{\widehat{\mathscr{D}}_n}+\sum_{i=c,e}\lambda_i(T)\mathbb{E}\big[(1-\ell_i)^{\phi-\gamma}-1\big]-\sum_{x\neq\mathbf{X}}\lambda_x\Big)\\&\quad+\Pi_{n,t}+\Pi_{n,S}S(1-S)\mu_S+\Pi_{n,T}\mu_T+\frac{1}{2}\Pi_{n,TT}\|\sigma_T\|^2+\frac{1}{2}\Pi_{n,SS}S^2(1-S)^2\|\sigma_S\|^2\\&\quad+\big(\Pi_{n,T}\sigma_T+\Pi_{n,S}S(1-S)\sigma_S\big)^\top\sigma_{\widehat{\mathscr{D}}_n}\end{aligned} \tag{B.12}$$

B.4 Risk Premiums

The dynamics of the asset price $P_n = \mathrm{e}^{\pi_n}\mathscr{D}_n$ follow by Itô's lemma. We obtain the following asset price dynamics

$$\begin{aligned}\frac{\mathrm{d}P_n}{P_{n-}} = \mu_n^p \mathrm{d}t + (\sigma_{\pi_n} + \sigma_{\mathscr{D}_n})^\top \mathrm{d}W + \sum_{i=c,e} \big((1-\ell_i)^\phi - 1\big)\mathrm{d}N_i - \lambda_i(T)\mathbb{E}\big[(1-\ell_i)^\phi - 1\big]\mathrm{d}t \\ + \sum_{x\neq \mathbf{X}} \Big[\big((1-j^x_{\Pi_n})(1-j^x_{\chi_n})^\phi - 1\big)\mathrm{d}N^x - \lambda_x\big((1-j^x_{\Pi_n})(1-j^x_{\chi_n})^\phi - 1\big)\Big],\end{aligned}$$

where the expected stock return and the volatility vector are given by

$$\mu_n^p = \mu_{\pi_n} + \mu_{\mathscr{D}_n} + \sigma_{\mathscr{D}_n}^\top \sigma_{\pi_n} + \frac{1}{2}\|\sigma_{\pi_n}\|^2 + \sum_{i=c,e} \lambda_i(T)\mathbb{E}\big[(1-\ell_i)^\phi - 1\big] + \sum_{x\neq \mathbf{X}} \lambda_x\big((1-j^x_{\Pi_n})(1+j^x_{\mathscr{D}_n}) - 1\big).$$

Now, the risk premium of asset n can be computed as the sum of its expected stock return, μ_n^P, and its dividend yield, $y_n^d = \mathrm{e}^{-\pi_n}$, minus the risk-free interest rate, r^f, i.e.

$$r_n^p = \mu_n^p + y_n^d - r^f.$$

To derive a semi-closed form solution of the equity premium and the carbon premium, we multiply risk exposures with the appropriate market prices of risk and obtain

$$\begin{aligned}r_n^p = \big(\Pi_{n,T}\sigma_T + \Pi_{n,S}S(1-S)\sigma_S + \phi\sigma_n + \phi\sigma_{\chi_n}\big)^\top \Big(\gamma\sigma_k - \frac{\theta-1}{\theta}\sigma_v + \frac{1}{\psi}\sigma_c\Big) \\ + \sum_{i=c,e} \lambda_i(T)\mathbb{E}\big[\big(1-(1-\ell_i)\big)^{-\gamma}\big((1-\ell_i)^\phi - 1\big)\big] \\ + \sum_{x\neq \mathbf{X}} \lambda_x\big(1-(1-j_v^x)^{1-1/\theta}(1-j_c^x)^{-1/\psi}\big)\big((1-j^x_{\Pi_n})(1+j^x_{\chi_n}) - 1\big).\end{aligned} \tag{B.13}$$

The decomposition (B.13) of the equity premium generalizes formulas similar to this as in van den Bremer et al. (2023) and Karydas and Xepapadeas (2022) to transition risk. It is known from the disaster risk literature that the disaster risk component in the second line typically makes the largest contribution to the equity premium while the diffusion component in the first line has only a small effect.

The novel component is the transition risk term in the third line. The first factor $\big(1-(1-j_v^x)^{1-1/\theta}(1-j_c^x)^{-1/\psi}\big)$ reflects the effect of a transition shock on the stochastic discount factor and is similar to the corresponding term in the risk-free rate. The second factor $\big((1-j^x_{\Pi_n})(1+j^x_{\chi_n})-1\big)$ reflects the impact of transition shock on the share price of sector n. If this price impact is positive, the last term contributes positively to the risk premium. Moreover, if the price impact of a certain type of shock is more pro-

nounced for the brown sector, then a carbon premium emerges. However, the carbon premium can also emerge from diffusive components as can be seen from the first line: In the CAP state, a temperature shock with volatility σ_T can have very distinct effects on the green and the brown sector if temperatures are close to two degrees, and thus the difference between $\Pi_{2,T}$ and $\Pi_{1,T}$ can drive to the carbon premium.

C Details on the Calibration

Here we provide further calibration details for all relevant parts of the core and extended models. We also present alternative calibrations used for sensitivity analyses and robustness checks.

C.1 Calibration of the Core Model

Our calibration is matched to the global economy[41] and is market-based. For the political Markov chain, we assume a constant probability of 4% that there is a switch from BAU to active climate policy, and a zero probability that there is a switch back to no carbon pricing again.

Macroeconomic Uncertainty We set annual volatility of capital diffusion risk to $\sigma_1 = \sigma_2 = 2\%$ matching the observed volatility of consumption or output (e.g., Wachter 2013). We assume a zero *instantaneous correlation* between the two capital stocks, $\rho_{12} = 0$ (cf. Cochrane et al., 2007). The total correlation between capital stocks is much higher than indicated by the value of ρ_{12} due to joint macroeconomic disaster shocks and common state variables that affect both sectors (cf. Hambel et al., 2024).

The recovery rate of macroeconomic disasters, $Z = 1 - \ell$, has a power distribution over $(0,1)$ with parameter $\alpha > 0$ and density functions $\zeta(Z) = \alpha Z^{\alpha-1}$, $Z \in (0,1)$ (Pindyck and Wang, 2013). The n^{th} moment of the recovery rate is $\mathbb{E}[Z^n] = \frac{\alpha}{\alpha+n}$. To calibrate the macroeconomic disaster-size distribution, we follow Wachter (2013) and define a disaster as an event destroying more than $\overline{\ell} = 10\%$ of GDP or aggregate consumption. She uses historical consumption data to estimate an annual disaster probability of 3.55% and an average consumption loss of 25% when a disaster strikes: $\lambda \int_0^{1-\overline{\ell}} \zeta(Z) \mathrm{d}Z = 0.0355$ and $\mathbb{E}[\ell | \ell > \overline{\ell}] = 0.25$. This pins down $\alpha = 5$ and $\lambda = 0.06$.

Economic Growth To jointly calibrate the production and preference parameters, we follow Hambel et al. (2024) and firstly consider a model with only one capital share in the spirit of Pindyck and Wang

[41] This is true for consumption, GDP, and capital stocks, but for lack of better data and following Pindyck and Wang (2013) we calibrate the returns on safe and risky assets to U.S. data.

(2013). Their model also abstracts from climate change, but it is nested in our two-sector model. The model is well-suited to explain *historical* asset returns, since dirty capital dominated the world economy in the past, while the influence of climate change on asset markets was modest. We assume that the single-capital stock evolves according to

$$\mathrm{d}K = \left(I - \frac{1}{2}\varphi\frac{I^2}{K} - \delta_k K\right)\mathrm{d}t + K\sigma\mathrm{d}W - K_-\ell_e\mathrm{d}N_e.$$

Besides, output is produced by capital K and energy E by a Cobb-Douglas production technology, $Y = AK^{1-\eta}E^{\eta} = I + C + bE$, where b is the price of one unit of the energy composite E. In the optimum, the model becomes a simple AK-technology with linear production function $Y = A^*K$ where productivity is

$$A^* = A\left(\frac{b}{\eta A}\right)^{\frac{\eta}{\eta-1}}.$$

This aggregate model closely follows Pindyck and Wang (2013), but involves an energy input E. We solve this model for a representative investor with Epstein-Zin-preferences and obtain a set of non-linear equations that pin down the model parameters.

Fixing the leverage parameter at $\phi = 2.6$ (Wachter 2013) and the elasticity of intertemporal subsitution at $\psi = 1.5$ (Bansal and Yaron 2004), we calibrate the remaining parameters to match an expected GDP growth rate of $\overline{\mu} = 2.52\%$ in normal times, i.e. in the absence of a disaster (Wachter 2013), an average consumption rate of $\frac{C}{Y} = 63\%$ of GDP, a risk-free interest rate of $r^f = 0.8\%$, an equity premium of $r^p = 6.6\%$, and a Tobin's Q of 1.548 (Pindyck and Wang 2013).

All real quantities (emissions, GDP, capital stocks, etc.) are calibrated to the global economy, but we follow Pindyck and Wang (2013) and take the safe rate to be the return on U.S. Treasury bills (0.8%) and the risky rate as the return on U.S. stocks (7.4%). This choice for the safe rate is not too bad as one can argue that the relevant safe return for the rest of the world is not that far off from the return on U.S. Treasury bills. And, it is difficult to find a figure for the global risk-free rate. Since U.S. assets take up more than 70% of the MSCI World Index, it is perhaps not too bad to follow Pindyck and Wang (2013) and use this figure of 7.4%. The *global* return on risky assets may be 0.2% lower than the U.S. return due to the higher return in emerging markets, so the effect on the coefficient of relative risk aversion and the elasticity of intertemporal substitution will be very small. For the sake of consistency we therefore stick to the returns on safe and risky assets used in Pindyck and Wang (2013) and other papers including van den Bremer and van der Ploeg (2021).

Following the calculations in Pindyck and Wang (2013) but taking leverage into account one obtains a non-linear system that involves five equations and five unknowns $A^*, \varphi, \delta_k, \delta, \gamma$. For the risk-free rate and the risk premium, one obtains

$$r^f = \delta + \frac{\overline{\mu}}{\psi} - \tfrac{1}{2}\gamma\Big(1+\frac{1}{\psi}\Big)\sigma^2 - \lambda_e\Big(\frac{\alpha_e}{\alpha_e-\gamma+1}\frac{1/\psi-\gamma}{1-\gamma} - \frac{\alpha_e}{\alpha_e-\gamma}\Big), \tag{C.1}$$

$$r^p = \phi\gamma\sigma^2 + \lambda_e\gamma\Big[\frac{\alpha_e}{\alpha_e-\gamma} - \frac{\alpha_e}{\alpha_e-\gamma+\phi} + \frac{\alpha_e}{\alpha_e+\phi} - 1\Big]. \tag{C.2}$$

Given the values of σ, λ_e, and α_e, (C.2) pins down the degree of relative risk aversion γ. Then, (C.1) can be solved for the time preference rate δ. Then, we determine the productivity by

$$A^* = \frac{q}{\chi}\Big[\delta + \Big(\frac{1}{\psi}-1\Big)\Big(\overline{\mu} - \tfrac{1}{2}\gamma\sigma^2 - \frac{\lambda_e}{1-\gamma}\frac{\alpha_e}{\alpha_e-\gamma+1}\Big)\Big]. \tag{C.3}$$

In equilibrium, the model generates an investment-capital ratio of $i = A^*(1-\chi-\eta)$ and Tobin's Q is $q = \frac{1}{1-\varphi i}$. Hence, the adjustment cost parameter φ is given by

$$\varphi = \frac{1-1/q}{i}. \tag{C.4}$$

Finally, the capital depreciation rate δ_k is given by

$$\delta_k = i - 0.5\varphi i^2 - \overline{\mu}. \tag{C.5}$$

We use the above equations to calibrate the remaining preference parameters, the depreciation rate, the investment adjustment cost parameters, and the total factor productivities given in Table 1 to match an expected GDP growth rate of $\overline{\mu} = 2.52\%$ in normal times without disasters (Wachter, 2013), a consumption share of $\frac{C}{Y} = 63\%$ of GDP, a risk-free interest rate of $r^f = 0.8\%$, an equity risk premium of $r^p = 6.6\%$, and a Tobin's Q of 1.548 (Pindyck and Wang, 2013).

Energy Consumption We set the energy shares in the production functions to $\eta_i = 0.043$ (van den Bremer and van der Ploeg, 2021).[42] We set the initial cost of fossil fuel to $b_f(S_0)$ = \$540/tC (cf. van den Bremer and van der Ploeg, 2021), but use a significantly higher initial cost of green energy, $b_g(S_0)$ = \$810/etC, in line with production costs in developed countries. We have learning by doing in the production of renewables as the unit production cost drops by 20% for every doubling of cumulative installed volume of renewables based on a voluminous literature on learning curves in accordance with Swanson's law (e.g. Lafond et al., 2018), hence the cost of green goods drops as the green transition

[42] This assumption is in line with Golosov et al. (2014) who use an energy share of 4%.

progresses.[43] This green technical progress is not exogenous and is an alternative to directed technical change (Acemoglu et al., 2012). We suppose that the cost parameter for green energy gradually declines over time as the green transition progresses by setting $b_g(S_t) = b_g(S_0)k_0(1-S_t)^{-k_1}$ with $k_0 > 0$ and $k_1 > 0$. This gives $k_0 = 0.5107$ and $k_1 = 0.3219$.

The green sector only uses renewable energy, so $\kappa_{1,1} = 1$, $\kappa_{2,1} = 0$, and ρ_1 can be chosen arbitrarily. The brown sector can be fueled by both energy sources. To calibrate the energy composite of the brown sector and the CES weights, we set the elasticity of intratemporal substitution to $\zeta_2 = 2$ corresponding to $\rho_2 = 0.5$ and the CES weights to $\kappa_{1,2} = 0.356$, $\kappa_{2,2} = 0.644$ (Golosov et al., 2014). With this calibration it is possible to fully replace fossil fuel by green energy withing this sector even though moving capital to the green sector may be more efficient.

Given those parameter choices, we determine the share of brown capital such that the model generates 19.77% of renewable energy in total energy demand in the BAU-scenario in 2020.[44] This gives an initial share of brown capital of $S_0 = 0.876$. We can thus back out the initial green and brown capital stocks (74.3 and 1353.9 trillion US $, respectively).

Emission Intensity Since the emission intensity ν follows $\mathrm{d}\nu = \nu_- \left[g_\nu \mathrm{d}t - \frac{\mathrm{d}K}{K_-} \right]$, industrial emissions are given by $E_t^{ind} = (f_{1t}(1-S_t) + f_{2t}S_t)K_0 \mathrm{e}^{\int_0^t g_\nu(s)\mathrm{d}s}$. In the BAU state, the social planner does not take account of the negative externalities caused by emissions but reallocates capital from the brown to the green sector for other reasons such as diversification purposes (e.g. Hambel et al. (2024) and the references therein). We now solve and simulate the pure BAU scenario over the next 100 years assuming a reallocation cost parameter of $\kappa = 2$. This parameter choice yields a BAU simulation of temperature, emissions, and energy that is well in line with the adjusted RCP8.5 scenario. Given the adjusted RCP8.5 emission data E_t and the simulated share of brown capital S_t, we approximate $p(t) = \frac{E_t}{\mathbb{E}[f_{1t}(1-S_t)+f_{2t}S_t]}$ by a cubic polynomial function of time, $p(t) = p_0 + p_1 t + p_2 t^2 + p_3 t^3$, with $p_0 = 2.08 \cdot 10^{15}$, $p_1 = 4.22 \cdot 10^{13}$, $p_2 = 1.01 \cdot 10^{12}$, $p_3 = -9.76 \cdot 10^9$, and $R^2 > 99\%$. The corresponding growth rate g_ν is then given by $g_\nu(t) = \frac{\mathrm{d}}{\mathrm{d}t} \ln p(t)$. Figure C.1 depicts the adjusted RCP8.5 emission data and the model fit. Panel (a) shows the simulated data $p(t)$ (o) determining the emission intensity and its cubic fit. Panel (b) depicts the median evolution of the BAU emissions (——) and compares it to the RCP8.5 emission predictions (o). It also shows the corresponding 5% and 95% quantile of BAU emissions (- - -). This calibration implies that the emission intensity ν_t tends to decline over time although it is exposed to stochastic shocks.

[43] Swanson's law is the solar industry specific application of Wright's Law which states there will be a fixed cost reduction for each doubling of manufacturing volume. More specifically, Swanson's law states that the price of solar panels drops by 20 percent every time the volume of panels shipped doubles, see https://www.economist.com/news/2012/11/21/sunny-uplands.

[44] We use world bank data on the share of renewable energy of total final energy consumption, see https://data.worldbank.org/indicator/EG.FEC.RNEW.ZS.

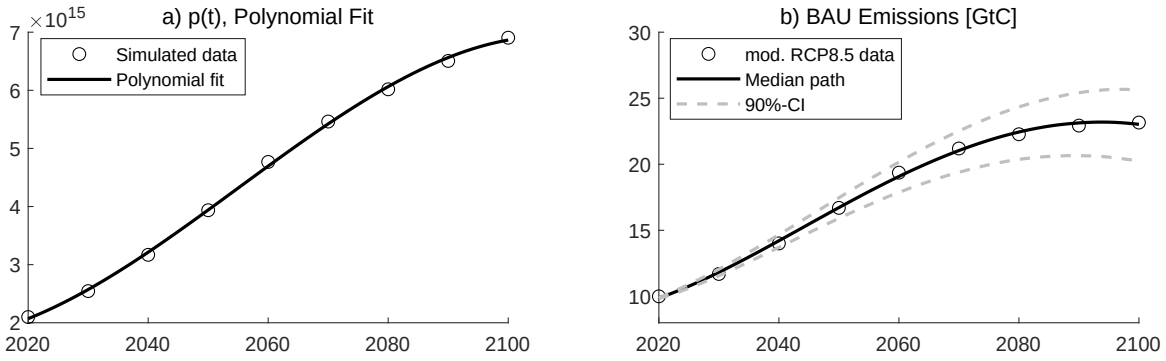

Figure C.1: Calibration of Emission Intensity. Panel (a) shows the simulated data $p(t)$ (o) determining the emission intensity and its cubic fit. Panel (b) depicts the median evolution of the BAU emissions (——) and compares it to the adjusted RCP8.5 emission data (o). It also shows the 5% and 95% quantiles of BAU emissions (- - -).

We thus calibrate the emission intensity such that the pure BAU simulation mimics the modified RCP8.5 scenario of the Fifth Assessment Report of the Intergovernmental Panel on Climate Change (Cambridge University Press, 2014). RCP8.5 is characterized by high emissions leading to a temperature increase of about 4.3°C relative to the pre-industrial level by the end of this century.[45] We slightly modify the emission data to take account of the lower emissions in reality compared to the RCP8.5 scenario. While the scenario predicts emissions of 12.44 GtC in 2020, emissions were only 10 GtC. Thus, we calibrate the emission intensity to adjusted RCP8.5 emission data that is 20% lower than the original data.

Temperature Dynamics Estimates of the transient climate response to cumulative emissions range from 0.8 to 2.4°C/TtC (e.g. Allen et al., 2009; Matthews et al., 2009). We take a TCRE of $\vartheta = 1.8$°C/TtC, which is in line with the temperature evolution in DICE-2016R and other climate-economic models such as Dietz and Venmans (2019). Moreover, we choose a constant temperature volatility of $\sigma_T = 0.033$ to match the temperature range of global mean temperature increase in the RCP scenarios.[46]

Damage Specification We use a standard, inverse quadratic damage function of the form $\Lambda(T) = \frac{1}{1+\theta T^2}$. The damage function parameter corresponding to Nordhaus (2017) is $\theta = 0.00236$. This leads to very low carbon taxes, and a prominent recent study suggests that damages are much higher leading to a benchmark SCC of around \$185/tCO$_2$, see Rennert et al. (2022).[47] Tol (2023) has conducted a meta

[45] The data is available from the RCP database, see `http://tntcat.iiasa.ac.at/RcpDb`.

[46] The temperature range in the year 2100 of the various RCP scenarios varies between 0.8°C around its mean in RCP2.6 to 1.1°C in RCP8.5.

[47] Bilal and Känzig (2024) obtain an even higher benchmark SCC of around \$1,000/tCO$_2$. We do not adopt this higher value, but will in Section 5 allow for temperature-dependent risks of climate disasters which pushes up the SCC considerably.

analysis and found that the estimates of the SCC have increased considerably. He finds an average SCC of about \$40/tCO$_2$ for a low discount rate corresponding to a market based-calibration although the SCC can easily reach three-digit numbers for lower discount rates. Since our calibration is market-based, we calibrate the damage parameter to match the \$40/tCO$_2$ in 2020, leading to $\theta = 0.0073$.[48]

C.2 Additional Calibration Details for Extended Model

Climate Tipping Risks Given the initial value of the TCRE in the pre-tip state, $\vartheta(X_0^c = 1) = 1.8^\circ\text{C/TtC}$, and the range of estimates up to 2.4°C/TtC for the TRCE, we choose a TCRE of $\vartheta(X^c = 2) = 2.1^\circ\text{C/TtC}$ for the intermediate state and $\vartheta(X^c = 3) = 2.4^\circ\text{C/TtC}$ for the post-tip state. From the pre-tip state, the transition intensity to the intermediate and post-tip state is $\lambda_c(\mathbf{S}, 1, j) = \widehat{\lambda}_c^{1,j}(T-1)$ with $\widehat{\lambda}_c^{1,j} = 0.012$ (cf. Cai and Lontzek, 2019).[49] This implies an annual initial tipping intensity of 0.324% at $T_0 = 1.27^\circ\text{C}$ corresponding to an expected duration of 309 years and a tipping intensity of 1.2% at $T = 2^\circ\text{C}$ corresponding to an expected duration of 83 years. The transition intensity for the post-tip state conditional on being in the intermediate state is $\lambda_c(\mathbf{S}, 2, 3) = \widehat{\lambda}_c^{2,3} = 0.02$ corresponding to an average duration of 50 years between the intermediate and the final climate tipping state. The climate can also jump directly from state 1 to state 3, so the total tipping intensity at the initial temperature $T_0 = 1.27^\circ\text{C}$ is 0.648% (cf. van den Bremer et al., 2023). Finally, we have irreversible climate tipping, so $\lambda_c(\mathbf{S}, i, j) = 0$ for $j < i$.

Negative Emission Technology For the calibration of the parameters of the marginal cost function for the negative emission technology $\frac{\partial b_d(S, X^t=2, D, K)}{\partial D} = K[a_1(S) + a_2(S)a_3(S)\exp(a_3(S)D)]$, we first average the data from the two scenarios described in Rebonato et al. (2023) and shown in their Figure 5. We neglect the very small share with low but steep marginal costs for removal that is close to zero. The averaged data—expressed in GtC—is depicted in Figure C.2 for the year 2050 (Panel a) and 2100 (Panel b). Then, we calibrate the truncated power functions of the form $a_j(S) = b_j \max(\zeta, S)^{c_j}$, $j \in \{1,2,3\}$ jointly to both curves by assuming that the time dependencies are only driven by variations in S. In this sense, S models technological progress towards a low-carbon economy. We simulate S and K for the optimal scenario (PIGOU) and calibrate the power functions a_1, a_2, a_3 such that the expected marginal costs at $\tau \in \{31, 81\}$, i.e., in the years 2050 and 2100, respectively, match the marginal cost curves as closely as possible in a least-squares sense. The parameters obtained are all strictly positive so that in particular $\frac{\partial^2 b_d(S, X^t=2, D, K)}{\partial D \partial S} > 0$, i.e., the greater the proportion of brown capital, the greater the marginal removal costs. The fit is visualized by the black line (——). The exponential marginal cost function performs very well with an R^2 exceeding 99%.

[48] This carbon price is computed along the optimal Pigouvian path without policy uncertainty (see Appendix E.3). With temperature-dependent risks of recurring climate disasters and climate tipping (see section 5), it becomes \$113/tCO$_2$.

[49] Climate tipping is only possible if temperature exceeds 1°C, which given our initial temperature is the case.

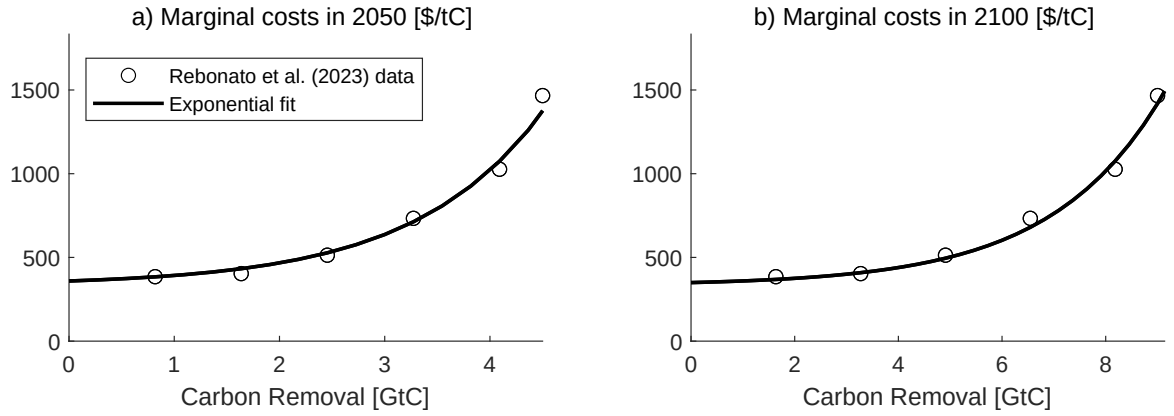

Figure C.2: Calibration of the Marginal Cost Function for NET. The figure shows the averaged data from the two scenarios in Rebonato et al. (2023) (o). Panel (a) shows the resulting marginal costs function for the year 2050 and Panel (b) for the year 2100, respectively. We fit an exponential function of the form $\frac{\partial b_d(S,X^t=2,D,K)}{\partial D} = K[a_1(S)+a_2(S)a_3(S)\exp(a_3(S)D)]$ to this data as shown by the black line (——), where $a_j(S) = b_j \max(\zeta,S)^{c_j}$ are truncated power functions of the share of brown capital.

More Realistic Model of Policy Tipping Ongoing global warming (exponentially) increases the likelihood of strengthening climate policy once temperature has crossed 1.5°C (Barnett, 2024). Although carbon taxes or cap-and-trade systems have never been completely abolished after they had been implemented, there is a significant hazard of climate change deniers coming (back) to power. To allow for transitions back to BAU, we model political transition intensities by

$$\lambda_p(\mathbf{S},i,j) = \widehat{\lambda}_p^{i,j} \exp\left(\widehat{\mu}[\max(T-1.5,0)-S]\right), \qquad i<j$$
$$\lambda_p(\mathbf{S},i,j) = \widehat{\lambda}_p^{i,j} \exp\left(\widehat{\mu}[\min(1.5-T,0)+S]\right), \qquad i>j$$

with $\widehat{\lambda}_p^{i,j} > 0$ for $i \neq j$ and $\widehat{\mu} > 0$. The probability for jumps to a more ambitious climate policy ($j > i$) thus rises in temperature if $T > 1.5$°C. It also falls in the share of brown capital as a result of lobbies to slow down the green transition;[50] also, as the green sector grows in size, green lobbies increase the chance of more stringent climate policies. Conversely, the probability for jumps back to a less ambitious climate policy ($j < i$), falls in temperature if $T > 1.5$°C and rises in the share of brown capital due to stronger brown and weaker green lobbies.

We choose parameters to roughly match the likelihood and resulting temperature increase of the various transition scenarios in Moore et al. (2022): about 48% of their simulations are in their modal scenario, which leads to an average temperature increase of 2.3°C. About 28% of their simulations lead to ag-

[50] For instance, more than 2400 lobbyists affiliated with oil and gas industries attended the recent climate summit COP28, e.g. https://www.theguardian.com/environment/2023/dec/05/record-number-of-fossil-fuel-lobbyists-get-access-to-cop28-climate-talks.

gressive climate action limiting global warming to up to 1.8°C. There is less ambitious or less effective climate action in the remaining scenarios (about 24%) with average temperature increases of around 3°C, of which less than two percent of the simulations lead to significantly higher temperatures. To replicate those figures with our model, we use the parameterization in Table 2. We thus find that the jump intensity from BAU to modest (PIGOU) or ambitious (CAP) climate policies at $T_0 = 1.27$°C and $S_0 = 0.876$ is 6.22% and 2.59%, respectively, which correspond to an expected duration of 16.08 or 38.56 years. The average time until the government takes climate action is half the harmonic mean of those average durations: 11.35 years. Compared to technological or climate tips, these are quick transitions. If BAU continues and temperature rises to say 2°C, expected durations shorten to 11.05 and 26.52 years, respectively. This cuts the average time until the government takes climate action to 7.80 years. Hence, we assume that ongoing global warming and a smaller share of brown capital make it more likely that policy makers start taking the climate serious.

D Additional Simulation Results for the Core Model

This section provides further details including the policy functions for the simulations of our core model.

D.1 Scenarios without Transition Risks.

Macroeconomic outcomes and temperature for the BAU and CAP policy simulations are presented in Figure D.3. As can be seen from Figure D.4, the risk-free rate and the risk premiums are hardly affected in this BAU scenario. This is in line with van den Bremer and van der Ploeg (2021), Hambel et al. (2024), who demonstrate that TFP damages alone are not sufficient to generate a *temperature risk premium* in the spirit of Bansal et al. (2017), Donadelli et al. (2017), Hong et al. (2019), and Gregory (2024). We therefore extend the model with climate-related disaster and climate tipping risks in section 5.

D.2 Policy Functions for the Core Model

Here we discuss the influence of the state variables and the policy states on the optimal decisions and asset returns, captured by the so-called policy functions. From this, we derive intuition for the influence of the share of brown capital and temperature on the optimal controls. In particular, we discuss how climate change affects the interest rate and asset returns. All the results are for the benchmark calibration of our core model for the year 2025. The policy functions are depicted in two figures and depend on the state variables, i.e. S, T and X^p. They are qualitatively similar for other years. Figure D.5 depicts policy functions for the BAU policy state, and Figure D.7 for the CAP policy

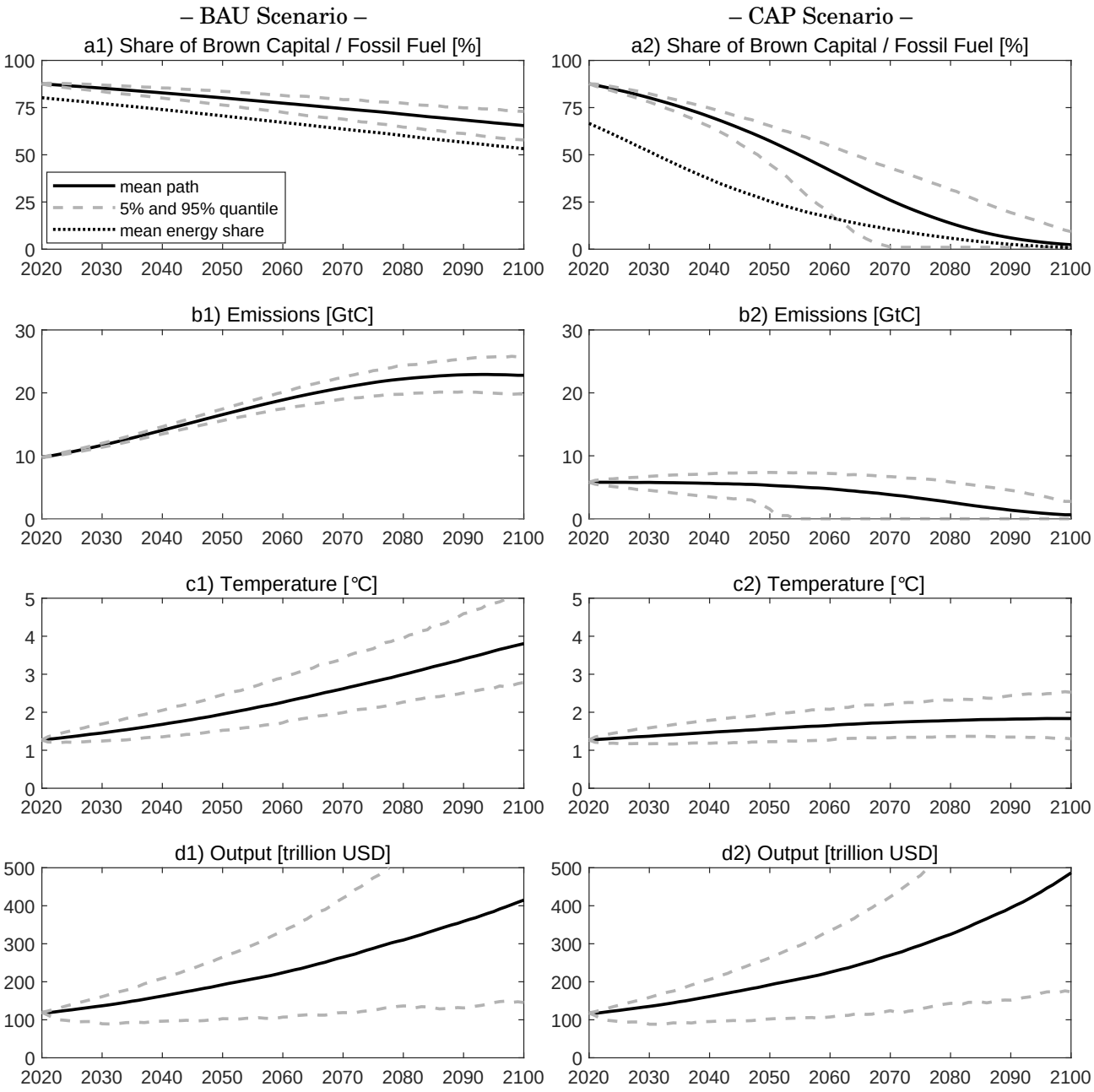

Figure D.3: BAU Scenario (left panels) and CAP scenario (right panels) without Transition Risks. Mean values are depicted by solid lines (——) and 5% and 95% quantiles by dashed lines (- - -). The dotted lines (·····) in Panels a1) and a2) depict the mean path of the share of fossil fuel in the global energy mix.

state. The dark lines (——) depict $S = 0.75$, the gray lines (——) refer to S = 0.5, and the light lines (——) to S = 0.25. The horizontal axis depicts the temperature in the range from 0°C to 4°C.

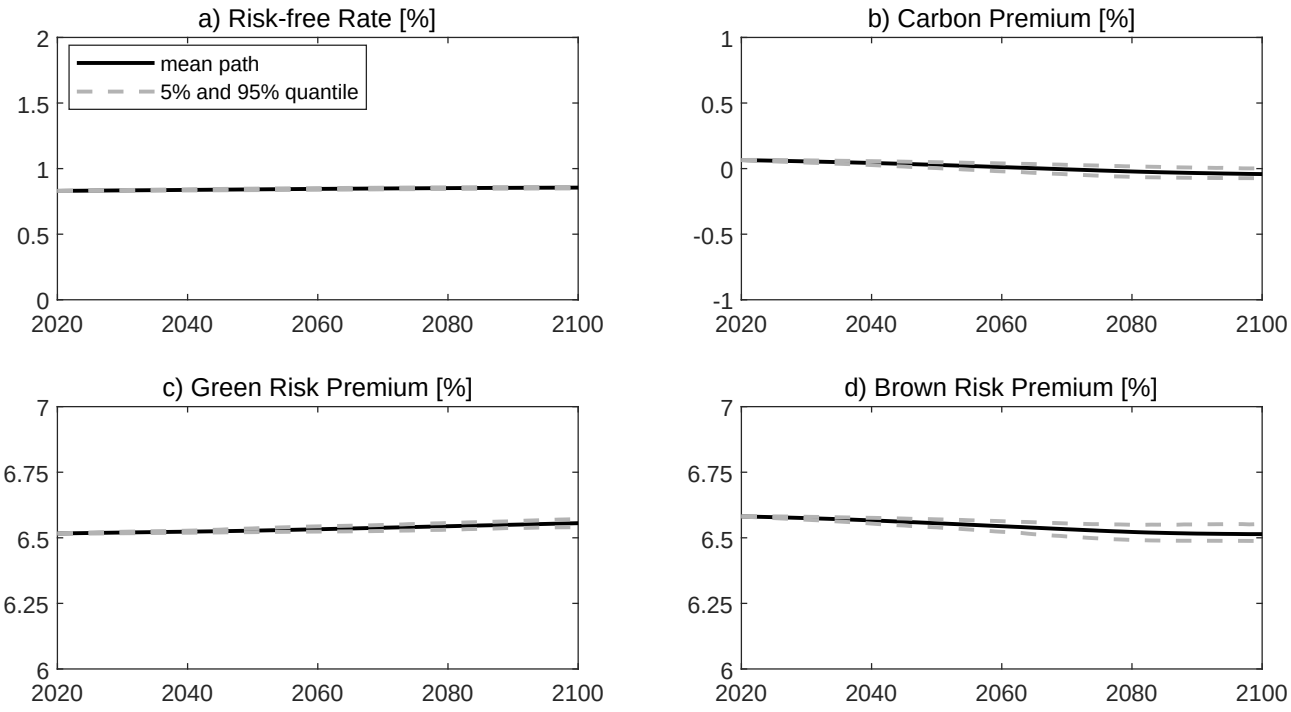

Figure D.4: Business-as-usual Scenario without Transition Risks: Asset Pricing. Average values are depicted by solid lines (——) and 5% and 95% quantiles by dashed lines (- - -). The dotted line (·····) in panel a) depicts the mean path of the share of fossil fuel in the global energy mix.

BAU Policy State Panel a) of Figure D.5 shows that in the BAU policy state the carbon tax is zero (panel c)). Optimal consumption hardly depends on the share of brown capital although it is high if the share of green capital is high. Panel b) depicts optimal capital reallocation from the brown sector to the green sector. As policy makers ignore the negative externality from carbon dioxide but has a motive for diversification, they reallocate capital from the brown to the green sector only if the capital share is above 50% (Hambel et al., 2024). The relocation does not depend on temperature in the BAU state. Panels d), e), and f) depict energy use relative to the respective capital stock, which does not vary with temperature, but brown energy is high and green energy use is low if the share of brown capital is high.

Since capital markets price in climate transition risks and anticipate both climate damages and potential climate policy that may eventually be implemented, the asset pricing moments depicted in panels g), h), and i) depend on temperature. Panel g) shows that the risk-free rate decreases in the share of brown capital and is heavily curbed for temperatures above the two degrees cap. If a policy shock from the BAU to the CAP policy state would hit the economy when temperatures are above the 2°C cap, the brown capital stock may not be operated anymore. This policy transition risk is priced in (see equation (3.2) and the discussion in the main text). Similar effects lead to a slight increase of the risk premiums of both risky assets around the critical temperature of two degrees, leading to a transition risk premium

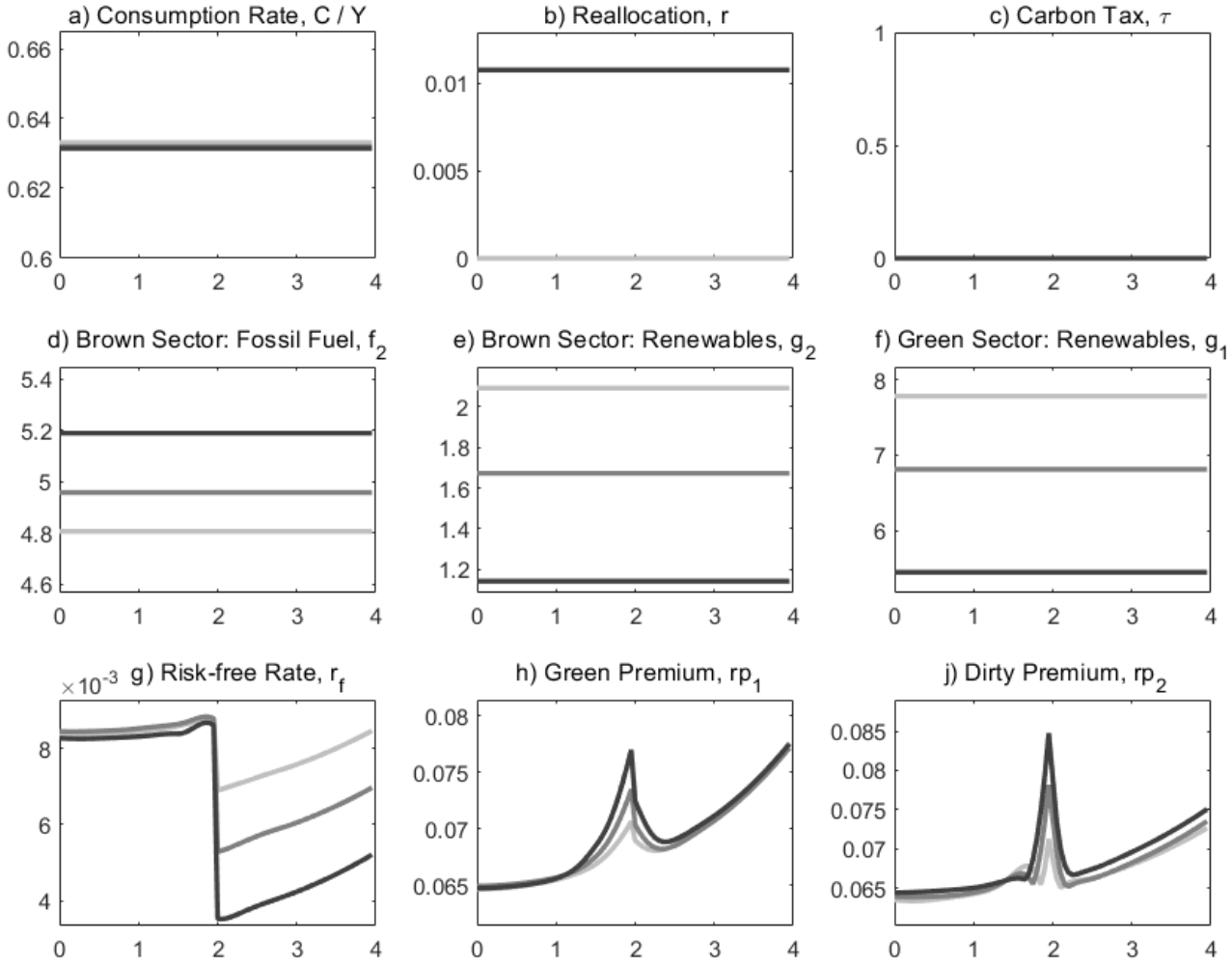

Figure D.5: Policy Functions for the BAU Policy State. The graphs depict policy rules as functions of the two state variables S and T and of the policy state. On the horizontal axis is temperature in the range 0°C to 4°C. The lines represent various levels of the brown capital share: dark lines (——) depict $S = 0.75$ the gray lines (——) refers to $S = 0.5$, and the light lines (——) to $S = 0.25$.

in the spirit of Engle et al. (2020). These transition risks are more pronounced if the share of brown capital in the total capital stock is large.

CAP Policy State Turning to the CAP policy state, Panel a) of Figure D.7, shows that the consumption-to-output ratio significantly increases when temperatures exceed 2°C. Because from then on fossil fuel must not be used anymore (panel d)), output and economic growth drop. This effect is more pronounced if the share of brown capital is large and society relies more on fossil fuel. The economy satisfies its desire for consumption smoothing by increasing the consumption-to-output ratio and the demand for renewable energy in the brown sector that can partially substitute fossil fuel (panel e)). Panel b) il-

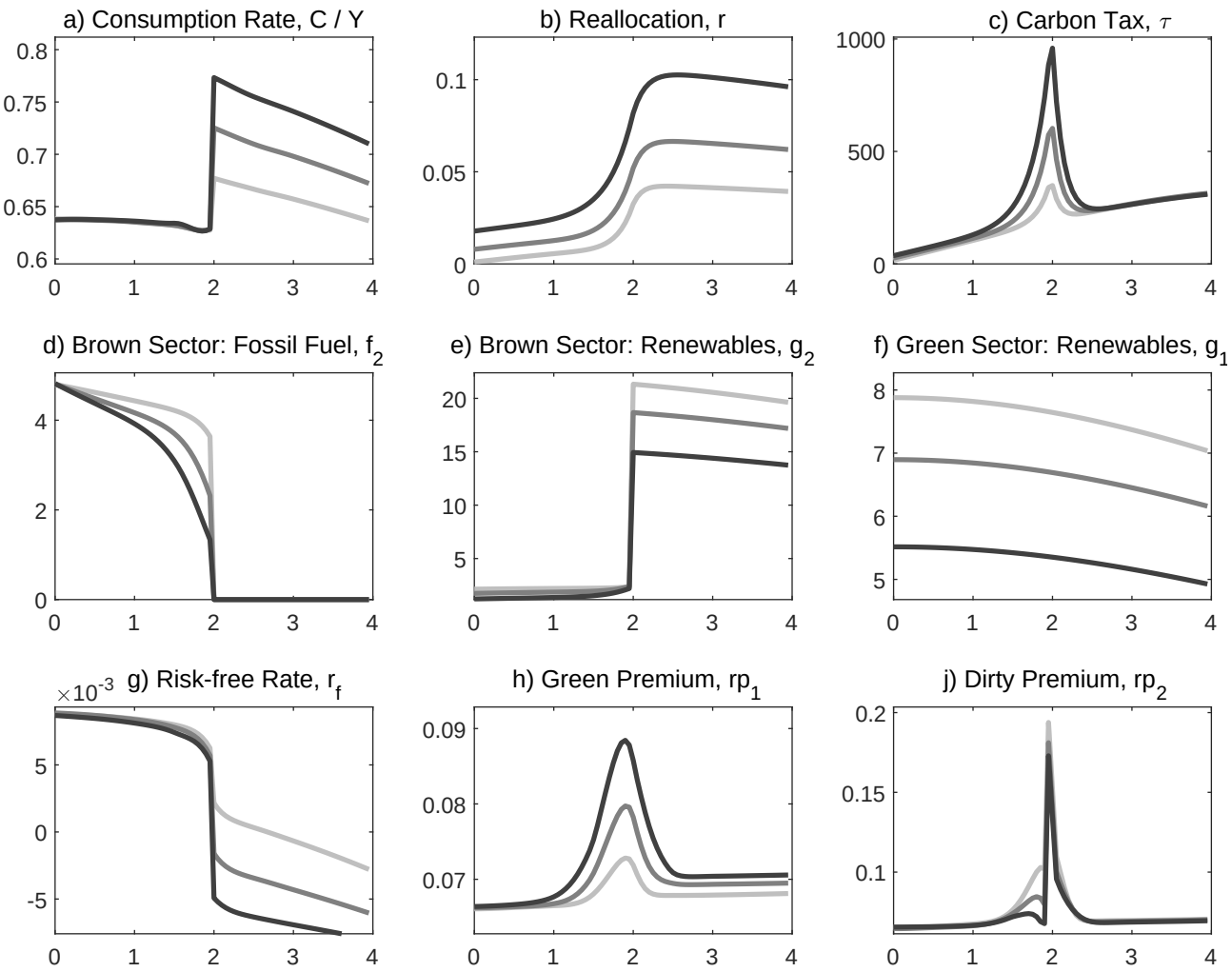

Figure D.6: Policy Functions for the CAP Policy State. The graphs depict policy rules as functions of the two state variables S and T. On the horizontal axis is temperature in the range 0°C to 4°C. The lines represent various levels of the brown capital share: dark lines (——) depict $S = 0.75$, the gray lines (——) refers to $S = 0.5$, and the light lines (——) to $S = 0.25$.

lustrates that capital reallocation takes place at a much faster rate than in the BAU state. Due to prevailing climate risks and policy, society keeps on reallocating even if the share of brown capital is already quite low. Panel c) illustrates that the carbon tax increases dramatically if temperatures are close to but still below two degrees in order to prevent them from crossing the cap. Once temperatures exceed the 2° cap, it becomes more and more unlikely that they will fall below 2° again. Thus for high temperatures, the carbon tax is merely a shadow price as carbon dioxide must not be emitted anymore.

Panel g) depicts the equilibrium risk-free rate. As in the BAU policy state, it drops drastically if temperatures are below two degrees. This is, however, not due to the jump component in equation (3.2), which is zero in the CAP policy state. This drop is mainly driven by the consumption smoothing component

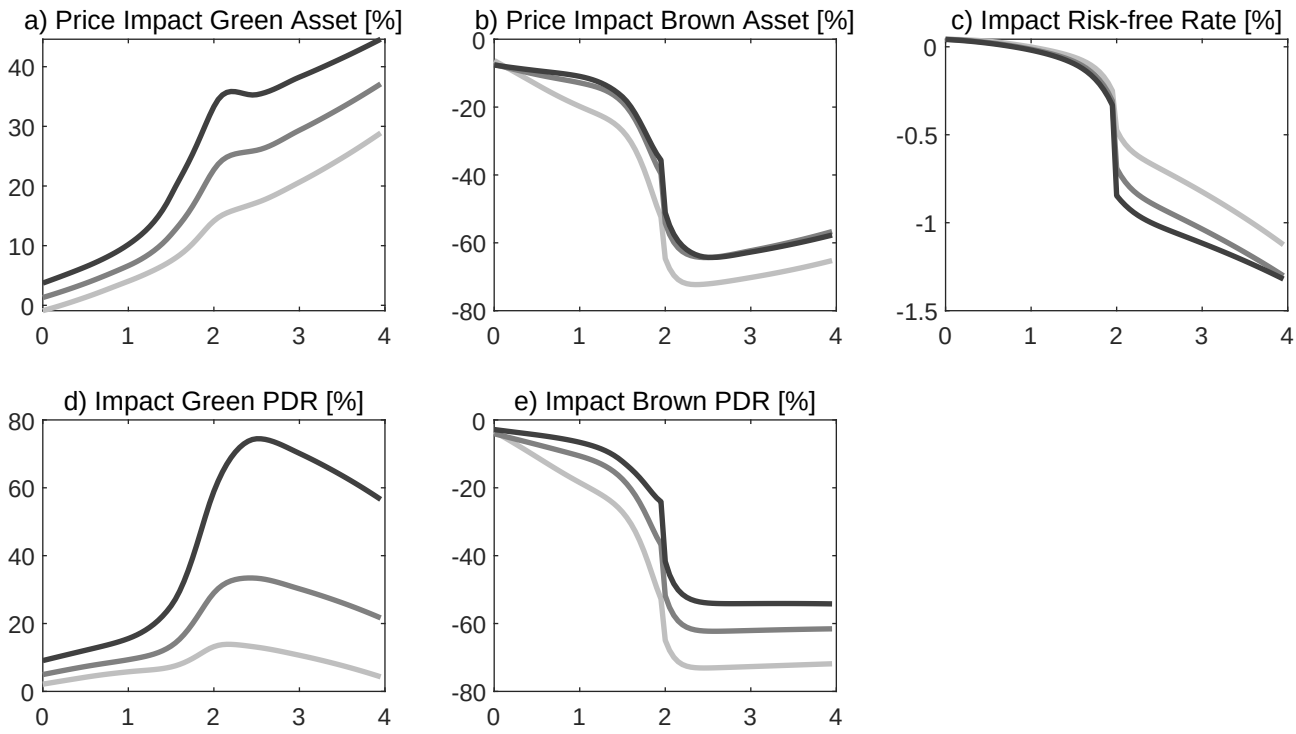

Figure D.7: Effect of Climate Policy on Financial Markets. The graphs depict the effect of a transition from the BAU state to the CAP policy state as functions of the two state variables S and T. On the horizontal axis is temperature in the range 0°C to 4°C. The lines represent various levels of the brown capital share: dark lines (——) depict $S = 0.75$, the gray lines (——) refers to $S = 0.5$, and the light lines (——) to $S = 0.25$.

$\frac{1}{\psi}\mu_C$. As fossil fuels must not be used anymore, the expected consumption growth rate is much lower than in the BAU state. Consequently, the risk-free rate experiences a negative shock, which is stronger if the economy relies a lot on brown capital. Finally, panels h) and i) depict the risk premiums of the two risky assets. Again, both assets price in the aforementioned transition risk, which corresponds to the first line of (B.13). Now the brown asset is much stronger affected than the green asset, leading to a positive carbon premium (see the second line of (3.4) and the discussion in the main text).

Effect of Climate Policy on Financial Markets We now examine the impact of a policy transition from the BAU to the CAP policy state. It turns out that such a policy transition has significant implications for financial markets. As can be seen from panels a) and b), the price of the green asset goes up drastically while the price of the brown asset is negatively affected. While the impact of such a policy shock is rather moderate for low temperatures, it increases drastically if temperatures are close to or above two degrees. The stark negative price effect on the brown asset is particularly pronounced if the temperature cap has been crossed and fossil fuel must not be used for production anymore. We also see that the positive price impact on the green asset is stronger if there is still much brown capital in

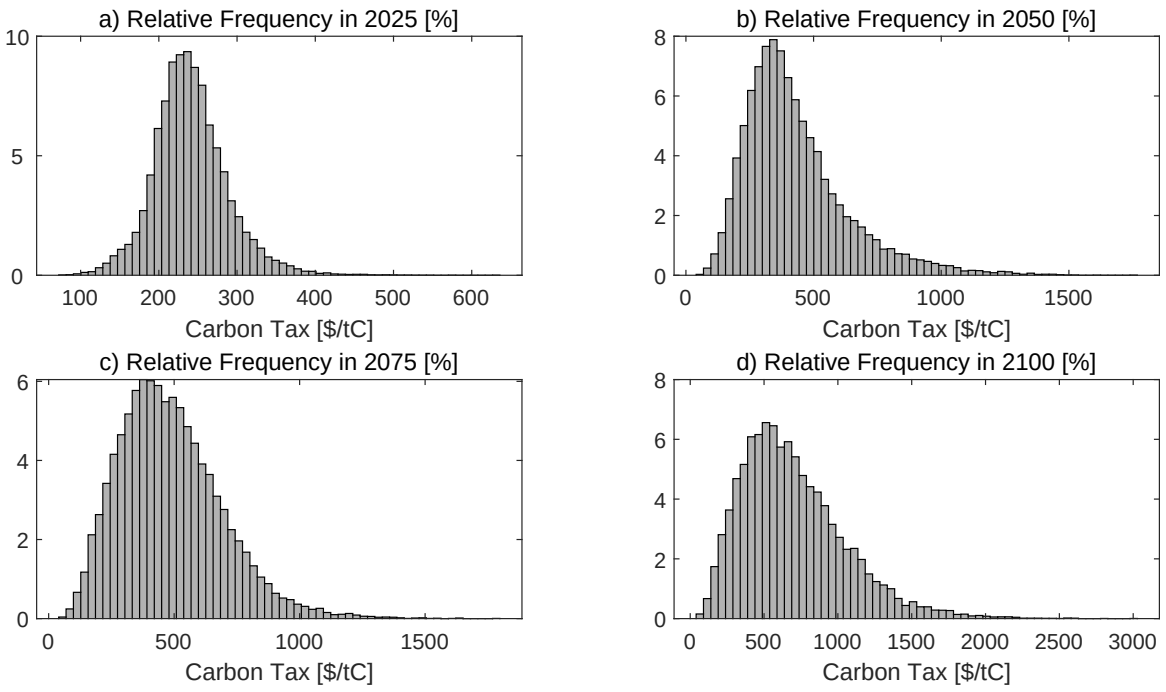

Figure D.8: Carbon Taxes. The figure shows histograms for the implemented carbon tax, i.e., conditional on being in the CAP policy state, for the years a) 2025, b) 2050, b) 2075, and d) 2100.

the economy. Then, the demand for green assets to compensate the loss in the brown sector is particularly strong. These findings are also reflected in panels e) and f), which illustrate the effect on the price-dividend ratios of both risky assets.

Panel c) now illustrates the effect of a policy transition shock on the risk-free rate, which is always negative. If temperatures are below the 2° cap, the risk of phasing out fossil fuel is now more pronounced and so the demand for precautionary savings increase. If temperatures are already above two degrees, production becomes more expensive as fossil fuel must not be used anymore. Consequently, consumption growth is slowed down and the term $\frac{1}{\psi}\mu_C$ in equation (3.2) becomes smaller after the policy transition.

D.3 Additional Material for the Core Simulations

Optimal Carbon Taxes Table D.1 reports the unconditional moments of the implemented carbon tax for the years 2025, 2050, 2075, and 2100. Since the carbon tax is implemented in only about 25% of the paths in 2025, its unconditional distribution is clearly right-skewed. Its skewness tends to decline over time as carbon taxes are implemented in more and more paths. Figure D.8 shows histograms for implemented carbon taxes for the years 2025, 2050, 2075, and 2100. Those histograms are generated with 20,000 paths conditional on being in the CAP policy state.

(a) Unconditional moments

	$\mathbb{E}[\tau]$	$\text{Med}(\tau)$	$\sigma(\tau)$	$q_{5\%}(\tau)$	$q_{95\%}(\tau)$	$\text{Skew}(\tau)$
2025	42	0	97	0	275	2.01
2050	372	345	366	0	1072	1.06
2075	465	457	300	0	957	0.74
2100	696	651	395	0	1402	0.65

(b) Conditional moments

	$\mathbb{E}[\tau]$	$\text{Med}(\tau)$	$\sigma(\tau)$	$q_{5\%}(\tau)$	$q_{95\%}(\tau)$	$\text{Skew}(\tau)$
2025	254	250	53	175	347	0.70
2050	562	481	309	215	1197	1.48
2075	538	501	254	210	989	1.48
2100	738	677	367	247	1416	0.93

Table D.1: Optimal Carbon Tax. The table reports summary statistics of (a) the unconditional optimal carbon tax and (b) the optimal carbon tax conditional on being implemented for the years 2025, 2050, 2075, and 2100.

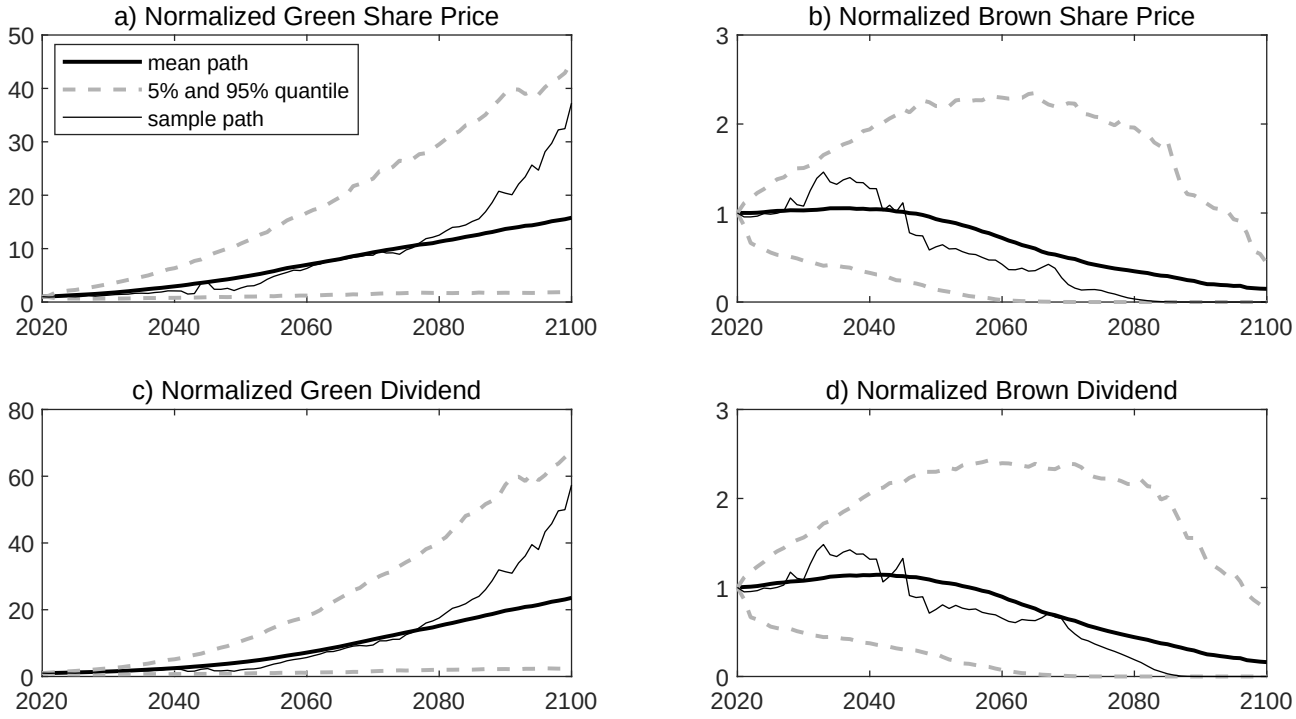

Figure D.9: An Illustrative Sample Path (Asset Prices). Average values are depicted by solid lines (——) and 5% and 95% quantiles by dashed lines (- - -). To simplify the comparison between the brown and green assets, we have normalized share prices in 2020 in panels (a) and (b) and dividends in 2020 in (c) and (d) to one in each case. The thin black lines (——) shows one illustrative sample path, where society switches from the BAU policy state to the CAP policy state in the year 2045.

An Illustrative Sample Path for Asset Prices Figure D.9 complements Figure 2 from the main text. In particular, it illustrates the simulated normalized dividends and share prices for both risky assets. Panels a) and b) illustrate the price impact of a climate policy shock from the BAU state to the

Scenario		Average Carbon tax [$/tCO$_2$]				Carbon premium [%]			
	λ_x	2025	2050	2075	2100	2025	2050	2075	2100
BAU	–	0	0	0	0	0.0	0.0	0.0	0.0
PIGOU	–	45	77	127	199	–0.1	0	0.2	0.6
CAP	–	66	117	132	190	–0.5	0.3	2.0	1.8
BAU → CAP	4%	11 (73)	99 (153)	122 (143)	190 (202)	–0.2	0.3	1.6	1.1
BAU → CAP	20%	45 (72)	129 (129)	134 (134)	195 (195)	–0.5	0.5	2.2	2.0
BAU → PIGOU	4%	8 (46)	54 (81)	119 (137)	207 (219)	0.0	0.0	0.1	0.4

Table E.2: SCC and the Carbon Premium in Alternative Scenarios. The table reports average carbon taxes and average carbon premiums or the years 2025, 2050, 2075, and 2100. The numbers in brackets refer to the average optimal carbon tax *conditional* on being implemented.

CAP state in the year 2045. This event is accompanied by a rise in the price of the green asset and a sharp fall in the price of the brown asset. The effect on prices is stronger than on dividends, whereby the price-dividend ratio of the green asset increases strongly and that of the brown asset decreases. The sharp rise in the price-dividend ratio of the green asset causes a decline in the dividend yield. However, the onset of climate policy will increase demand for the green asset in the long term, causing the expected growth rate to rise sharply. This overcompensates for the decline in the dividend yield and leads to an increase in the green premium. Conversely, the increase in the brown risk premium can be explained by the now significantly increased risk of fossil fuels phasing out.

E Sensitivity of Core Results

E.1 Higher Transition Risk

We first examine the extent to which the carbon premium and the carbon tax depend on transition probabilities (see rows 4 and 5 of Table E.2). With an annual transition probability of 20% (rather than 4%) for switching to the CAP policy state, the unconditional average carbon tax is higher because more paths will implement climate policy. It is significantly higher in the short than in the long run, since over time more and more paths will have switched to the CAP policy state and the difference in carbon taxes diminishes. The unconditional average carbon tax is smaller than in the benchmark case as climate action has started earlier and policy makers do not have to catch up on so much that was missed in the BAU policy state. The carbon premiums are higher too in later years.

E.2 Tighter Temperature Cap

The second sensitivity exercise is to examine a temperature cap of 1.5°C instead of 2°C (see Appendix E.4 and Figure E.10). Carbon pricing is then in the next two decades more ambitious to avoid the potentially devastating effects of overshooting the carbon budget, but in the distant future damages and the optimal carbon tax have grown so much that temperature caps no longer bite and the difference in carbon pricing disappears. The carbon premium becomes earlier economically relevant than when the economy is in the CAP state and temperature is close to 1.5°C.

E.3 Carbon Pricing without Temperature Cap

The third sensitivity exercise is to examine what happens if we replace the CAP policy state with a more modest carbon prices called the PIGOU policy state, which internalizes the global warming externalities but does not enforce the temperature cap (see last row of Table E.2). First, consider modest carbon pricing without policy transition risk. In line with the equivalent simulation with the CAP state without transition risk, the carbon premium is initially very small and negative (–0.1%), but remains below 0.75% due to the absence of transition risk. Thus, the magnitude of the carbon premium is small and economically not significant. It only becomes relevant at the end of this century when sizable carbon taxes are implemented.

Second, we consider the scenario with transition risk and the BAU and PIGOU policy states. Simulations starts with BAU until there is a policy switch and policy makers start pricing carbon modestly. Like the BAU and PIGOU scenarios without transition risk, there are no significant carbon premiums. Compared to the PIGOU scenario without transition risk, policy makers implement slightly higher carbon taxes after a transition to the PIGOU policy state to make up for the omitted carbon pricing in the BAU policy state. For instance, in the year 2050, the average carbon tax in the PIGOU policy state is \$81/tCO_2, which is slightly higher than in the pure PIGOU scenario (\$77/tCO_2).

Hence, the risk of exceeding a temperature cap, not policy transition risk, is at the root of a sizeable carbon premium. In this sense, the risk of exceeding a temperature cap is a form of transition risk.

E.4 CAP Scenario without Policy Transition Risks

Figure E.12 provides the simulation results when the model starts in the CAP state and excludes policy transitions to the BAU or PIGOU state (i.e. with the political Markov chain switched off). In contrast to the PIGOU scenario, the carbon premium can be sizable if temperatures are close to 2°C. This scenario leads to an even faster transition to net zero than the PIGOU scenario and policy makers implement more stringent carbon prices.

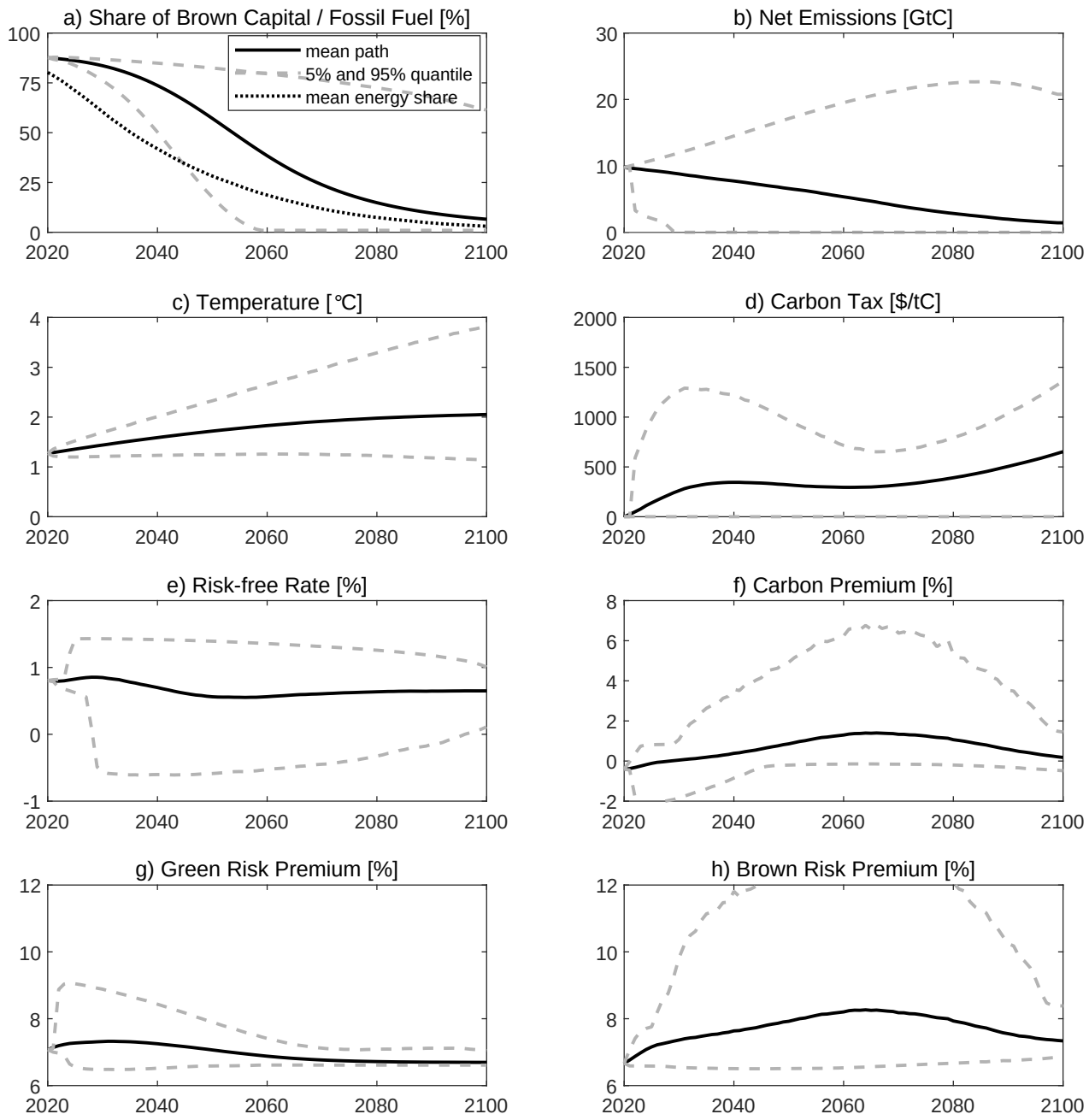

Figure E.10: Core Model with a Tighter Carbon Budget. Average values are depicted by solid lines (——) and 5% and 95% quantiles by dashed lines (- - -). The dotted line (·····) in Panel a) depicts the mean path of the share of fossil fuel in the global energy mix.

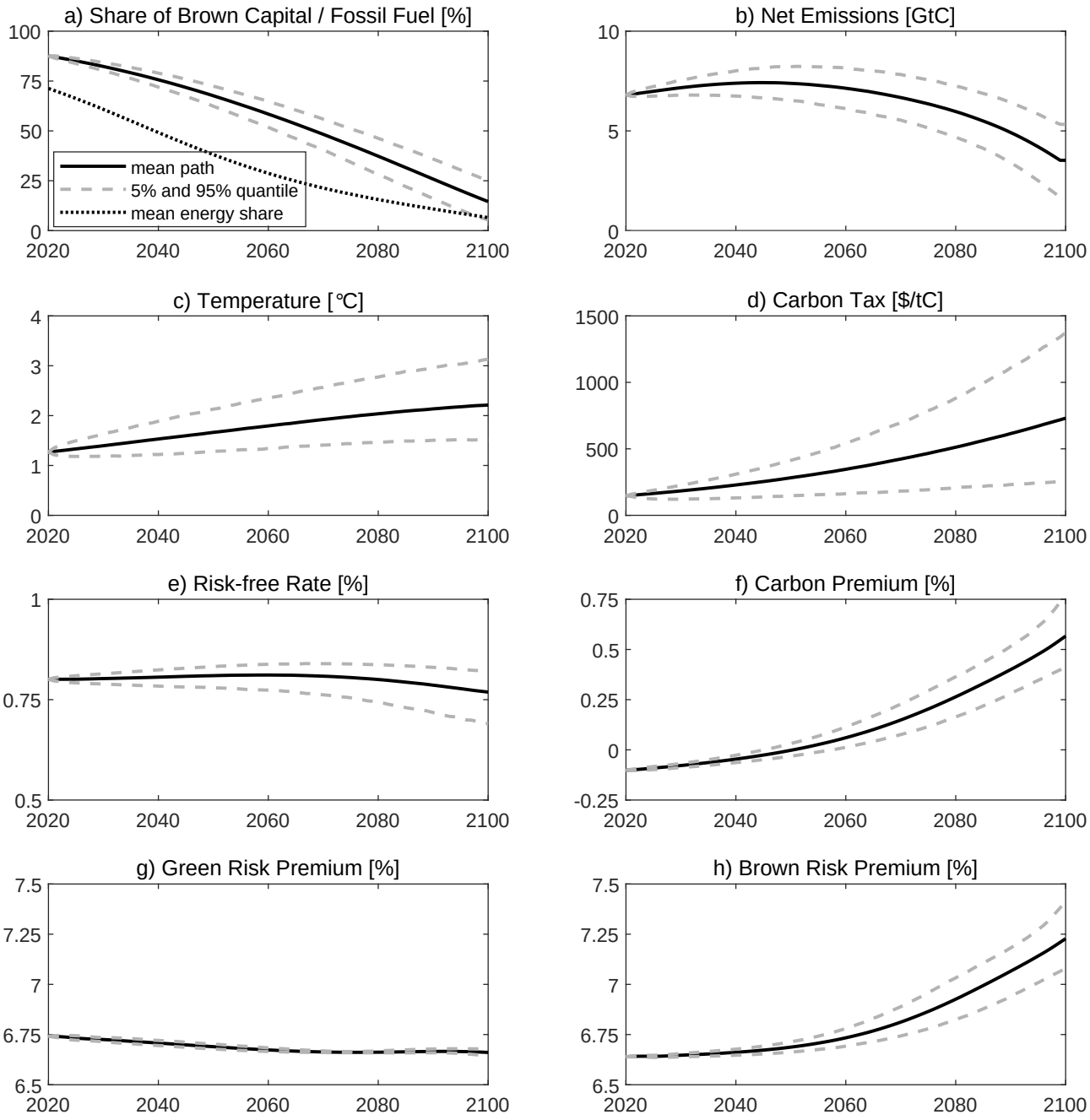

Figure E.11: PIGOU Scenario without Transition Risks (Optimal Carbon Taxes, No Temperature Cap). Average values are depicted by solid lines (——) and 5% and 95% quantiles by dashed lines (- - -). The dotted line (·····) in Panel a) depicts the mean path of the share of fossil fuel in the global energy mix.

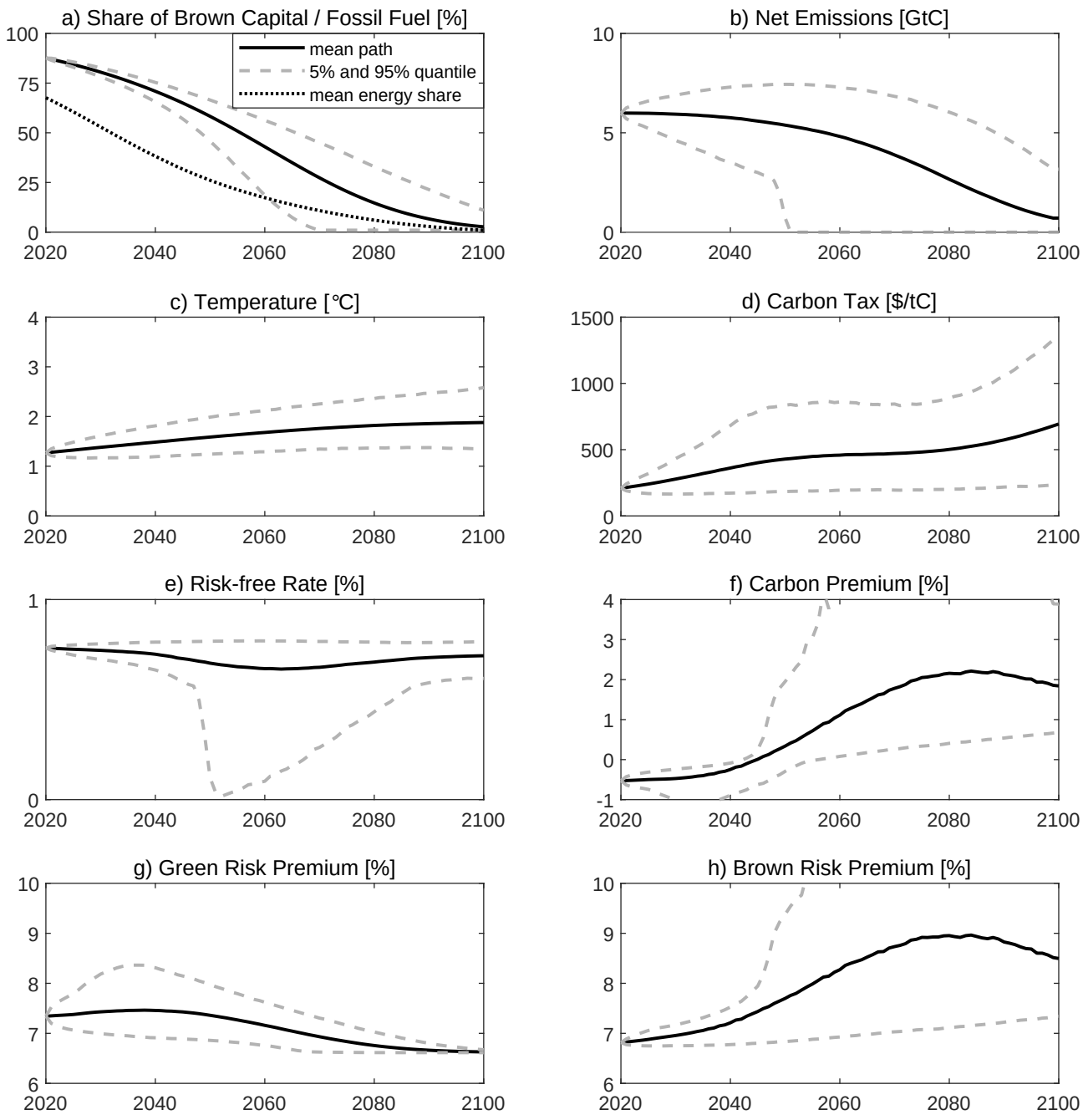

Figure E.12: CAP Scenario without Transition Risks. Average values are depicted by solid lines (——) and 5% and 95% quantiles by dashed lines (- - -). The dotted line (·····) in Panel a) depicts the mean path of the share of fossil fuel in the global energy mix.